



universität
wien

**Characterization and Functional Analysis of
a Novel PP2C Phosphatase AP2C2
from *Arabidopsis***

Dissertation

zur Erlangung des Akademischen Grades der Doktorin
der Naturwissenschaften *Doctor rerum naturalium*
an der Fakultät für Lebenswissenschaften der Universität Wien

Verfasserin:

Chonnanit Choopayak

Matrikel-Nummer:

0409975

Dissertationsgebiet (lt. Studienblatt):

090441 Genetik-Mikrobiologie (Stzw)

Betreuerin:

Univ. Doz. Dr. Irute Meskiene

Wien, am 24. September, 2008

ZUSAMMENFASSUNG

Um zu überleben haben Pflanzen geeignete Signalwege entwickelt, um auf spezifische Reize und Einflüsse aus der Umgebung passend reagieren zu können. Proteinphosphorylierung ist eine der zellulären Hauptstrategien, um Umweltbelastungen wahrzunehmen und damit umzugehen. In *Arabidopsis* spielen Proteinphosphatasen vom Typ 2C (PP2C) wichtige Rollen in der Stressreaktion. In der vorliegenden Arbeit wird eine *Arabidopsis* PP2C namens AP2C2 als Regulator von Signalwegen bestimmter Stressreaktionen aufgezeigt. AP2C2 zeigt insbesondere eine wichtige Rolle in ROS Signalwege, welche durch biotische und abiotische Belastungen aktiviert werden. ROS induziert die Expression von AP2C2, deren Lokalisation sich örtlich an den Stellen der ROS Ansammlung befindet. Es wird dargelegt, dass AP2C2 die Signalkaskade stress-aktivierter MAP-Kinasen (MAPK) kontrolliert. AP2C2 interagiert und inaktiviert Stress-MAPK durch Dephosphorylierung der Aminosäure Threonin am essentiellen pTEpY Motiv der MAPK. In der Pflanzenzelle ist AP2C2 einerseits mit dem Zellkern assoziiert, andererseits auch an Plastiden lokalisiert, was mehrere Rollen von AP2C2 in verschiedenen Zellkompartimenten andeuten kann. Die intrazelluläre Lokalisation der Wirkung von AP2C2 auf MAP-Kinasen könnte sowohl der Zellkern als auch das Cytoplasma sein, da Komplexe von AP2C2 und MAP-Kinasen im Zellkern und zum Teil auch im Cytoplasma detektiert wurden. Modifikationen der Expression von AP2C2 weisen darauf hin, dass AP2C2 eine Stressantwort in der Pflanze reguliert, da festgestellt wurde, dass *ap2c2* Pflanzen mit ausgeschalteter AP2C2 eine höhere Resistenz gegenüber Salz und Paraquat zeigten. Es liegt nahe, dass AP2C2 ein möglicher negativer Regulator der Jasmonsäurebiosynthese ist. *ap2c2* Pflanzen zeigen eine vermehrte Expression des Jasmonsäure-responsives Transkripts *Thi2.1* nach Verwundung. Die Funktion von AP2C2 könnte mit der von anderen Phosphatasen wie AP2C1 und MKP1 redundant sein. *ap2c1/ap2c2* mutante Pflanzen zeigten einen deutlicheren Phänotyp des Wurzelwachstums, und *ap2c2/mkp1* Pflanzen wiesen ein offensichtliches Entwicklungsphänotyp. Zusammengefasst stehen die Funktionen von AP2C2 mit Stressabwehr und Pflanzenentwicklung in Verbindung. Zusätzlich zu der Regulierung von Stress-aktivierten MAP-Kinasen werden möglicherweise Pflanzenhormone durch AP2C2 reguliert.

ABSTRACT

In order to survive, plants developed the proper signaling for responses to the specific stimuli. Protein phosphorylation is the principal strategy that plants use to cope with environmental stress. In *Arabidopsis*, protein serine/threonine phosphatases of type 2C (PP2Cs) play important roles in stress responses. Here, an *Arabidopsis* PP2C, named AP2C2, is demonstrated as a regulator of stress response signaling, in particular ROS signaling activated by both biotic and abiotic stresses. AP2C2 expression is induced by ROS and is localised at the site of ROS accumulation. It is demonstrated that AP2C2 controls the stress-activated MAPK cascade. AP2C2 interacts with and inactivates stress-MAPKs by dephosphorylating the threonine residue at pTEpY motif of MAPKs. In plant cell, AP2C2 is associated with the nucleus, and also localized to plastids suggesting the multiple functions of AP2C2 in different compartments of the cell. The site of action of AP2C2 on MAPKs might be in the nucleus or cytoplasm of the cell because the complexes of AP2C2 and MPKs were detected in the nucleus and to some extent in the cytoplasm. Modification of AP2C2 expression suggests that AP2C2 regulates plant stress response as *ap2c2* plants were found to be more resistant to high salt and paraquat. AP2C2 is proposed to negatively regulate JA biosynthesis. *ap2c2* plants upregulated JA-responsive transcript, *Thi2.1* upon wounding stress. The function of AP2C2 may be redundant with other protein phosphatases, including AP2C1 and MKP1. *ap2c1/ap2c2* had stronger root growth phenotype than the single knockout plants and *ap2c2/mkp1* plants showed developmental phenotype. Taken together, AP2C2 functions are related to stress response and plant development. In addition to regulate stress-activated MAPK signaling, AP2C2 possibly regulate plant stress hormones.

ACKNOWLEDGEMENTS

I am thankful to *Univ. Doz. Dr. Irute Meskiene* for her scientific supervision, providing me the opportunity to work in her group and for always reminding me to learn useful things for my country.

My appreciation goes to *Dr. Alois Schweighofer* for supervising me, showing me how to discover the scientific world when I was new here.

I wish to thank *Univ. Ass. Prof. Dr. Holger Bohlmann* and *Prof. Dr. Francesca Cardinale* for their valuable comments and suggestions during the final stage of my PhD.

My sincere thanks to *a.o.Univ. Prof. Dr. Andrea Barta* for lab space, *Univ. Doz. Dr. Friedrich Kragler* for work discussions and *Dr. Doz. Zdravko Lorkovic* for sharing tools and kindly support.

My special thanks go to *Dr. Wilfried Rozhon* for sharing the tools, friendly suggestions and work discussion, *Mag. Monika Kastler* for kindly availability and suggestions, *Mag. Andrej Belokurov* for technical assistance, *Dr. Manfred Schwanninger* for ethylene measurement and *a.o.Univ. Prof. Dr. Angela Witte* for her help with the bureaucracy.

I am also thankful to my colleagues *Dr. Vaiva Kazanaviciute*, *Mag. Julija Umbrasaite* and for their assistance, discussion and friendship in the group. Special thanks go to *Mag. Zahra Ayatollahi* for her kindness, friendly and translation.

I am thankful to the *Thai government* and *Naresuan University* for financial support throughout my study.

I owe a great debt to my dear friends; *Dr. Sutira Lerdragool* for warm mental support and for coordinating all of my affairs in Thailand throughout the period of my study Also to *Dr. Apinun Limmongkon* for showing me how to adapt and live in Austria.

Finally, my deepest appreciation and thanks to *my family, Mum, Dad, sister and brother*. Their unconditional love, support, encouragement and understanding, helped me overcome all the difficult situations and achieve the golden goal.

TABLE OF CONTENTS

	pages
ZUSAMMENFASSUNG	ii
ABSTRACT	iii
ACKNOWLEDGEMENTS	iv
TABLE OF CONTENTS	v

1. INTRODUCTION

1.1. Aims of this work	2
1.2. Protein phosphatases in plants	2
1.2.1. Protein Ser/Thr phosphatases	2
1.2.2. Protein Tyr phosphatases	4
1.3. Reactive oxygen species (ROS)	5
1.4. Roles of ROS in plants	7
1.5. Sources of ROS production in plants	8
1.5.1. Photosynthesis	9
1.5.2. Respiration	9
1.5.3. Photorespiration	10
1.5.4. NADPH oxidase	12
1.5.5. Cell wall peroxidase	12
1.6. Defence mechanisms against ROS in plants	13
1.7. ROS production and signal transduction under stress factors	15
1.7.1. ROS and MAPK cascade	15
1.7.2. Pathogen challenges	18
1.7.3. Wounding	20
1.7.4. High light (HL)	21
1.7.5. Salinity	23
1.7.6. Heat	25
1.7.7. Paraquat	26
1.7.8. Combination of different stresses	28
1.8. Hormone biosynthesis and signalling pathways	28
1.8.1. Salicylic acid	29

	pages
1.8.2. Ethylene	30
1.8.3. Jasmonic acid	35
1.9. Hormone-mediated signalling	37
1.9.1. under Biotic stresses	37
1.9.2. under Abiotic stresses	38
1.9.3. in Mutation plants	40
 2. MATERIALS AND METHODS	
2.1. Plasmid constructs	46
2.1.1. Vectors	46
2.1.2. Plasmids	48
2.2. Oligonucleotides	49
2.2.1. PCR primers	49
2.2.2. RT-PCR primers	50
2.2.3. Primers for construction of Loss-of-function mutations	50
2.2.4. Primers for AP2C2-RNAi construction	50
2.3. Antibodies	51
2.3.1. Primary antibodies	51
2.3.2. Secondary antibodies	51
2.4. DNA work	52
2.4.1. Southern blotting	52
2.4.2. DNA extraction from leaf tissues	53
2.4.3. Creation of loss-of-function mutations of AP2C2	53
2.4.3.1. Site directed mutagenesis	53
2.4.3.2. AP2C2-RNAi plasmid construction	54
2.5. RNA work	54
2.5.1. RNA extraction	54
2.5.2. Reverse transcription	55
2.6. Protein work	55
2.6.1. Protein extraction from plants and protoplasts	55
2.6.2. Determination of protein concentration	56
2.6.3. SDS PAGE	56

	pages
2.6.4. Western blotting	56
2.6.5. Expression and purification of GST-fusion proteins	57
2.6.6. <i>In vitro</i> kinase assay	57
2.6.7. In gel kinase assay	58
2.6.8. <i>In vitro</i> phosphatase assay	59
2.6.8.1. Casein substrate labelling	59
2.6.8.2. MPK6 substrate labelling	59
2.6.8.3. Substrates dephosphorylation	60
2.6.9. Catalase activity measurement	60
2.7. Bacterial work	61
2.7.1. <i>Escherichia coli</i>	61
2.7.1.1. Production of competent <i>E.coli</i>	61
2.7.1.2. Transformation of <i>E.coli</i>	61
2.7.2. <i>Agrobacterium tumefaciens</i>	61
2.7.2.1. <i>A. tumefaciens</i> strains	61
2.7.2.2. Cultivation of <i>A. tumefaciens</i>	62
2.7.2.3. Preparation of <i>A. tumefaciens</i> electrocompetent cells	62
2.7.2.4. <i>Agrobacterium</i> transformation by electroporation	62
2.7.2.5. Selection of transformants	63
2.7.2.6. Preparation of <i>Agrobacterium</i> frozen stocks	63
2.8. Yeast work	63
2.8.1. Yeast strains	63
2.8.2. Yeast one-step transformation	63
2.8.3. β -galactosidase assay	64
2.8.4. cDNA library screening	65
2.8.4.1. Two-hybrid library and yeast vectors	65
2.8.4.2. Yeast transformation	65
2.8.4.3. Characterization of putative interacting proteins	65
2.8.4.3.1. Plasmid rescue from yeast	66
2.8.4.3.2. Sequencing of interacting clones	66
2.9. Plant work	66
2.9.1. Plant lines	66

	pages
2.9.2. Plant growth conditions	66
2.9.2.1. Non-sterile <i>Arabidopsis</i> growth	67
2.9.2.2. Sterile <i>Arabidopsis</i> growth	67
2.9.3. Surface sterilization of <i>Arabidopsis</i> seeds	68
2.9.4. <i>A. tumefaciens</i> mediated transformation of <i>Arabidopsis</i> by floral dip	68
2.9.5. Selection of transgenic plants	68
2.9.5.1. Segregation analysis	68
2.9.5.2. Analysis of <i>ap2c2</i> knockout line	69
2.9.6. Plant tissue culture methods:	69
2.9.6.1. Cultivation of <i>Arabidopsis</i> suspension culture	69
2.9.6.2. Protoplast isolation	69
2.9.6.3. Protoplast transformation	70
2.10. Expression analysis	70
2.10.1. Promoter-reporter analysis	70
2.10.2. Stress treatment	70
2.10.2.1. Abiotic stress treatment	71
2.10.2.2. Biotic stress treatment	72
2.10.2.3. Hormone treatment	72
2.10.3. Histochemical staining and microscope	72
2.11. Bacterial pathogen resistance assays	72
2.11.1. Bacterial growth	72
2.11.2. Plant inoculation with <i>Pseudomonas syringae</i> DC3000	73
2.11.3. Scoring plant disease resistance to <i>P. syringae</i>	73
2.12. Ethylene production measurements	74

3. RESULTS

3.1. Interaction of AP2C2 with other proteins	75
3.2. Subcellular localization of AP2C2	80
3.3. Subcellular localization of IMP α 1	82
3.4. Expression analysis of AP2C2	82
3.5. Phosphatase activity of AP2C2	91

	pages
3.6. MAP kinases inactivation by AP2C2 in protoplasts	93
3.7. Characterization of <i>ap2c2</i> plant	94
3.8. Characterization of AP2C2 overexpressing plants	96
3.9. MAP kinases inactivation by AP2C2 <i>in planta</i>	97
3.10. <i>Thionin2.1</i> was transiently upregulated in <i>ap2c2</i> plant after stresses	100
3.11. Modification of AP2C2 expression affects seed germination and seedling survival	100
3.12. Modification of AP2C2 expression affects root phenotype under stress conditions	103
3.13. Production and characterization of AP2C2-RNAi plants	104
3.14. No difference in sensitivity to <i>P. syringae</i> DC3000 of AP2C2 modified plants	104
3.15. <i>ap2c2 mkp1</i> plants showed developmental phenotypes.	105
3.16. <i>ap2c1/2</i> plants had longer primary root.	107
3.17. Lack of AP2C2 complements fertility phenotype in <i>ap2c2/AP2C2 acx1/5</i> plants	107
3.18. Production of ethylene in AP2C2 modified plants.	109
 4. DISCUSSION	 110
 5. REFERENCES	 119
 6. APPENDIX	 127
6.1. Abbreviations	127
6.2. Curriculum Vitae	130

INTRODUCTION

AP2C2 is a putative *Arabidopsis* protein phosphatase of type 2C (PP2C) identified *in silico* by phosphatase catalytic domain of the protein (Schweighofer et al., 2004). It is encoded by a nuclear gene At1g07160 and comprises 380 amino acids with molecular weight of ~40.7 kDa (www.arabidopsis.org). AP2C2 protein structure contains predicted chloroplast transit peptide (cTP) of 67 amino acids and a MAP kinase interaction motif (KIM) in the N-terminus, and 11 catalytic subdomains with metal binding site (Mn^{2+} or Mg^{2+}) in the C-terminus (Bork et al., 1996; Das et al., 1996). AP2C2 is grouped in cluster B of *Arabidopsis* PP2C according to the amino acid sequence homology to MP2C, the alfalfa PP2C (*Medicago sativa*). A close homolog of AP2C2 is AP2C1 (At2g30020) (Schweighofer et al., 2004).

Several evidences suggested that AP2C2 might be involved in stress response signalling in *Arabidopsis*. First, MP2C and its close homolog AP2C1 play an important role as the regulators of signal transduction in response to environmental stresses. MP2C was identified as a negative regulator of stress-induced MAP kinase pathways in yeast and plants (Meskiene et al., 1998; Meskiene et al., 2003). AP2C1 was reported as a negative regulator of stress-induced MAP kinase cascade by interacting with and inactivating *Arabidopsis* MPK4 and MPK6. AP2C1 modulates innate immunity, and stress hormones such as jasmonic acid and ethylene levels in *Arabidopsis* (Schweighofer et al., 2007). Second, AP2C2 was shown to be highly upregulated in catalase-deficient plants CAT2HP1 exposed to high light stress (Vanderauwera et al., 2005). Microarray data reported that AP2C2 transcript is induced by several biotic and abiotic stresses (AtGenExpress).

Thus AP2C2 is interesting as the possible component of stress response signalling cascade, however, its function was not characterized. Possibly, it may regulate stress response in any specific way and/or it may function redundantly with the close homolog, AP2C1. To characterise and analyse function of AP2C2, the combination of genetics, molecular biology, biochemical and cell biology strategies both *in silico*, *in vitro* and *in vivo* were applied. The results obtained from this work provide indications what might be the role of AP2C2 and useful suggestions for further experiments.

1.1. The aims of this work

The main objective of this work was **to characterise the function of a putative *Arabidopsis* protein phosphatase of type 2C, named AP2C2**. Towards this aim the following questions were asked:

- What are the interacting proteins of AP2C2?
- Where are the AP2C2 and its interacting complexes localized in cell?
- What are the inducers of AP2C2 expression?
- What are the signalling pathways that regulated by AP2C2?
- What physiological or hormonal responses are controlled by AP2C2?

1.2. Protein phosphatases in *Arabidopsis*

Reversible protein phosphorylation modulates many cellular functions including hormone and other environmental stimuli, metabolic control, and developmental processes. As a paradigm, protein kinases and phosphatases add or remove phosphate groups on regulatory enzymes and proteins, thereby influencing their activity, localisation or stability. Based on phospho-amino-acid substrate specificity, protein phosphatases can be grouped into Ser/Thr, Tyr, and dual-specificity phosphatase classes (Wang et al., 2007).

1.2.1. Protein Ser/Thr Phosphatases

Based on sequence and structural similarity, the type one (PP1), type 2A (PP2A), and type 2B (PP2B) protein phosphatases are related enzymes and, hence, are defined as the PPP family. The type 2C protein phosphatases (PP2C) and other Mg^{2+} -dependent Ser/Thr phosphatases share no sequence homology with PPP and, thus, are defined as the PPM family (Barford and Neel, 1998). Despite their lack of sequence similarity, members of the PPP and PPM families share a similar structural fold (Das et al., 1996), suggesting a common mechanism of catalysis. PP1 proteins and PP2 proteins groups are divided based upon differential sensitivity to small molecule inhibitors. PP2 proteins are further distinguished by metal ion requirements: PP2Cs require Mg^{2+} or Mn^{2+} and PP2Bs require Ca^{2+} , whereas PP2As have no ion requirement. The crystal structure of human PP2C reveals a novel protein fold with a catalytic domain composed of a central beta-sandwich that binds two manganese ions, which is surrounded by alpha-helices. Mn^{2+} -bound water molecules at the binuclear metal centre coordinate the phosphate group of the substrate and

provide a nucleophile and general acid which is essential in the dephosphorylation reaction (Das et al., 1996).

Seventy-six *Arabidopsis* PP2C genes candidates are divided into 10 groups (Schweighofer et al., 2004). Group A contains most of the identified genes that are associated with abscisic acid (ABA) signal transduction, such as *ABI1* and *ABI2*. Group B is characterised by homology to an alfalfa PP2C that regulates MAPK signalling, MP2C, such as AP2C1 and a putative phosphatase AP2C2 (Figure 1.1.). A common feature of all PP2C is the presence of 11 characteristic subdomains in the catalytic part of the protein. The catalytic domain of most (44 out of 76) *Arabidopsis* PP2Cs is located at the C-terminus, with different N-terminal extensions. A protein domain search identifies several motifs. Many of which are related to intracellular signalling, such as a transmembrane spanning region and a MAP kinase interaction motif (KIM). In alfalfa MP2C and most of the B-group phosphatases, the PP2C catalytic domain is fused to the N-terminal extension containing KIM.

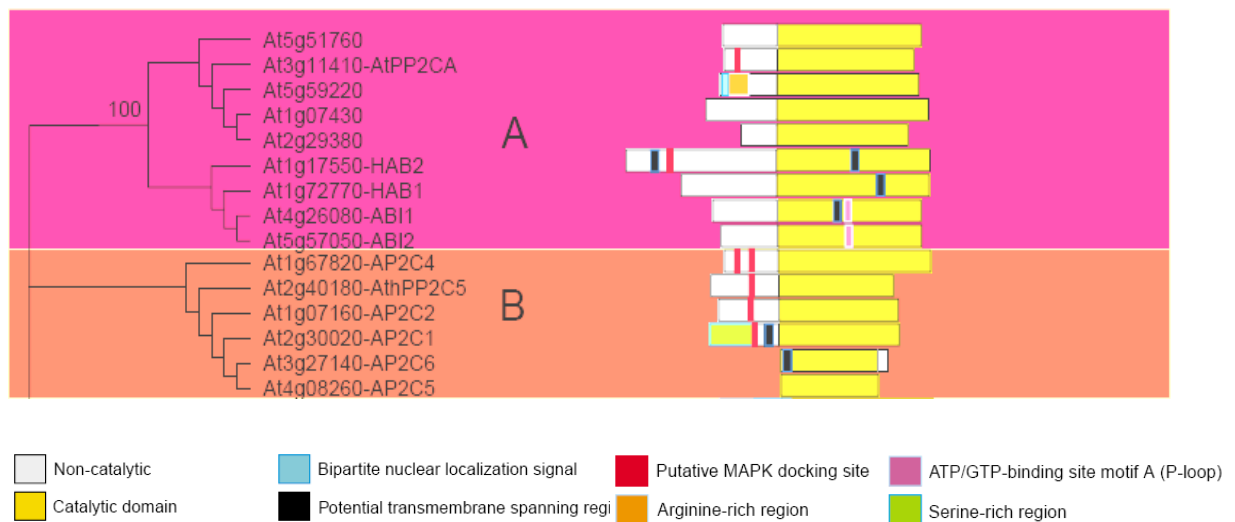


Figure 1.1. Topographic cladogram and domain structures of *Arabidopsis* PP2C group A and B. Modified from (Schweighofer et al., 2004).

PP2Cs function as negative regulators of stress-induced MAPK signalling. The activity of MAPKs is known to be strictly regulated via phosphorylation of the conserved TXY motif. A given MAPK is phosphorylated and activated by a corresponding MAPK kinase to transduce signal downstream. Once transiently activated, MAPKs cannot be reactivated within at least 30 min of the refractory term (Bogre et al., 1997), implying the presence of a possible system to inactivate MAPK. Alfalfa MP2C has been shown to be responsible for the dephosphorylation of activated MAPKs. Upon stress, such as wounding, MP2C is

strongly induced in leaves in a manner that correlates with the timing of SIMK inactivation. MP2C directly interacts and inactivates SIMK through threonine dephosphorylation of the pTEpY motif (Meskiene et al., 1998; Meskiene et al., 2003). *Arabidopsis* AP2C1 is involved in regulating stress hormone levels, defense responses, and the stress-responsive MAPKs MPK4 and MPK6. Mutant *ap2c1* plants produce significantly higher amounts of jasmonate upon wounding and as a consequence are more resistant to phytophagous mites (*Tetranychus urticae*). Plants with increased AP2C1 levels display lower wound activation of MAPKs, reduced ethylene production, and compromised innate immunity against the necrotrophic pathogen *Botrytis cinerea* (Schweighofer et al., 2007).

1.2.2. Protein Tyrosine phosphatases

Protein tyrosine phosphatases (PTPs) can be classified into tyrosine-specific PTPs that act on phosphotyrosine and dual-specificity protein tyrosine phosphatases (DSPs), which can dephosphorylate both phosphotyrosine and phosphoserine/phosphothreonine.

Of the 112 phosphatase candidates, there is only 1 PTP and 18 DSPs in the *Arabidopsis* genome (Kerk et al., 2002). The function of PTPs in plants is related to stress response (Xu et al., 1998). AtPTP1 expression is strongly induced under high-salt stress conditions. The *Arabidopsis* genome encodes five potential dual-specificity MAPK phosphatases (MKPs), including: DsPTP1, AtMKP1, AtMKP2, PHS1, and IBR5. AtDsPTP1 was demonstrated to be able to dephosphorylate and inactivate AtMPK4 (Gupta et al., 1998).

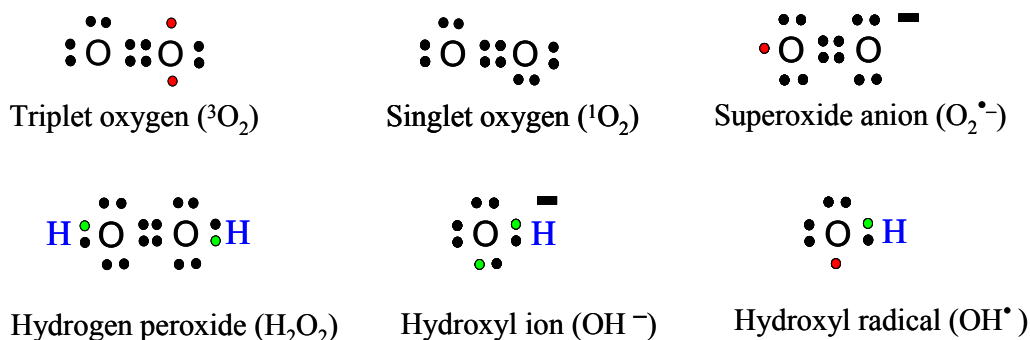
MKP1 regulates plant response to salinity and genotoxic stresses through the regulation of MAPK activities. *mkp1* is hypersensitive to genotoxic stress, UVC and methyl methanesulphonate, (Ulm et al., 2001) and is tolerant to salt (Ulm et al., 2002). A yeast two-hybrid assays demonstrated that MKP1 interacts with MPK3, MPK4, and MPK6, which are key signalling components in a diverse set of stress and environmental signalling responses.

MKP2 participates in the regulation of cellular homeostasis in ozone-challenged tissue. Suppression of AtMKP2 creates a marked ozone sensitivity phenotype in *Arabidopsis* plants, and this hypersensitivity is accompanied by prolonged activation of both MPK3 and MPK6. MKP2 dephosphorylates the conserved -pTEpY- motif of MPK3 and MPK6 *in vitro* (Lee and Ellis, 2007).

1.3. Reactive oxygen species (ROS)

Reactive oxygen species are molecules or ions formed by the incomplete one-electron reduction of oxygen. These reactive oxygen intermediates include singlet oxygen; superoxides; peroxides; hydroxyl radical; and hypochlorous acid.

A radical (sometimes called a "free radical") is a molecule that has an unpaired electron (represented by a dot next to the chemical structure, e.g. A^\bullet) in its outermost shell of electrons. Most radicals are highly reactive and thus unstable. A radical needs to pair its unpaired electron with another, and will react with another molecule in order to obtain this missing electron. If a radical achieves this by "stealing" an electron from another molecule, that molecule itself becomes a radical, and a self-propagating chain reaction is begun.



Triplet oxygen ($^3\text{O}_2$) : Oxygen in the air we breathe is in its "ground" (not energetically excited) state. It is a free radical-in fact, it is a diradical, as it has two unpaired electrons. Ground-state oxygen is in the triplet state. Its two unpaired electrons have parallel spins that do not allow them to react with most molecules. Thus, ground-state or triplet oxygen is not very reactive. However, triplet oxygen can be activated by the addition of energy, and transformed into *reactive oxygen species*.

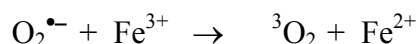
Singlet oxygen ($^1\text{O}_2$) : If triplet oxygen absorbs sufficient energy to reverse the spin of one of its unpaired electrons, it forms the singlet state. Singlet oxygen has a pair of electrons with opposite spins ($\uparrow\downarrow$); though not a free radical it is highly reactive. Singlet oxygen is produced as a result of natural biological reactions and photosensitization by the absorption of light energy. Singlet oxygen must transfer its excess energy to another molecule in order to relax to the triplet state.

Superoxide radical ($\text{O}_2^{\bullet-}$) : Triplet oxygen can also be transformed into a reactive state if it accepts a single electron. The result of monovalent reduction of triplet oxygen is a radical called superoxide. Superoxide can act both as an oxidant (by accepting electrons) or

as a reductant (by donating electrons). However, superoxide is not particularly reactive. It is a precursor to other oxidizing agents, including hydrogen peroxide, and other highly reactive molecules. In fact, superoxide is necessary as a signalling molecule to regulate cellular processes. Superoxide is a charged molecule and cannot cross biological membranes. Subcellular compartment of defence mechanisms is, therefore, crucial for the removal of superoxide anions at their sites of generation throughout the cell.

Hydrogen peroxide (H₂O₂) : Under biological conditions, the main reaction of superoxide is to react with itself to produce hydrogen peroxide and oxygen, a reaction known as "dismutation". Superoxide dismutation can be spontaneous or can be catalysed by the enzyme superoxide dismutase (SOD). H₂O₂ is important in biological systems because it can pass readily through cell membranes and cannot be excluded from cells. H₂O₂ is actually necessary for the function of many enzymes, and thus is required for a signalling function in defence responses (Kotchoni and Gachomo, 2006).

Hydroxyl radical (OH•) : The highly reactive hydroxyl radical is produced from superoxide. In this process, superoxide actually acts as a reducing agent, not as an oxidizing agent. This is because superoxide donates one electron to reduce ferric ion (Fe³⁺).



The reduced ferrous ion (Fe²⁺) then catalyzes the breaking of the oxygen-oxygen bond of hydrogen peroxide to produce a hydroxyl radical and hydroxide ion. This reaction is called the Fenton reaction.



Like hydrogen peroxide, the hydroxyl radical passes easily through membranes and cannot be kept out of cells. Hydroxyl radical damage is "diffusion rate-limited" by how far and fast it can diffuse in the cell. This highly reactive radical can add to an organic substrate in a chain reaction. This type of chain reaction is common in the oxidative damage of fatty acids and other lipids. Similar damage can occur in proteins and with nucleic acids (mainly DNA). Proteins are highly susceptible to oxidative damage, particularly at sites where sulphur containing amino acids are found. DNA can be oxidative damaged at both the nucleic bases and at the sugars. Oxidative damage of DNA results in degradation of the bases, breaking of the DNA strands by oxidation of the sugar linkages, or cross-linking of DNA to protein. Although all cells have some capability of repairing oxidative damage to proteins and DNA, excess damage can cause mutations or cell death. However, OH• can

promote on cell growth. Apoplastically generated OH^\bullet can cause cell wall loosening leading to elongation growth of maize coleoptiles or hypocotyls of soybean (Schopfer, 2001).

1.4. Roles of ROS in plants

Although the chemical nature and reactivity of ROS prove them to be potentially harmful to cells, it is now well accepted that ROS accumulation is crucial to plant development as well as in defence responses (Foyer and Noctor, 2005). Plants use them as secondary messengers in signal transduction cascades regulating diverse processes such as mitosis, tropisms, cell death and defence mechanisms (Pavet et al., 2005). Under normal conditions, ROS are rapidly metabolised with help of antioxidant enzymes and other non-enzymatic antioxidant molecules such as vitamins, proteins and non-protein thiols. However, when subjected to environmental stresses such as cold, high light, ozone, drought, salt stress, UV irradiation, and pathogen challenge (Langebartels et al., 2002; Torres et al., 2006), excessive ROS is generated (Figure 1.2.). ROS are known to play dual roles depending on their accumulation levels. High intracellular levels of ROS in plants exposed to biotic and abiotic stresses causes plants to oxidative stress. ROS rapidly oxidize and damage lipids in cellular membranes, proteins and other cellular components, leading consequently to cellular dysfunction and ultimately to cell death, or appearance of necrotic lesions (Foyer and Noctor, 2005). However, this excessive accumulation of ROS necessitates the activation of additional defences. Moderate accumulations of ROS function as key inducers for secondary programmed metabolisms, defence signal, cell wall differentiation and activation of mitogen-activated protein kinases (MAPKs) leading to the environmental stress tolerance (Mittler, 2006). Localized generation of H_2O_2 is one of the earliest cytologically detectable defence responses to penetration of plant cell walls by various fungal pathogens (Mellersh et al., 2002). H_2O_2 generation was the only response detected to account for fungal penetration failure. Enzymatic removal of H_2O_2 resulted in increased penetration success of fungi in the host plant cells.

1.5. Sources of ROS production in plants

There are several known sources of ROS production in plants. The major sources are organelles with a highly oxidizing metabolic activity such as chloroplasts and mitochondria (Dat et al., 2000). Other sources are photorespiration in the peroxisomes, and potential enzymatic sources including plasma membrane NADPH-dependent oxidases and cell wall peroxidases (Langebartels et al., 2002).

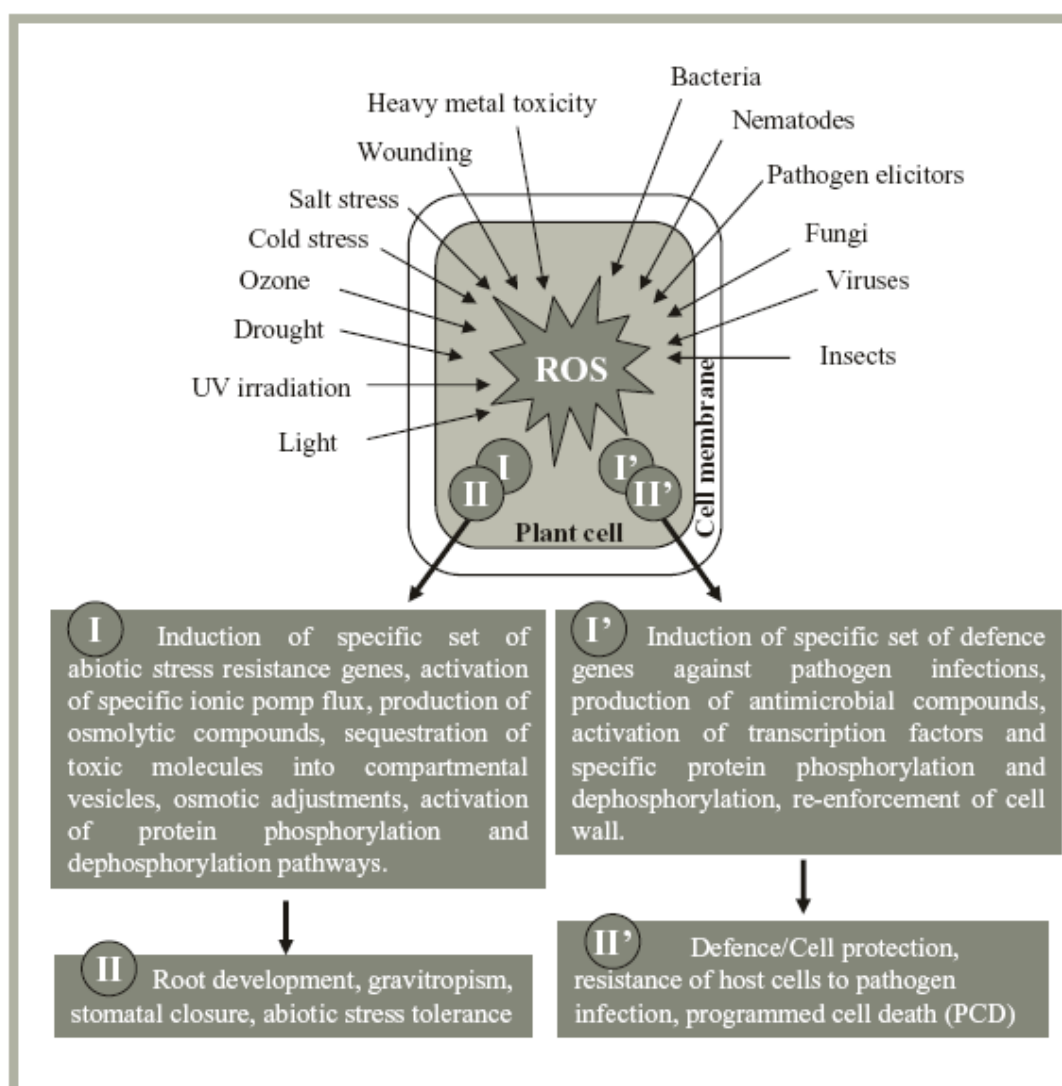


Figure 1.2. Involvement of ROS in cellular metabolic processes of plants response to both various environmental stresses. I and II indicate the subsequent downstream events mediated by ROS in plant cells exposed to abiotic stresses, while I' and II' indicate the subsequent downstream events mediated by ROS in plant cells exposed to pathogens and pathogen-elicitors (Kotchoni and Gachomo, 2006).

1.5.1. Photosynthesis

Chloroplasts are considered to be the most powerful source of ROS in plants. The primary sources of ROS production are the Mehler reaction and the antenna pigments. Some electron passing down the electron transport chain leak away from the main path (especially as they pass through ubiquinone) and go directly to reduce oxygen molecules to the superoxide anion. Moreover, photosynthesis is a combination of successive redox reactions during light energy absorption by the light-harvesting complexes, transferred to the reaction centres of the photosystems and then electrons are passed on to a final electron acceptor, generally CO₂. However, because plants have limited rates of CO₂ fixation, alternative acceptors are used, including oxygen. Conditions limiting CO₂ fixation will inevitably lead to an enhancement of ROS accumulation, as more O₂ molecules will be used as electron acceptors. The environmental conditions limit CO₂ fixation, such as drought (Dat et al., 2000), salt and temperature stress (Suzuki and Mittler, 2006) as well as the combination of these conditions with high-light stress. The photosynthetic electron transport chain components at the acceptor side of photosystem I (PSI) include Fe-S centres, reduced thioredoxin, and ferredoxin. These electron transport components are auto-oxidizable and under conditions limiting the availability of NADP⁺, O₂^{•-} can be formed. Superoxide can then initiate a chain reaction leading to the production of more toxic radicals.

1.5.2. Respiration

Although ROS production in plant mitochondria has received little attention in the past, recent evidence suggests that mitochondria are an important source of ROS under specific conditions. The mitochondria electron transport chain is made of several dehydrogenase complexes that reduce a common pool of ubiquinone. The ubiquinone pool is then oxidized by either the cytochrome or the alternative pathway. In general, the main O₂^{•-} generators in mitochondria are the ubiquinone radical and NADH dehydrogenases. O₂^{•-} is formed by the auto-oxidation of the reduced components of the respiratory chain.

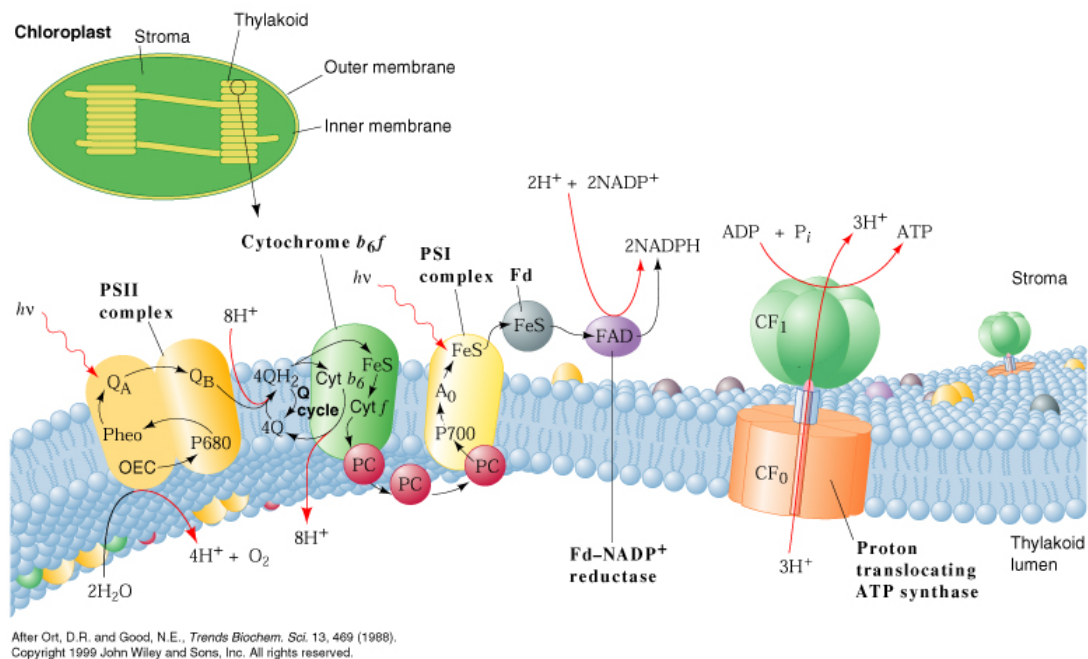


Figure 1.3. Linear electron transport in the thylakoid membrane. The electrons in photosynthesis pass from PSII via Cytochrome b_6f and PSI to NADP and carbohydrates. PSII replenishes its lost electrons by splitting water. The PSII antenna delivers the light energy to the reaction centre chlorophyll P680. Upon excitation, it can donate an electron to the primary acceptor, pheophytin (Pheo). The redox potential energy drives the electron further down the electron-transport chain; Q_A , Q_B , PQ, Cyt b_6f , PC, and PSI. Upon arrival at the PSI donor-side, the electron has lost its redox potential energy and another light quantum is needed for the PSI reaction centre to push the electron further to the rest of the electron carriers. Finally, the electron is transferred to $NADP^+$ and used in the dark phase of photosynthesis to reduce CO_2 . The energy freed during this electron transport is used to transfer a proton from the stroma into the lumen. Thus, the proton gradient is generated. The protons accumulated in the lumen of the thylakoid membrane pass through the ATP-synthase and generate ATP (Ort and Good, 1988).

1.5.3. Photorespiration

There is another route by which H_2O_2 can be produced during photosynthesis. Photorespiration is the alternate pathway for production of glyceraldehyde 3-phosphate (G3P) by RuBisCO, the main enzyme of the light-independent reactions of photosynthesis (known as the Calvin cycle). This usually occurs when oxygen levels are high; for example, when the stomata are closed to prevent water loss on dry days. It involves three cellular organelles: chloroplasts, peroxisomes, and mitochondria. Although RuBisCO prefers carbon dioxide to oxygen, oxygenation by RuBisCO occurs frequently. Oxygenation yields two glycolates that are then transported from the chloroplasts to the peroxisomes. There, glycolate oxidation is catalysed by glycolate oxidase yielding H_2O_2 and glyoxalate. Serine is produced in mitochondria and reenters the peroxisomes. Finally, glycerate reenters back to the chloroplast and subsequently the Calvin cycle.

Photorespiration is a wasteful process because G3P is created at a reduced rate and higher metabolic cost (2ATP and 1 NAD(P)H) compared with RuBP carboxylase activity. G3P produced in the chloroplast is used to create "nearly all" of the food and structures in the plant. While photorespiratory carbon cycling results eventually in G3P, it also produces waste ammonia that must be detoxified at a substantial cost to the cell in ATP and reducing equivalents. However, it may function as a "safety valve", preventing excess energy to damage reaction centers of photosystem.

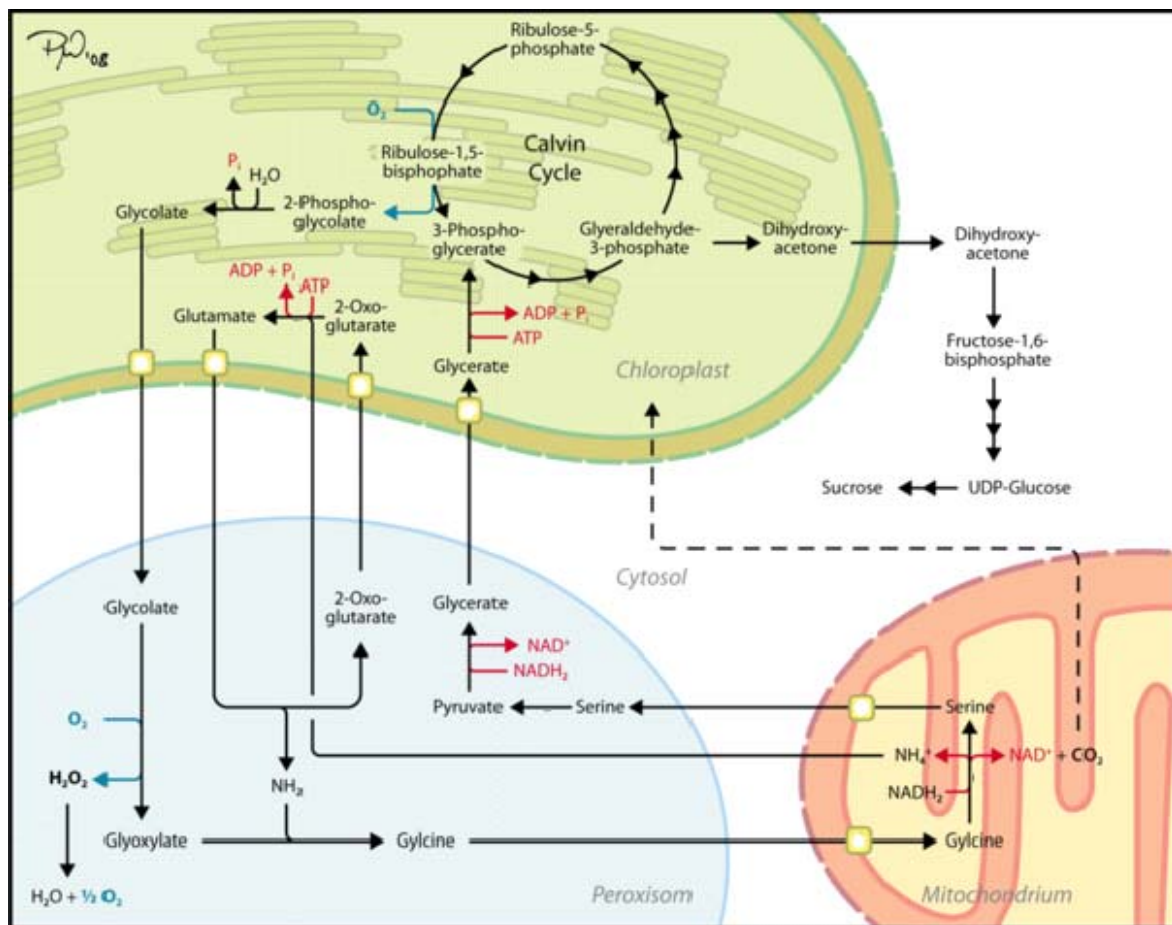


Figure 1.4. Diagram of the reactions of photorespiration, involving chloroplast, peroxisome and mitochondrion. The process begins with the oxidative reaction of rubisco in the chloroplast stroma, producing glycolate, which enters peroxisomes by a special porin protein channel in their membrane. Its conversion to glyoxylate releases hydrogen peroxide (broken down by catalase). Transamination to glycine, subsequent conversions in mitochondria, and return to peroxisomes and thence to chloroplasts allows some of the original carbon to conserve by its re-entry into the photosynthetic carbon reduction cycle. Modified from http://en.wikipedia.org/wiki/Image:Photorespiration_eng.png

1.5.4. NADPH-oxidase

The NADPH oxidase, also known as the respiratory burst oxidase (RBO), is the enzymatic subunit of this oxidase and transfers electrons to molecular oxygen to generate superoxide. *Arabidopsis* (*Arabidopsis thaliana*) has 10 *Atrboh* (*Arabidopsis* RBO homolog) genes. The members of the *Rboh* family mediate the production of apoplastic ROS during the defence responses, as well as in response to abiotic environmental and developmental cues (Torres and Dangl, 2005). Cellular fractionation of plant tissue indicates that RBOH proteins are located in the plasma membrane. The precise submembrane distribution of RBOH is likely critical for its function, as noted in the asymmetric distribution of RBOH activity in *AtrbohC*-dependent ROS signalling in root hair growth (Foreman et al., 2003; Carol et al., 2005).

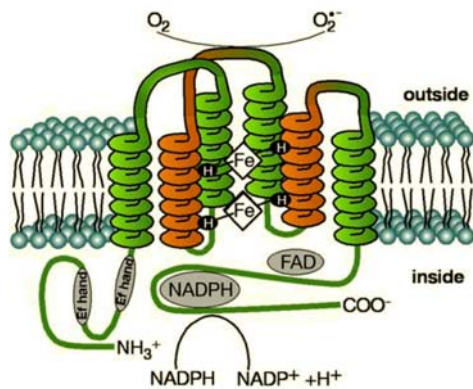


Figure 1.5. Schematic diagram of Rboh structure. It was predicted to be located in the membrane, showing the irreversible transfer of charge from cellular NADPH to extracellular oxygen. Shown are the N-terminal region EF hands juxtaposed to the C-terminal end to indicate an interaction by which calcium-dependent activity is regulated (Sagi and Fluhr, 2006).

1.5.5. Cell wall peroxidase

Peroxidases form a complex family of proteins that catalyze the oxidoreduction of various substrates using H_2O_2 . In particular, pH-dependent peroxidases in the cell wall can catalyse the production of OH^\bullet by the Haber-Weiss reaction. The cell-wall polysaccharides can be depolymerised by peroxidases acting in the OH^\bullet -generating mode *in vitro* (Schweikert et al., 2000).

1.6. Defence mechanisms against ROS

Cells have a variety of defences against the harmful effects of ROS. These include three mechanisms.

Enzymatic ROS scavenging mechanisms

Major ROS-scavenging enzymes of plants include: superoxide dismutase (SOD), ascorbate peroxidase (APX), catalase (CAT), glutathione peroxidase (GPX) and peroxiredoxin (PrxR). SODs act as the first line of defence against ROS, by dismutating two superoxide anions to a molecule of hydrogen peroxide and one of oxygen. APX, GPX and CAT subsequently detoxify H_2O_2 . Unlike most other organisms, plants have multiple genes encoding SOD and APX isoforms that are specifically targeted to chloroplasts, mitochondria and peroxisomes and are differentially regulated in a tissue-dependent manner during oxidative stress responses (Mittler et al., 2004).

Non-enzymatic ROS scavenging mechanisms

Nonenzymatic antioxidants include ascorbate and glutathione (GSH), and tocopherol, flavonoids, alkaloids, carotenoids and anthocyanins (Foyer and Noctor, 2005). Ascorbate and GSH are major cellular redox buffers (Pitzschke et al., 2006). The cellular pools of the antioxidants ascorbic acid and glutathione are maintained in their reduced state.

ROS themselves

ROS themselves play a role in intracellular redox sensing, activating antioxidant resistance mechanisms. A number of redox sensitive transcription factors have been identified in plant cells (Chen et al., 2002).

ROS can be produced in different compartments of the cells. The rigorous defence mechanisms of ROS at the site of ROS production are necessary. Although the mechanisms in the different compartments are separated from each other, H_2O_2 can easily diffuse through membranes and antioxidants such as glutathione and ascorbic acid (reduced or oxidized) can be transported between the different compartments. Mainly, the enzymatic pathways respond to ROS detoxification as shown in Figure 1.6. The water–water cycle detoxifies O_2^- and H_2O_2 , and alternative oxidase (AOX) reduces the production rate of O_2^- in thylakoids. ROS that escape this cycle and/or are produced in the stroma undergo detoxification by SOD and the stromal ascorbate–glutathione cycle. Peroxiredoxin (PrxR) and glutathione peroxidase (GPX) are also involved in H_2O_2 removal in the stroma. ROS produced in peroxisomes during photorespiration, fatty acid oxidation

or other reactions are decomposed by SOD, catalase (CAT) and ascorbate peroxidase (APX). SOD and other components of the ascorbate–glutathione cycle are also present in mitochondria. In addition, AOX prevents oxidative damage in mitochondria. In principle, the cytosol contains the same set of enzymes found in the stroma. The enzymatic components responsible for ROS detoxification in the apoplast and cell wall are only partially known, and the ROS-scavenging pathways at the vacuole are unknown.

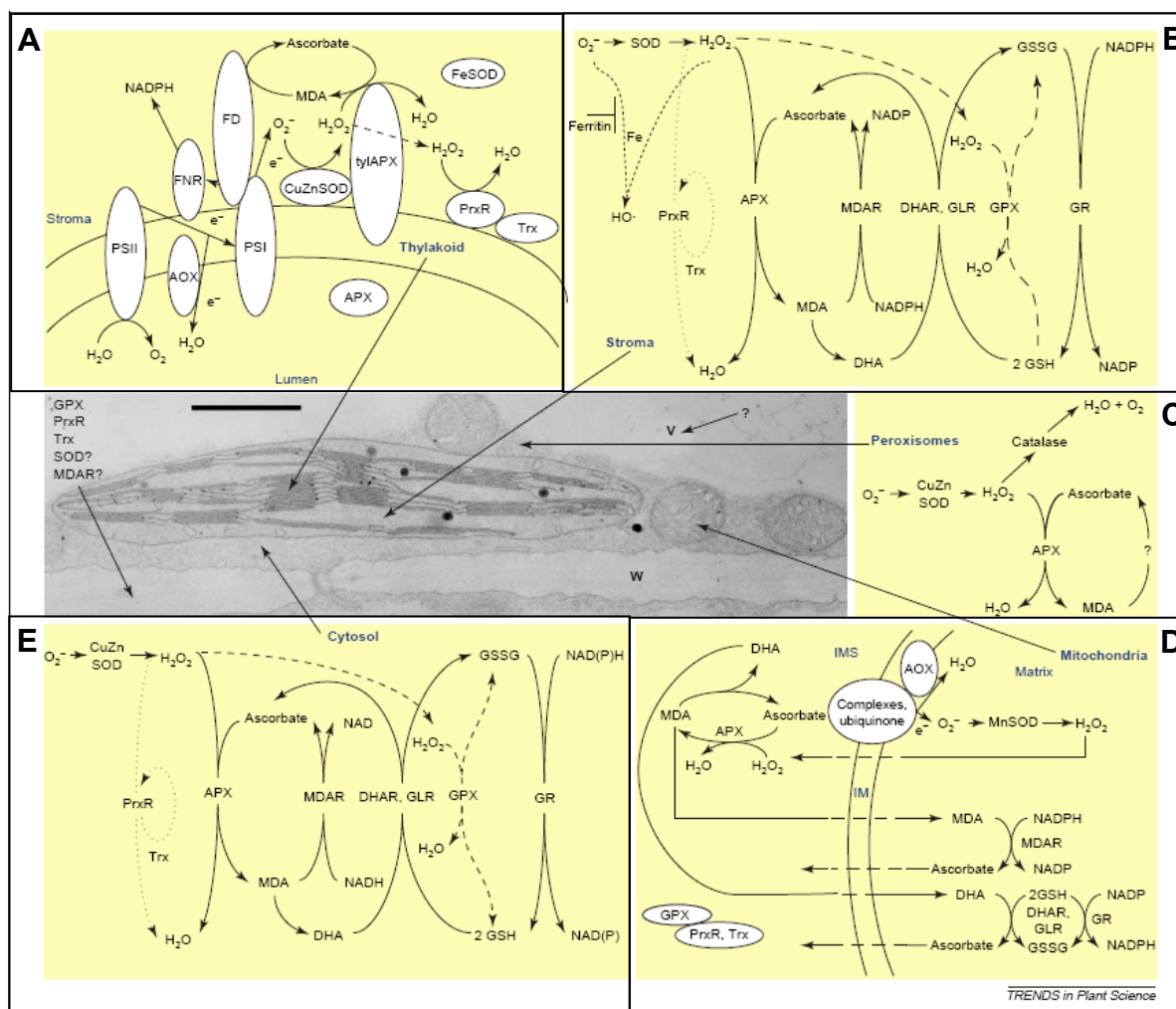


Figure 1.6. Localization of reactive oxygen species (ROS) scavenging pathways in plant cells. The enzymatic pathways responsible for ROS detoxification are shown. **A - in the chloroplast lumen;** the water–water cycle and alternative oxidase (AOX). **B - in the chloroplast stroma,** SOD, ascorbate–glutathione cycle, peroxiredoxin (PrxR) and glutathione peroxidase (GPX). **C - in peroxisomes,** SOD, catalase (CAT) and ascorbate peroxidase (APX). **D - in mitochondria;** SOD, AOX and other components of the ascorbate–glutathione cycle. **E - in the cytosol** contains the same set of enzymes found in the stroma. GPX pathways are indicated by dashed lines and PrxR pathways are indicated by dotted lines in the stroma and cytosol. Abbreviations: DHA, dehydroascorbate; DHAR, DHA reductase; FD, ferredoxin; FNR, ferredoxin NADPH reductase; GLR, glutaredoxin; GR, glutathione reductase; GSH, reduced glutathione; GSSG, oxidized glutathione; IM, inner membrane; IMS, IM space; MDA, monodehydroascorbate; MDAR, MDA reductase; Trx, thioredoxin; tyl, thylakoid (Mittler et al., 2004).

1.7. ROS production and signal transduction under stress factors

Increasing evidence indicates that H_2O_2 functions as a signalling molecule in plants. H_2O_2 generation during the oxidative burst is one of the earliest cellular responses to potential pathogens and elicitor molecules. Although the receptors for ROS are unknown at present, it has been suggested that plant cells sense ROS via unidentified receptor proteins or redox-sensitive transcription factors (Mittler et al., 2004). H_2O_2 also activates mitogen-activated protein kinases (MAPKs) and protein phosphatase type 2C (PP2C) (Vanderauwera et al., 2005). The expression of defense-related genes such as *GST* and different transcription factors, including members of WRKY, Zat, RAV, GRAS and Myb families, is enhanced by ROS (Figure 1.7.).

1.7.1. ROS and Mitogen-activated protein kinase (MAPK) cascade

In plants, the signal transduction is controlled by protein phosphorylation and dephosphorylation involving MAPKs, conserved signalling kinases that modulate gene expression, and transduce cellular responses to extracellular stimuli (Liu and Zhang, 2004). Induction of MAPK activity has been detected after exposure of plants to various stresses (Teige et al., 2004; Doczi et al., 2007). It was recently discovered that ROS mediate the activation of MAPK cascade and subsequent responses of plants to external stimuli. The MAPK-signalling pathways involve three distinct components of the protein kinase family including, MAPK, MAPK kinase (MAPKK) and MAPKK kinase (MAPKKK). During signal transduction, the MAPKKKs are phosphorylated and could then be able to activate particular MAPKKs, which become phosphorylated and thereafter activate specific MAPKs. Activated MAPKs (phosphorylated MAPKs) are often imported into the nucleus, where they phosphorylate and activate specific downstream signalling components such as transcription factors (Figure 1.8.).

Serine/Threonine protein kinase OXI1 has been shown to play a central role in ROS sensing and the activation of mitogen-activated-protein kinases (MPK3 and MPK6) by Ca^{2+} (Rentel et al., 2004). A MAPK cascade involving MPK3/6 acts downstream of OXI1 and controls the activation of different mechanisms in response to ROS stress.

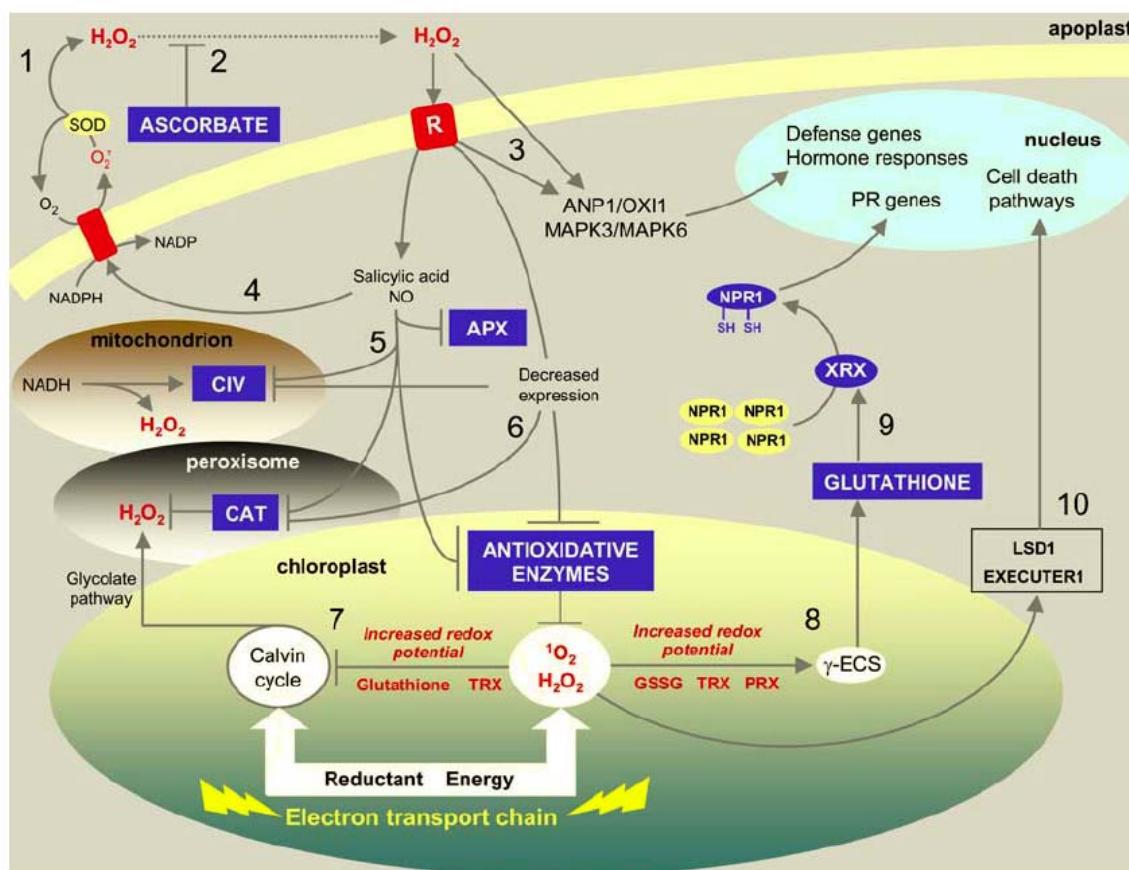


Figure 1.7. Oxidant and antioxidant signalling in plant stresses and orchestrated responses.

The hypothetical scheme draws together some of the redox-modulated elements recently identified in plants and others likely to be influential. Components that promote an oxidative signal are shown in red, and those that oppose such signals or transmit a reductive signal are shown in dark blue. Plasma membrane NADPH oxidases are activated by elicitor or hormone-mediated signalling and produce H_2O_2 (1). Production of H_2O_2 can oxidize putative membrane receptors, and this function is opposed by apoplastic ascorbate (2). ROS production activates signalling through specific MAP kinases (3), and some of these components are also important in ROS-mediated hormone and growth responses. A key factor in specification of pathogenesis and cell death responses is secondary production of ROS, either by positive feedback enhancement of the primary oxidative signal (4) or by withdrawal and inactivation of antioxidative capacity. Downregulation of the antioxidative system could occur by posttranslational modulation of heme functions by salicylic acid and nitric oxide (5) and/or programmed withdrawal of antioxidative enzyme expression (6). Oxidative inhibition of chloroplast metabolism by glutathionylation and/or inactivation of thioredoxin-modulated enzymes may also be crucial in increasing chloroplastic flux to oxygen to enhance ROS production (7). Greater availability of ROS activates glutathione synthesis (8), and the resulting increase in cytosolic glutathione is somehow linked to induction or activation of a thioredoxin or glutaredoxin that is able to reduce NPR1 (9). NPR1 reduction is associated with its accumulation in the nucleus and its interaction with TGA transcription factors to induce *PR* gene expression. Enhanced chloroplastic levels of ROS such as singlet oxygen may also activate the pathways that (10) set in train the cell death program. APX, ascorbate peroxidase; CAT, catalase; CIV, cytochrome oxidase; SOD, superoxide dismutase (Foyer and Noctor, 2005).

The ANP (*Arabidopsis* homologous of NPK1, Nicotina protein kinase) class of MAPK kinase-kinases (MAPKKKs) from *Arabidopsis* is induced specifically by H_2O_2 (Tena et al., 2001), which subsequently induces the activation of other set of specific classes of MAPKs under environmental stresses (Kovtun et al., 2000). Increased accumulation of ROS in transgenic plants activates several MAPKs, which regulate the state of cellular redox and enhances tolerance to multiple stresses. At present, putative functions in *Arabidopsis* are assigned to only MPKs 3/4/6, and all three are linked to diverse stress responses (Ichimura et al., 2000; Kovtun et al., 2000; Asai et al., 2002). MPK4 is involved in the integration of SA- and JA-dependent signals to evoke the appropriate responses against pathogens and other stresses by acting as a negative regulator of salicylic acid (SA) and systemic acquired resistance and a positive regulator of jasmonate (JA)-activated gene expression (Petersen et al., 2000). MAPK cascade is inactivated by phosphatases. Protein phosphatases including ser/thr phosphatases and dual-specificity MAPK phosphatases (MKP) dephosphorylate MAPKs in a specific manner.

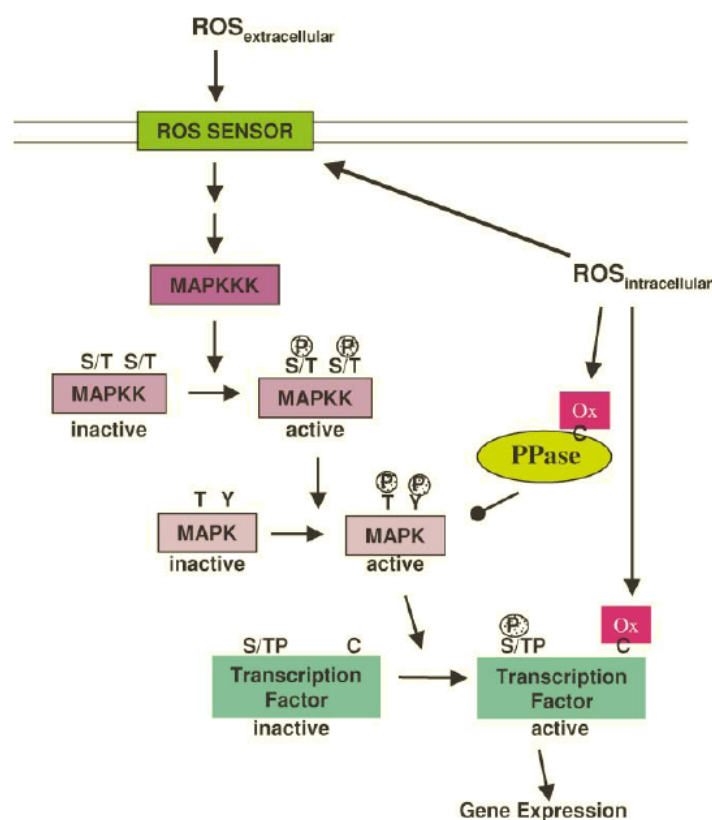


Figure 1.8. Schematic depiction of cellular ROS sensing and signalling mechanisms. ROS sensors such as membrane-localized histidine kinases can sense extracellular and intracellular ROS. Intracellular ROS can also influence the ROS-induced mitogen-activated protein kinase (MAPK) signalling pathway, protein phosphatases (PPases) or downstream transcription factors. ROS regulation occurs by oxidation of cysteine residues. Modified from (Apel and Hirt, 2004).

1.7.2. ROS production and signal transduction under pathogen challenges.

The resistance of plants to pathogen infections involves an elaborate system of signal perception and transduction to activate cellular defence. After perception of pathogen attack, plants activate basal defences following perception of PAMPs (Pathogen-associated molecular patterns). The host cell synthesizes various molecules including ROS, protein-kinases and transcription factors, relaying the pathogen-perception signal to activate downstream defence responses (Figure 1.9.) (Kotchoni and Gachomo, 2006). The production of ROS is one of the earliest cellular responses which influence plant defence responses, including cell death. Apoplastic generation of $O_2^{\bullet-}$, or its dismutation product H_2O_2 , has been documented following recognition of a variety of pathogens.

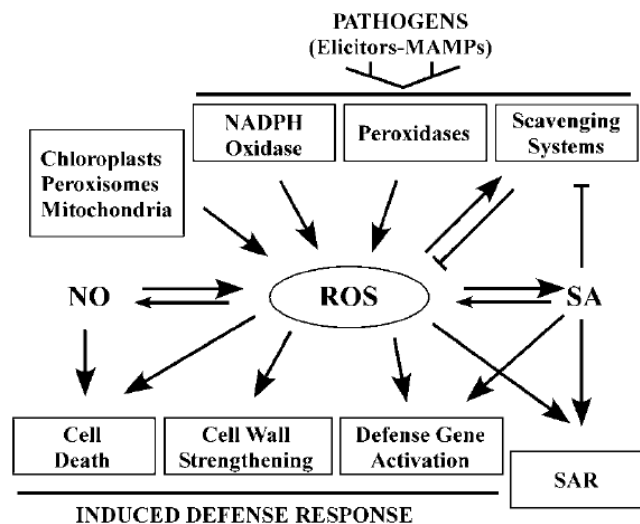


Figure 1.9. ROS production and functions in response to pathogens (Torres et al., 2006).

Upon pathogen infection, the avirulence signal (avr) carried by pathogens is recognized by a specific plant resistance (R) gene product. This avr/R interaction is called gene-for-gene resistance and often triggers a strong defense mechanism that includes the programmed cell death of plant cells at the site of infection (known as the hypersensitive response), resulting in efficient containment of the pathogen. The recognition elicits a biphasic ROS accumulation with a low-amplitude, transient first phase, followed by a sustained phase of much higher magnitude that correlates with disease resistance. However, virulent pathogens that avoid host recognition induce only the transient, low-amplitude first phase of this response, suggesting a role for ROS in the establishment of the defences.

Rapid production of ROS could also inhibit pathogen growth by restricting pathogen penetration via cross-linking of host cell wall glycoproteins, by induction of phytoalexin accumulation. Accumulation of ROS inhibits mitochondrial electron transport leads to ATP depletion. Both ROS accumulation and ATP depletion lead rapidly to Ca^{2+} influx, which triggers programmed cell death (PCD) in plants (Figure 1.10.A.). Moderate concentration of ROS activates the cellular defence response by induction of defence-related genes, leading to systemic acquired resistance (SAR) (Kotchoni and Gachomo, 2006). SAR provides systemic immunity to secondary infection by a range of pathogens that have diverse modes of infection. SAR requires both local and systemic salicylic acid (SA) accumulation and the induction of a subset of the pathogenesis-related (PR) genes. A slight alteration of intracellular ROS triggers the expression of a specific set of genes generally encoding for antioxidant proteins, compatible molecules, oxidative scavengers, and protein phosphorylation cascade via activated MAPK proteins.

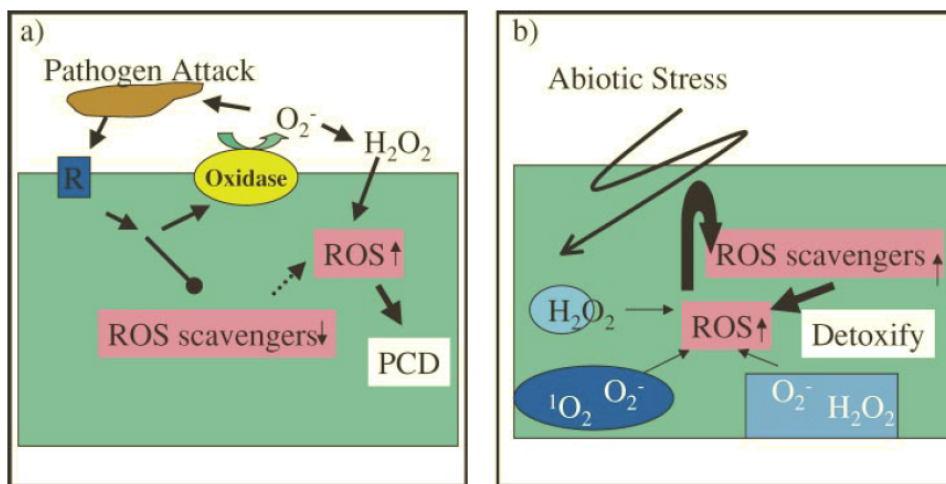


Figure 1.10. Different roles of ROS under conditions of (a) pathogen attack or (b) abiotic stress. Upon pathogen attack apoplast-localized oxidases produce ($\text{O}_2^{\bullet -}$) that are highly toxic and can kill the invading pathogen. On the other hand, $\text{O}_2^{\bullet -}$ is rapidly dismutated into H_2O_2 which can readily cross the plasma membrane. Intracellular ROS levels increase due not only to extracellular production of ROS but also by downregulation of ROS scavenging mechanisms. ROS amounts increase to critical levels and induce PCD. During abiotic stress, ROS production occurs mainly in chloroplasts and mitochondria at the sites of electron transport, increasing intracellular ROS amounts to toxic levels. The cellular response encompasses upregulation of ROS scavenging mechanisms to detoxify increased amounts of ROS (Apel and Hirt, 2004).

In *Arabidopsis*, bacterial flagellin activates a MAPK cascade composed of MEKK1-MKK4/MKK5-MPK3/MPK6 via flagellin receptor FLS2 (Asai et al., 2002) leading to expression of basal defence-related genes. MEKK1 has been shown to be required for

flg22-induced activation of MPK4 (Rodriguez et al., 2007) (Figure 1.11.). The MPK4 substrate MKS1 interacts, in a JA-independent manner, with two WRKY transcription factors, WRKY 25 and WRKY 33. PAD4/EDS1 (phytoalexin deficient4/ enhanced disease susceptible1) mutations are proposed to act as central mediators of SA/JA signalling to a kinase cascade (Brodersen et al., 2006).

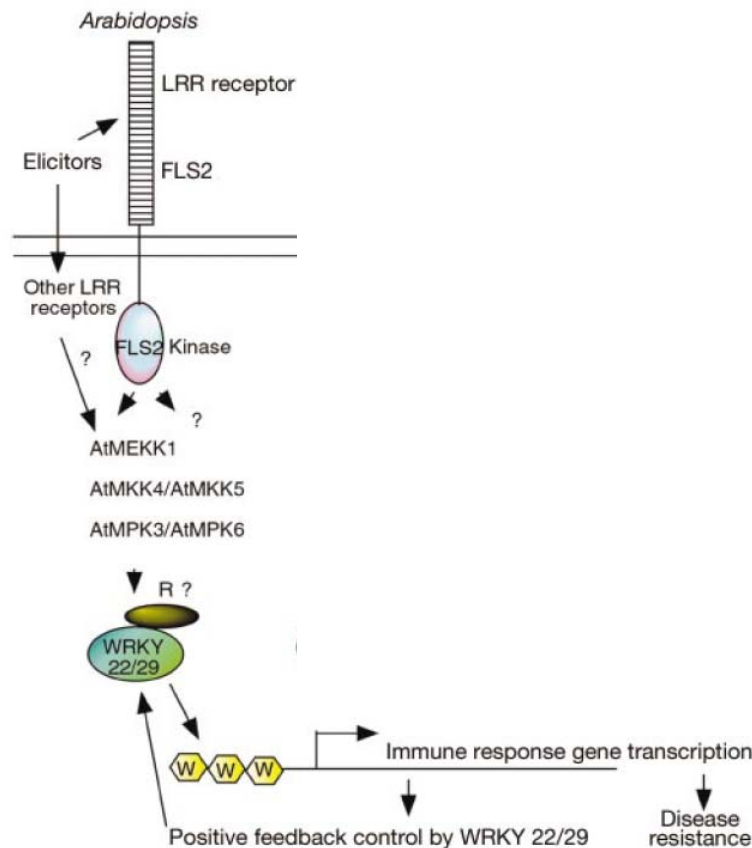


Figure 1.11. Model of flg22 signalling in *Arabidopsis*. Flg22 activates plant innate immunity through MAPK cascade (MEKK2, MKK4/MKK5 and MPK3/MPK6) and WRKY22/WRKY29 transcription factors that function downstream of the flagellin receptor FLS2, a leucine-rich-repeat (LRR) receptor kinase. Modified from (Asai et al., 2002).

1.7.3. ROS production and signal transduction under wounding stress

The oxidative burst is highly regulated by wounding. A number of genes for the enzymes involved in hydrogen peroxide production and processing are activated by wounding. H_2O_2 can act as a local signal, as a diffusible signal in adjacent cells and as a second messenger for the induction of defence genes.

Two major groups of the wounded-responsive genes identified were genes for signalling/regulatory components and those for effectors (Cheong et al., 2002). The

signalling/regulatory components include RLKs, non-receptor protein kinases, protein phosphatases, calcium-binding proteins, G-proteins, PI pathway enzymes, and transcription factors. The effectors include defence-related proteins and enzymes in the secondary metabolism involved in activation of the defence response. RLK proteins perceive external stimuli and transduce the signals through phosphorylation cascade that leads to the expression of appropriate target genes. Wounding induces expression of a large number of genes encoding transcription factors; AP2, WRKY, and MYB families that regulate the transcription of a number of flavonoid genes (Figure 1.12.).

Among the late response genes regulated by wounding are a number of genes involved in secondary metabolism and cell wall modifications. Their respective gene products were defined as effectors involved in late defence responses. Most striking is the activation of the phenylpropanoid pathway that produces many secondary metabolites, which act as anti-pathogen and anti-insect agents. Some of them are important intermediates for lignin biosynthesis during cell wall thickening. Enzymes involved in the Trp and alkaloid biosynthetic pathways are also activated at the transcriptional level. The *Arabidopsis* Trp pathway can lead to the biosynthesis of the phytoalexin camalexin and other secondary compounds.

1.7.4. ROS production and signal transduction under high light (HL)

Exposure of plants to high light intensities that exceed the capacity of CO₂ fixation, leads to the inhibition of photosynthesis. To protect the photosynthesis apparatus against photo-inhibition, 2 essential elements are needed; first, the thermal dissipation of excess excitation energy in the PSII antennae (non-photochemical quenching), and second, the ability of PSII to transfer electrons to acceptors within the chloroplast (photochemical quenching) (Ort and Baker, 2002). Recent studies indicate that the proportion of absorbed photons that are thermally dissipated through the non-photochemical pathway reaches a maximum before saturating irradiances are reached. Thus, photochemical quenching is crucial for photo-protection under high light intensities. When plants are exposed to environmental stresses and the availability of CO₂ within the leaf is restricted, the reduction of oxygen by both the photorespiratory and the Mehler ascorbate peroxidase pathways appears to play a critical photo-protective role.

Under such conditions, molecular oxygen (O₂) can be used as an alternative electron acceptor to CO₂ in two ways (Bechtold et al., 2008). First, O₂ can be photo-reduced by PSI

to produce superoxide anion radicals ($O_2^{\bullet-}$), which are rapidly converted to H_2O_2 by SOD. Secondly, photorespiration can also take up photosynthetic reducing equivalents and indirectly produce H_2O_2 . Such processes serve to dissipate excitation energy in excess of that required for photosynthetic metabolism. Failure to quench excess excitation energy leads to over-reduction of components of the electron transport system. Under such conditions, chlorophyll triplet states form in PSII and react with oxygen to form singlet oxygen (1O_2), leading to PSII reaction centre damage (Figure 1.13.).

Since plants are unable to avoid oxidative damage caused by light, they employ broad protective mechanisms, including minimization of light absorption, avoidance of ROS overaccumulation, and repair of damaged proteins, lipids, and photosystems.

ROS generated in the chloroplast during high light (HL) stress have been implicated as triggers of signalling pathways that influence expression of nuclear-encoded genes which may initiate acclimation processes or trigger cell death responses, depending on the degree of photo-oxidative stress suffered. Examples of the transcriptional response include the induction of heat shock proteins (HSPs), the cytosolic isoforms of APX, APX1 and APX2 and transcription factors (Vanderauwera et al., 2005).

AP2C2 (At1g07160), a putative *Arabidopsis* protein phosphatase type 2C, was found to be upregulated 52.4 fold in a catalase-deficient plant (CAT2HP1) compared with a control plant exposed to high light, (Vanderauwera et al., 2005). The CAT2HP1 plant was reported retaining 20% of total residual catalase activity levels and accumulating higher H_2O_2 upon high light irradiation than the control plant (Vandenabeele et al., 2004). It might be that H_2O_2 production in this condition induces protein phosphatase expression.

The members of *Arabidopsis* ZAT (zinc finger transcription factor) gene family, ZAT10 or ZAT12, have been shown to respond to drought, salt, cold and high light. Partial HL exposure of a leaf or leaves rapidly induced ZAT10 mRNA in distal, shaded photosynthetic tissues, including the floral stem, cauline leaves, and rosette, but not in roots (Rossel et al., 2007). ZAT10 overexpression resulted in enhanced tolerance to photo-inhibitory light and exogenous H_2O_2 , increased expression of antioxidative genes. Constitutive expression of ZAT12 in *Arabidopsis* results in the enhanced expression of light stress-response transcript (Davletova et al., 2005).

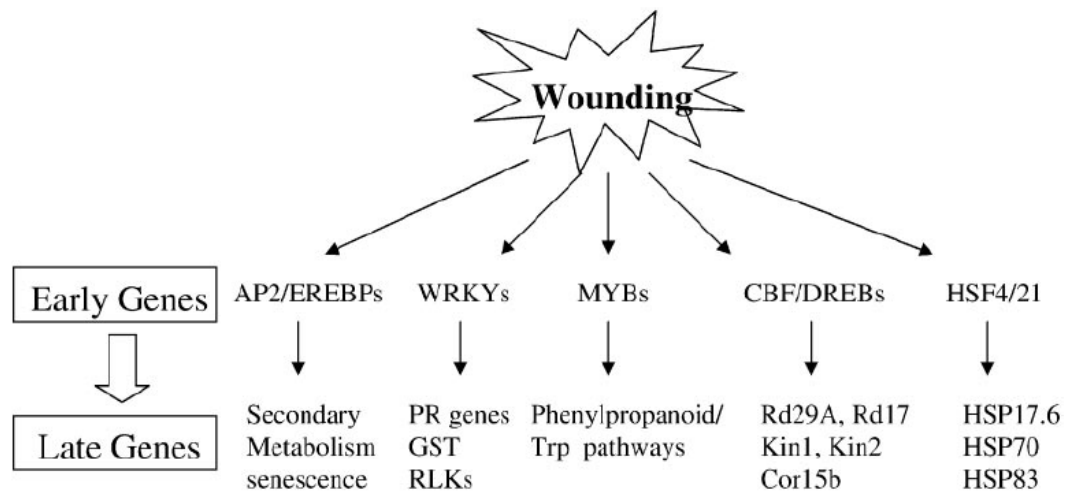


Figure 1.12. A hypothetical model for early wound-responsive transcription factors to activate late responsive genes in wounding signal transduction pathways (Cheong et al., 2002).

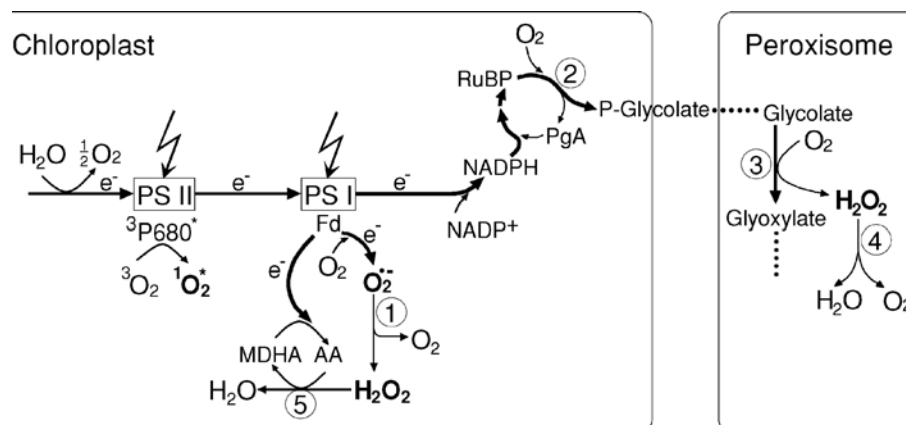


Figure 1.13. The principal features of photosynthetic electron transport under high light stress that lead to the production of ROS in chloroplasts and peroxisomes. Two electron sinks can be used to alleviate the negative consequences of over-reduction of the photosynthetic electron chain: (a) the reduction of oxygen by PSI that generates superoxide and H_2O_2 , and (b) the Rubisco oxygenase reaction and the photorespiratory pathway that lead to H_2O_2 generation within the peroxisome. Under light stress, increasing amounts of singlet oxygen are produced within PSII. Bold arrows show the main routes of electron transport. Key enzymes are shown in numbers: 1) superoxide dismutase, 2) Rubisco, 3) glycolate oxidase, 4) catalase, and 5) ascorbate peroxidase (Apel and Hirt, 2004).

1.7.5. ROS production and signal transduction under salt stress

Salt stress elevates intracellular Ca^{2+} level, which activates the SOS signalling pathway. The SOS pathway includes three key components: SOS1, a plasma membrane Na^+/H^+ antiporter (Shi et al., 2000). SOS2, a serine/threonine protein kinase (Liu et al., 2000); and SOS3, a Ca^{2+} sensor (Liu and Zhu, 1998).

High Na^+ stress leads to an increase of cytosolic free Ca^{2+} concentration. SOS3, Ca^{2+} binding protein binds to this Ca^{2+} and activates the protein kinase SOS2, a serine/threonine protein kinase. Activated SOS3-SOS2 kinase complex is necessary for increased expression of SOS1, a plasma membrane Na^+/H^+ antiporter. The activation of SOS1 would cause rapid apoplastic alkalization and cytosolic acidification. This pH change may then activate the plasma membrane-bound NADPH oxidase (Chung et al., 2008). All plant NADPH oxidases carry a presumably cytosolic 300-amino-acid amino-terminal extension with two EF-hands that bind Ca^{2+} . Activation of the plasma membrane-bound NADPH oxidase promotes the production of apoplastic $\text{O}_2^{\cdot-}$. In the presence of transition metals such as Fe^{2+} , the extremely reactive hydroxyl radical can be generated from H_2O_2 (Figure 1.14.).

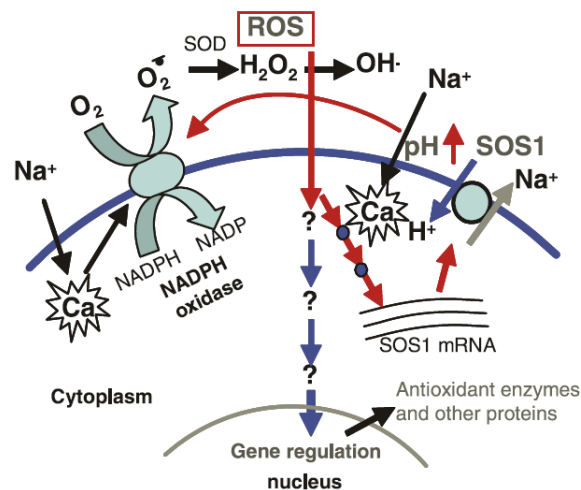


Figure 1.14. A proposed signalling pathway controlling SOS1 mRNA stability and SOS1-conferred paraquat sensitivity. Hypothetical model showing the early signalling events and downstream signal transduction regulating the stability of SOS1 mRNA. Under Na^+ stress, operation of SOS1 would cause extracellular pH elevation, which could be required for activation and/or maintenance of the plasma membrane-bound NADPH oxidase activity that produces extracellular ROS. Extracellular ROS could serve as signalling molecules to trigger gene regulation (Chung et al., 2008).

SOS2 and possibly other Ca^{2+} -activated protein kinases initiate a protein phosphorylation cascade channelled downstream through mitogen-activated protein (MAP) kinases. *In vitro* and *in vivo* evidence suggests that MKK2 mediates stress signalling by a MEKK1-MKK2-MPK4/MPK6 (Teige et al., 2004) (Figure 1.15.). MKK2 modulates salt tolerance through expression of a set of genes including genes for CDPK1, protein phosphatase AP2C1, transcription factor, AtbZIP17, STZ/ZAT10, water channels (PIP1a/2a), and Pro transporters (Liu et al., 2007). This gene expression and transporter activity regulation

brings about homeostasis of ions such as Na^+ and K^+ and consequently plant tolerance to Na^+ stress (Zhu, 2000).

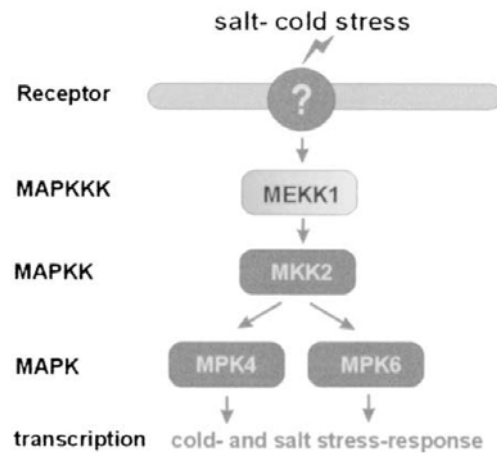


Figure 1.15. Model proposed for the salt stress-triggered MKK2 pathway involving MEKK1 as an upstream activator and the downstream MAPKs MPK4 and MPK6 (Teige et al., 2004)

1.7.6. ROS production and signal transduction under heat stress

Photochemical reactions in thylakoid lamellae and carbon metabolism in the stroma of chloroplast have been suggested as the primary sites for injury at high temperatures. PSII is highly thermolabile, and its activity is greatly reduced under high temperatures. Heat stress may lead to the dissociation of the oxygen evolving complex (OEC), resulting in an imbalance between the electron flow from OEC toward the acceptor side of PSII in the direction of PSI reaction centre (Figure 1.16.). Heat stress causes dissociation of a Mn-stabilising protein at PSII reaction centre complex followed by the release of Mn atoms.

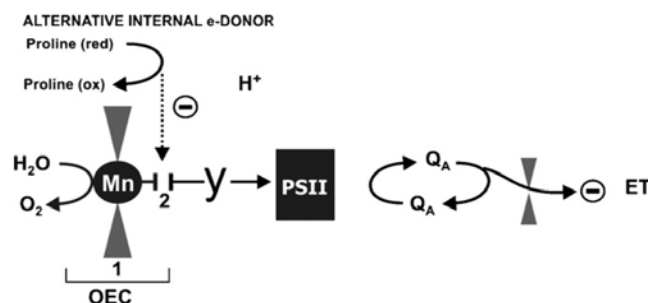


Figure 1.16. Heat induced inhibition of oxygen evolution and PSII activity. Heat stress leads to either (1) dissociation or (2) inhibition of the oxygen evolving complexes (OEC). This enables an alternative internal e--donor such as proline instead of H_2O to donate electrons to PSII (Wahid et al., 2007).

HSPs facilitate growth and survival of plants under conditions of severe heat stress. The expression of heat shock genes is regulated by HSFs (Figure 1.17.).

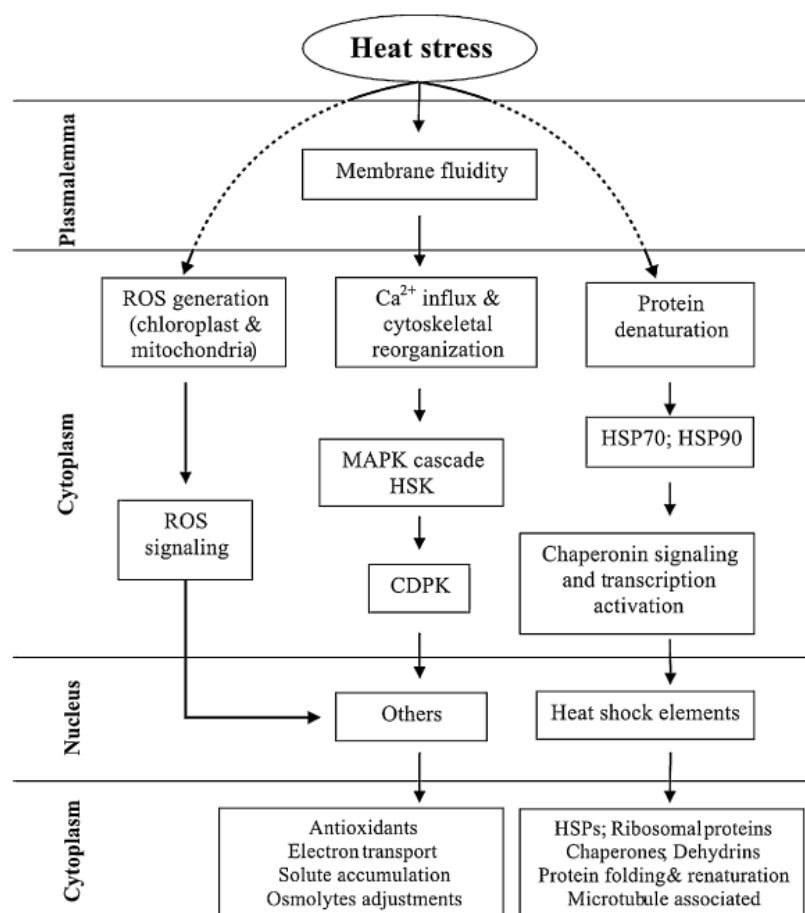


Figure 1.17. Proposed mechanisms of heat-stress tolerance in plants. HAMK, heat shock activated MAPK; HSE, heat shock element; HSPs, heat shock proteins; CDPK, calcium dependent protein kinase; HSK, histidine kinase (Wahid et al., 2007).

1.7.7. ROS production and signal transduction under Paraquat

Paraquat (Bipyridinium herbicides) has a redox potential of -446 mV, which is critical to its function as a free-radical generator. There are two possible models for paraquat action. One is by generating highly reactive, oxygen-centered free radicals within chloroplasts when treated plants are exposed to sunlight (Table 1.1.). The divalent paraquat cation, PQ^{2+} , accepts an electron from PSI in chloroplasts to produce the monocationic paraquat radical, $PQ^{\bullet+}$, which in turn is rapidly oxidized by molecular oxygen to regenerate PQ^{2+} with concomitant reduction of oxygen to superoxide, $O_2^{\bullet-}$ (Table 1.1.A.). The paraquat molecule is then ready for another cycle of reduction and oxidation. $O_2^{\bullet-}$ and H_2O_2 that

escape detoxification by SOD, catalase (in peroxisomes) (Table 1.1.B.), and peroxidases may then participate in two pathological pathways leading to the generation of highly toxic OH^\bullet radicals. One is the superoxide-driven Fenton reaction (Table 1.1.C.), involving trace amounts of iron. Another is a Fenton-like reaction (Table 1.1.D.), in which the reduced paraquat radical, $\text{PQ}^{+\bullet}$, reacts with hydrogen peroxide either directly or in the presence of very small, catalytic concentrations of iron.

Table 1.1. Mode of Paraquat-induced free readical generation (Babbs et al., 1989)

A. Paraquat-induced oxidative stress	
	PSI
	$\text{paraquat}^{2+} \rightarrow \text{paraquat}^{+\bullet}$,
	$\text{O}_2 + \text{paraquat}^{+\bullet} \rightarrow \text{O}_2^{\bullet-} + \text{paraquat}^{2+}$
B. Normal detoxification of superoxide	
	$2 \text{H}^+ + 2 \text{O}_2^{\bullet-} \rightarrow \text{H}_2\text{O}_2 + \text{O}_2$ (SOD reaction)
	$2 \text{H}_2\text{O}_2 \rightarrow 2 \text{H}_2\text{O} + \text{O}_2$ (catalase reaction)
C. Superoxide-driven Fenton reaction	
	$\text{O}_2^{\bullet-} + \text{Fe}^{3+} \rightarrow \text{O}_2 + \text{Fe}^{2+}$
	$2 \text{O}_2^{\bullet-} + 2 \text{H}^+ \rightarrow \text{H}_2\text{O}_2 + \text{O}_2$
	$\text{H}^+ + \text{Fe}^{2+} + \text{H}_2\text{O}_2 \rightarrow \text{HO}^\bullet + \text{Fe}^{3+} + \text{H}_2\text{O}$
D. Winterbourn's reaction	
	$\text{paraquat}^{+\bullet} + \text{H}_2\text{O}_2 \rightarrow \text{paraquat}^{2+} + \text{OH}^- + \text{HO}^\bullet$ (original version)
	$\text{paraquat}^{+\bullet} + \text{Fe}^{3+} \rightarrow \text{paraquat}^{2+} + \text{Fe}^{2+}$ (trace Fe catalyzed)
	$\text{H}^+ + \text{Fe}^{2+} + \text{H}_2\text{O}_2 \rightarrow \text{HO}^\bullet + \text{Fe}^{3+} + \text{H}_2\text{O}$

Another possible mode of action for paraquat is based on the observation that *sos1* mutation confers tolerance to paraquat (Chung et al., 2008). In this paradigm, formation of free radicals promoted by PQ would require the activity of the plasma membrane NADPH oxidase. NADPH oxidase causes the divalent cation paraquat²⁺ (PQ^{2+}) to form a free radical $\text{PQ}^{+\bullet}$ (Figure 1.18.). Since this molecule is unstable, it is rapidly reoxidized in the presence of oxygen to yield the original divalent cation. During this oxidation process, electrons are transferred to molecular oxygen to form $\text{O}_2^{\bullet-}$. Superoxide radicals are then enzymatically converted to H_2O_2 , which could subsequently produce toxic hydroxyl radicals. The PQ^{2+} ion would then be available again for another cycle. Thus this herbicide would function as a catalyst for transferring electrons to oxygen. In fact, the NADPH oxidase has been identified as an enzymatic source of electrons that trigger PQ redox cycling and extracellular ROS production in mammalian cells. According to this model, SOS1 plays a pivotal role in control of NADPH oxidase activity and apoplastic ROS production. When SOS1 is functional, the activity of NADPH oxidase would be maintained, which enhances PQ redox cycling and extracellular ROS production. Since

apoplastic ROS could either be signalling molecules at a low concentration or cause cell damage by oxidative stress at high concentration, a large amount of ROS produced through PQ redox cycling would be extremely toxic to plant cells (Figure 1.18.).

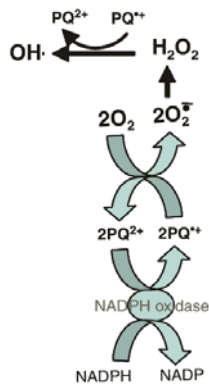


Figure 1.18. Redox cycling of paraquat (PQ) coupling with the plasma membrane NADPH oxidases. The plasma membrane-bound NADPH oxidase could be an enzymatic source of electrons for the formation of free radical paraquat ($PQ^{\bullet +}$) from normal divalent cation paraquat (PQ^{2+}). Rapid reoxidation of $PQ^{\bullet +}$ causes production of ROS through transfer of electrons to molecular oxygen. The PQ redox cycling, which causes enormous extracellular ROS production deleterious to plant cells, could be dependent on SOS1 activity that would be required for activation and/or maintenance of the NADPH oxidase activity. See the Discussion in the text for a detailed explanation (Chung et al., 2008).

1.7.8. ROS production and signal transduction under combination of different stresses.

Recent studies have revealed that the molecular and metabolic response of plants to a combination of two different abiotic stresses is unique and cannot be directly evaluated from the response of plants to each of the different stresses (Mittler et al., 2004). The simultaneous exposure of a plant to different abiotic stress conditions results in the co-activation of different stress-response pathways. These might have either a synergistic or antagonistic effect on each other. For examples, heat stress was found to silence the UVB response of parsley (Walter, 1989), whereas ozone induces pathogen responses in *Arabidopsis* (Bowler and Fluhr, 2000). Different members of gene families involved in the protective mechanism against pathogen attacks were up-regulated in plants under several abiotic stresses (Rizhsky et al., 2004). The wounding of *Arabidopsis* leaves causes powerful but transient protection against *Botrytis* infection (Chassot et al., 2008). Wounding alone did not lead to camalexin production but its accumulation after inoculation with *B.cinerea*.

1.8. Hormone biosynthesis and signalling pathways

1.8.1. Salicylic acid synthesis and signalling

Salicylic acid (SA) mediates plant defenses against pathogens, accumulating in both infected and distal leaves in response to pathogen attack. Pathogenesis-related gene expression and the synthesis of defensive compounds associated with both local and systemic acquired resistance (LAR and SAR) in plants require SA. In *Arabidopsis*, exogenous application of SA sufficiency to establish SAR, resulted in enhanced resistance to a variety of pathogens.

1.8.1.1. Salicylic acid biosynthesis

Although SA can be synthesised from phenylalanine, the main pathway for *de novo* SA biosynthesis during pathogen infection is via an isochorismate pathway. The enzymes isochorismate synthase (ICS) and isochorismate pyruvate lyase (IPL) catalyze the two steps from chorismate to SA. An alternative pathway synthesizes SA from phenylalanine via benzoic acid. Phenylalanine ammonia lyase (PAL) catalyzes the first step in this pathway, which is the conversion of phenylalanine to trans-cinnamic acid. Trans-cinnamic acid is subsequently converted into benzoic acid. A benzoic-acid-2-hydroxylase (BA2H) catalyzes the final step, the conversion of benzoic acid to SA (Wildermuth et al., 2001) (Figure 1.19.).

1.8.1.2. Salicylic acid signalling

Activation of *R*-gene-mediated signalling activates SA synthesis. *EDS1* is required for the development of a HR and for the activation of defence signalling mediated by *R* genes. In addition, *EDS1* and *PAD4* are required for basal resistance and for increased SA accumulation in response to the challenge by various pathogens. *EDS5* (a predicted transporter protein) most likely acts upstream of *SID2* (a putative chloroplast-localized ICS) in regulating SA biosynthesis. SA can activate an expression of the pathogenesis-related (*PR*) gene and resistance via two mechanisms, NPR1 dependent and independent manners. The first requires the *NPR1* gene. Interaction of NPR1 with TGA2 activates the expression of the *PR-1* gene, presumably by countering the inhibitory effect of SUPPRESSOR OF *npr1-1* INDUCIBLE1 (SNI1). An SFD1-generated lipid signal is required for the activation of the NPR1 pathway by SA. Ethylene and JA signalling

potentiate signalling through this NPR1-independent pathway. *CPR5* is shown to repress lesions independently of *EDS1* and *PAD4*. The wild type *SSI2* gene represses plant defence by affecting the generation of a lipid molecule that is required for the activation of SA synthesis and the NPR1-independent pathway. *SSI2* also represses lesion development. The *SSI2* gene encodes a desaturase, which primarily catalyzes the desaturation of stearic acid to oleic acid. *SFD1* encodes a glycerol-3-phosphate (G3P) dehydrogenase that synthesizes G3P for glycerolipid biosynthesis. The wild type *NPR1* allele represses SA accumulation through a feedback mechanism. Pathogen-activated expression of *SID2* was higher in the *npr1* mutant, and so this negative feedback regulation is exerted before *SID2* action. In addition, a positive feedback mechanism involving SA enhances the expression of several *R* genes, and of *EDS1*, *PAD4*, *EDS5* and *SID2* (Figure 1.20.).

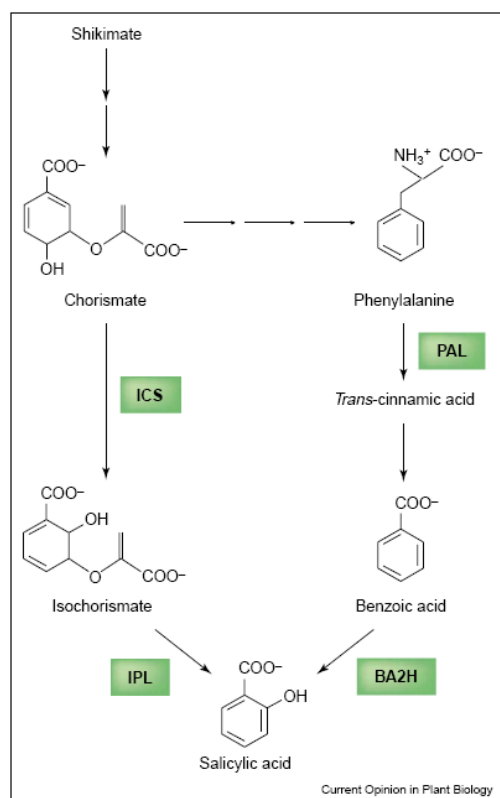


Figure 1.19. Proposed pathways for the biosynthesis of SA in plants. The shikimate pathway provides chorismate, which can be converted into SA. The main chorismate pool occurs in the chloroplast. The *Arabidopsis* *SID2* gene encodes a predicted ICS that has a putative plastid-transit sequence. The *SID2*-encoded ICS is proposed to catalyze the conversion of chorismate to isochorismate, presumably in the chloroplast. By analogy to the mechanism of SA biosynthesis in bacteria, it is suggested that an IPL catalyzes the conversion of isochorismate to SA. An alternative pathway that has been studied in tobacco synthesizes SA from phenylalanine via benzoic acid. Phenylalanine ammonia lyase (PAL) catalyzes the first step in this pathway, which is the conversion of phenylalanine to *trans*-cinnamic acid. *Trans*-cinnamic acid is subsequently converted into benzoic acid. A benzoic-acid-2-hydroxylase (BA2H) catalyzes the final step, the conversion of benzoic acid to SA (Shah, 2003).

1.8.2. Ethylene synthesis and signalling

Ethylene plays a role in plant growth and development and is involved in a number of processes, including seed germination, root hair development, senescence, abscission, and fruit ripening. Ethylene also participates in a variety of defence responses and abiotic stress responses.

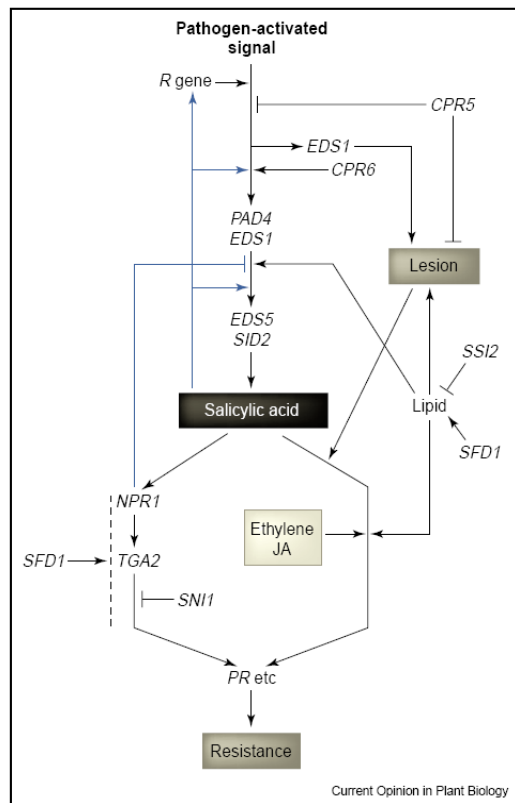


Figure 1.20. Model for the SA signalling in *Arabidopsis thaliana*. Arrows indicate positive effects whereas lines ending with a bar indicate inhibitory effects. Blue lines indicate feedback regulation (Shah, 2003).

1.8.2.1. Ethylene biosynthesis

The production of ethylene is tightly regulated by internal signals during development and in response to environmental stimuli such as pathogen attack or wounding. *S*-AdoMet is the precursor for ethylene biosynthesis. The first step of ethylene biosynthesis is the conversion of *S*-AdoMet to ACC by ACC synthase (ACS). In addition to ACC, ACS also produces 5'-methylthioadenosine (MTA) in this reaction, which is then converted to methionine. The recycling of MTA back to methionine conserves the methylthio group and is able to maintain a constant concentration of cellular methionine even when ethylene is rapidly synthesized. Malonylation of ACC to MACC deprives the ACC pool and reduces the ethylene production. Finally, ACC is oxidized by ACC oxidase to form ethylene, CO₂, and cyanide, which is detoxified to β-CAS to prevent toxicity by accumulated cyanide during high rates of ethylene synthesis (Figure 1.21.).

The rate-limiting step of ethylene synthesis is the conversion of *S*-AdoMet to ACC by ACC synthase (ACS). Ethylene biosynthesis is tightly controlled because the active ACS is labile and present at low levels. Both positive and negative feedback regulation of ethylene biosynthesis have been reported in different plant species. In *Arabidopsis*, ACS are substrates of MPK6. Phosphorylation of ACS2 and ACS6 by MPK6 leads to the

accumulation of ACS protein and, thus, elevated levels of cellular ACS activity and ethylene production (Liu and Zhang, 2004) (Figure 1.22.).

The regulation of ET synthesis by MAPK can be influenced by phosphatases that control MAPK activity. In tobacco, overexpression of the dual-specific MAPK phosphatase, NtMKP1, which represses wound-activation of both SIPK and WIPK57, leads to reduced ET production after wounding (Seo et al., 2007). The *Arabidopsis* PP2C-type MAPK phosphatase, AP2C1, which inactivates the wound responsive MPK4 and MPK6, leads to reduction of wound-ET production in plants overexpressing AP2C1 (Schweighofer et al., 2007).

1.8.2.2. Ethylene signalling

Ethylene is perceived by a family of the endoplasmic reticulum (ER) membrane-localized receptors that are homologous to bacterial histidine kinases involved in sensing environmental changes (Chen et al., 2002). Five ethylene receptors exist in *Arabidopsis*: ETR1, ETR2, ERS1, ERS2, and EIN4. Ethylene receptors are inactivated by ethylene binding in a hydrophobic pocket located at the N terminus of the receptors. The binding requires a transition metal, copper, as a cofactor (Rodriguez et al., 1999). RAN1 is involved in delivery of copper to the ethylene receptor and this copper-delivery pathway is required to create functional ethylene receptors in plants.

CTR1, Ser/Thr protein kinase is placed downstream of the ethylene receptors in the ethylene signalling pathway. It acts as a negative regulator of downstream signalling events by directly interacting with the kinase domain of ethylene receptors ETR1 and ERS1 (Clark et al., 1998). This association is required to turn off the ethylene-signalling pathway (Huang et al., 2003). EIN2 act as a positive regulator of the ethylene signalling, downstream of CTR1. The N-terminal portion of EIN2 is necessary for sensing the ethylene signal from upstream components in the pathway, whereas the EIN2 C-terminal portion (CEND) is required for transducing the signal to the downstream components. EIN3 are nuclear transcription factors that target the ethylene response element in the promoter of the ERF1 gene. ERF1 belongs to a large family of plant-specific transcription factors referred to as ethylene-response-element binding proteins (EREBPs). EREBPs were originally identified on the basis of their ability to bind to the GCC box, a DNA motif associated with ethylene- and pathogen-induced gene expression. ERF1 may regulate one branch of the ethylene response pathway downstream of EIN3 (Figure 1.23.).

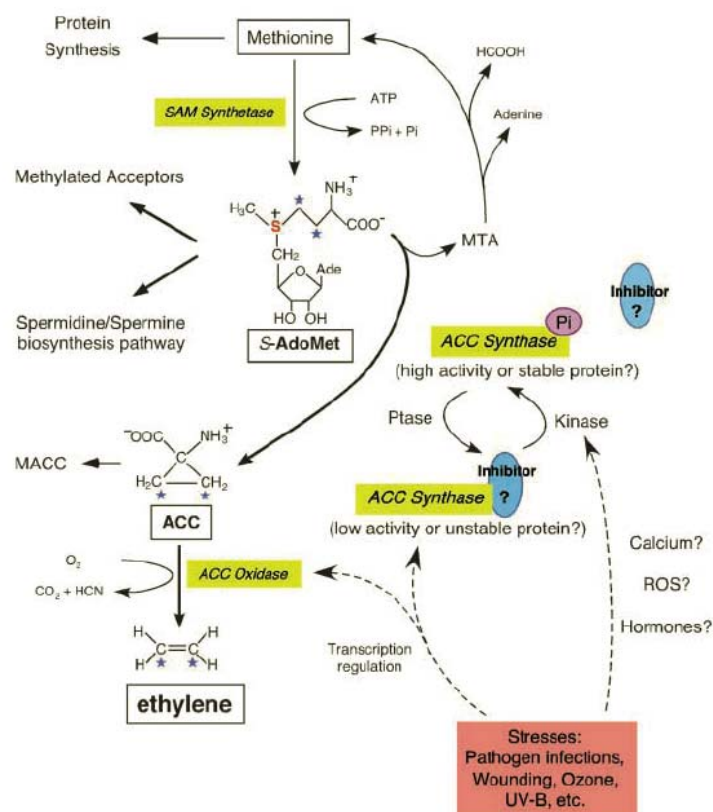


Figure 1.21. Biosynthetic pathway and regulation of ethylene. Transcriptional regulation of both ACC synthase (ACS) and ACC oxidase (ACO) is indicated by dashed arrows (Wang et al., 2002).

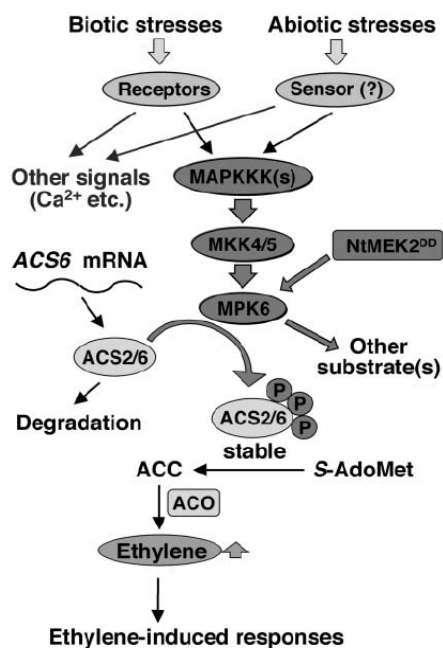


Figure 1.22. A Model depicts the role of MPK6 cascade in stress-induced ethylene production. Phosphorylation of ACS2/ACS6 by MPK6 stabilizes the ACS proteins in vivo, which leads to the accumulation of ACS protein, elevated levels of cellular ACS activity, ethylene production, and ethylene-induced phenotypes (Liu and Zhang, 2004).

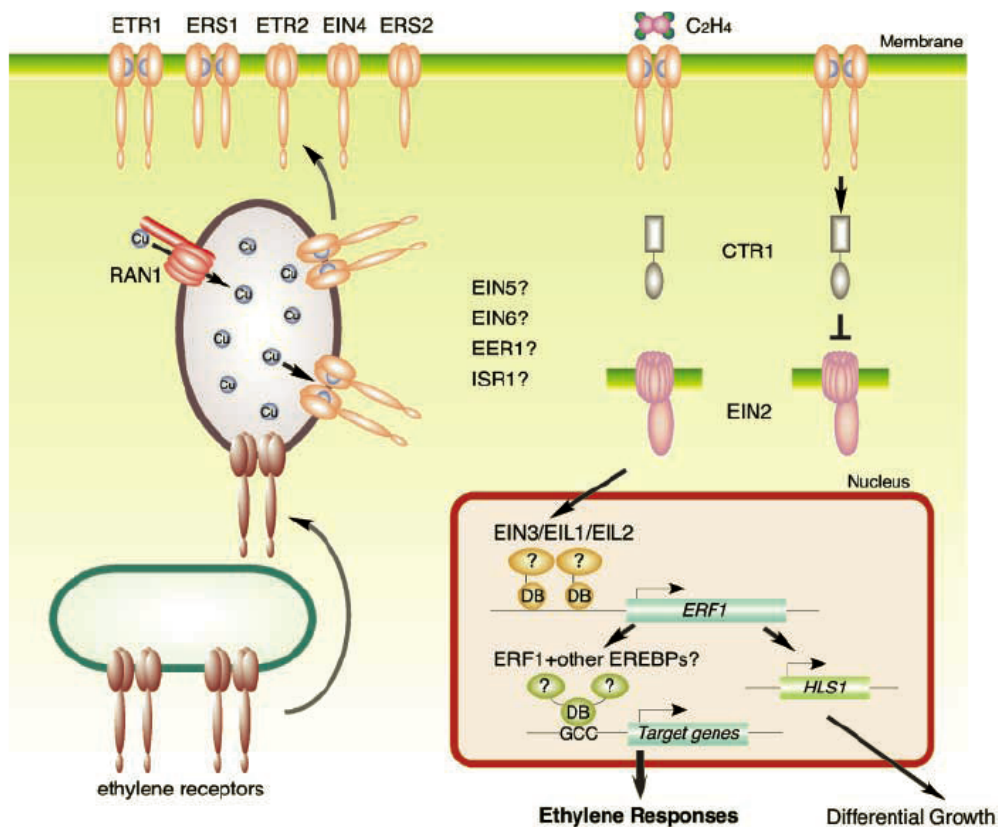


Figure 1.23. Model of the ethylene signal transduction pathway. There are 5 ethylene receptors in *Arabidopsis*, ETR1, ETR2, EIN4, ERS1, and ERS2. In the absence of an ethylene signal, ethylene receptors activate a Raf-like kinase, CTR1, and CTR1 in turn negatively regulates the downstream ethylene response pathway, possibly through a MAP-kinase cascade. Binding of ethylene inactivates the receptors, resulting in deactivation of CTR1, which allows EIN2 to function as a positive regulator of the ethylene pathway. EIN2 positively signals downstream to the EIN3 family of transcription factors located in the nucleus. EIN3 binds to the promoter of *ERF1* gene and activates its transcription in an ethylene-dependent manner. Transcription factors ERF1 and other EREBPs can interact with the GCC box in the promoter of target genes and activate downstream ethylene responses (Wang et al., 2002).

MAPK cascades have been shown to play a positive role in ethylene signalling. Transgenic *Arabidopsis* plants over-expressing SIMKK have constitutive MPK6 activation and also show induction of several ethylene-induced target genes. The positive role of MAPK cascade on ethylene signalling is proposed in two different ways, either by activating EIN2 (Figure 1.25.) (Chen et al., 2005) or by stabilising EIN3 transcription factor (Yoo et al., 2008). The binding of ethylene to its receptors inactivates CTR1, leading to MAPK activation. The activated MAPKs then activate EIN2 or stabilise EIN3, positively regulating the downstream ethylene response pathway. In the absence of ET, CTR1 block the MKK9-MPK3/MPK6 activity, leading to EIN3 transcription factor degradation. However, the inhibition of CTR1 upon the perception of ET activates MKK9-MPK3/MPK6, leading to EIN3 stabilisation (Figure 1.24.).

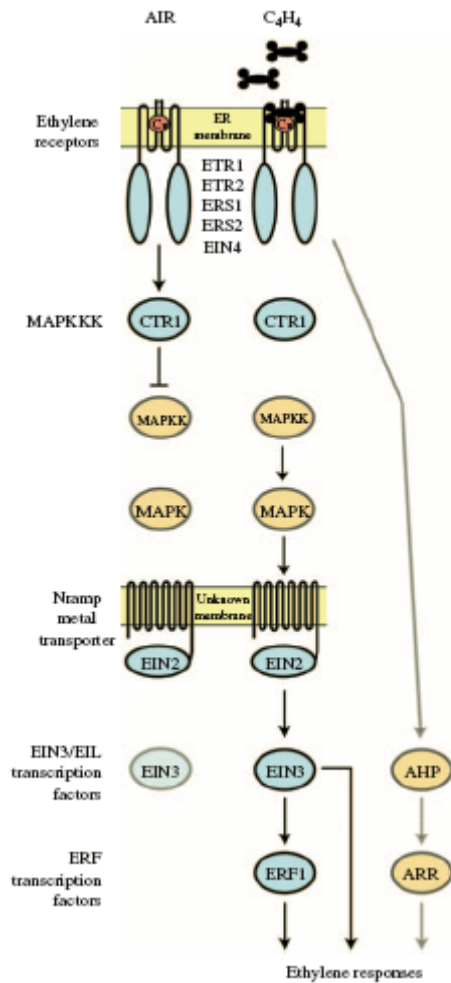


Figure 1.24. Proposed model for ethylene signal transduction and MAPK cascade. In air, ethylene receptors maintain CTR1 in an active state that serves to repress ethylene responses. In ethylene, the repression is relieved. Binding of ethylene inactivates the receptors, thereby inactivating CTR1, leading to MAPK activation. As a result, EIN2 is activated and a transcriptional cascade involving the EIN3/EIL and ERF transcription factors is initiated (Chen et al., 2005).

1.8.3. Jasmonic acid synthesis and signalling

Plants responses to biotic and abiotic stresses are orchestrated locally and systemically by signalling molecules known as jasmonates (JAs). Jasmonates include the biologically active intermediates in jasmonic acid biosynthesis, as well as the biologically active derivatives of jasmonic acid. These compounds are widely distributed in plants and affect a variety of processes, including fruit ripening, production of viable pollen, root growth, tendrils coiling, plant response to wounding, abiotic stress and defences against insects and pathogens.

1.8.3.1. Jasmonate biosynthesis

JA biosynthesis starts from oxylipins generation in the lipoxygenase pathway from α -linolenic acid (18:3) (LA). The biosynthesis of 12-oxo-phytodienoic acid (OPDA) from LA occurs in the chloroplast. LA released by lipase activity on chloroplast membranes is the substrate for oxylipins. Lipoxygenases (LOXs) catalyze the oxygenation of fatty acids

to 13-hydroperoxy-octadecatrienoic acid, a substrate for allene oxide synthase (AOS). AOS catalyses the dehydration of 13-hydroperoxy-octadecatrienoic acid to an unstable epoxide, which is converted to OPDA by allene oxide cyclase (AOC). AOC catalyzes the stereospecific cyclisation of unstable allene oxide to (9S,13S)-12-oxo-(10,15Z)-phytodienoic acid. *Arabidopsis* OPDA reductase (OPR3) catalyses the reduction of OPDA to 3-oxo-2-(2'(Z)-pentenyl)-cyclopentane-1-octanoic acid (OPC-8:0). OPR3 is probably located in the peroxisome, indicating that its substrate, OPDA, is transported from the chloroplast to the peroxisome. OPC-8:0 undergoes three rounds of β -oxidation to form jasmonic acid. This probably occurs in the peroxisome. (Z)-jasmone is a common component of plant volatiles and is probably formed by a further round of α -oxidation of jasmonic acid. Its release from plants can be induced by damage, for example during insect herbivory. The methylation of jasmonic acid to MeJA is catalysed by an S-adenosyl-L-methionine:jasmonic acid carboxyl methyltransferase (JMT) from *Arabidopsis*.

1.8.3.2. Jasmonic acid signalling

Following synthesis, JAs are perceived by, as yet, unknown receptor proteins, and this presumably activates a signal transduction pathway that culminates in the transcriptional activation or repression of a large number of JA-responsive genes. The involvement of protein degradation pathways in JA signalling became apparent after the identification of the COI1 gene encoding an F-box protein with Leu repeats (Xie et al., 1998). Indeed, COI1 or SCFCOI1 is an integral part of a highly conserved multi-protein complex called the SCF E3 ubiquitin ligase complex. In the absence of a JA signal, JAZ1 and JAI3/JAZ3 repress JIN1/MYC2. This repression most likely occurs in the nucleus. Upon sensing the JA signals, JAZ repressors are recruited to the SCF E3 complex for ubiquitination and subsequent degradation by the proteasome. The removal of these repressors then paves the way for JIN1/MYC2 to regulate JA-dependent gene expression. In addition to insect resistance, JIN1/MYC2 positively regulates JA-mediated oxidative stress tolerance and flavonoid metabolism. In contrast, JA-dependent pathogen defense and the biosynthesis of secondary metabolites (e.g. biosynthesis of indole glucosinolates) are negatively regulated by JIN1/MYC2 (Dombrecht et al., 2007). It was proposed that these regulatory controls are mediated by JIN1/MYC2 by coordinating a transcriptional cascade involving a number of other transcription factors (AP2/ERFs, MYBs, zinc fingers, and WRKYs), each with demonstrated roles in regulating downstream gene expression (Dombrecht et al., 2007). In

Arabidopsis, MPK4 is activated 2 to 5 min after wounding (Ichimura et al., 2000). MPK4 cascade simultaneously suppress SA biosynthesis and promotes the JA perception/response required for induction of *PDF1.2* and *Thi2.1*.

1.9. Hormone mediated signalling

Plant responses to different environmental stresses are achieved through integrating signalling networks and mediated by the synergistic or antagonistic interactions with the phytohormones SA, JA, ET and ROS. How plants response to particular stresses and provide the output specificity remains largely unknown; it is likely both temporal and spatial hormonal balances contribute significantly.

1.9.1. Hormone mediated signalling under biotic stress.

It is generally accepted that SA plays a main role in the activation of defences against biotrophic pathogens, whereas JA and ET are more associated with defence against necrotrophic pathogen attack (Adie et al., 2007). Additionally, SA and JA/ET defence pathways are mutually antagonistic (Turner et al., 2002).

The activation of the hypersensitive response triggers a long-lasting response known as systemic acquired resistance (SAR). SAR provides immunity against subsequent infections caused by a broad spectrum of virulent pathogens. In many cases, systemic acquired resistance is characterized by an increase in endogenous salicylic acid (SA) levels and expression of a subset of PR genes. However, some pathogens can induce plant defence responses via activation of the ET and JA signalling pathways. *Arabidopsis* plants with defects in ethylene perception (*ein2*) or JA signalling (*coi1*) fail to induce a subset of PR gene expression, including the plant defensin gene *PDF1.2* and a basic chitinase (*PR-3*), resulting in enhanced susceptibility toward certain pathogens (Penninckx et al., 1998). This suggests that the induction of *PDF1.2* requires both intact JA and ethylene signalling. The ethylene and JA pathways interact with each other, co-regulating expression of some genes involved in the plant defence mechanism. Nevertheless, ethylene and JA signalling may also function independently to regulate distinct defence responses.

1.9.2. Hormone mediated signalling under wounding stress.

Wounding responses involve a number of plant hormones, including JA, SA, and ethylene. The synergistic effects of JA with ethylene and antagonistic effects with SA in the wound response are supported by several reports. The synthesis of JA and ethylene is positively regulated by each other under wounding stress, whereas SA suppresses JA synthesis and the subsequent ethylene production. JA accumulates in wounded plants and activates expression of various defence genes such as Proteinase inhibitors (PIN2), Thionin (Thi2.1), and enzymes involved in secondary metabolism. A number of genes which are involved in biosynthesis of JA, are up-regulated by wounding. It has been also well documented that wounding induces ethylene production that affects the downstream wound response. Two mechanisms might be involved in the interaction between ethylene signalling and wound response (Cheong et al., 2002). First, ACS genes, which are involved in ethylene biosynthesis, have been identified as early wound-response genes. Following the induction of ACS genes, the induction of ethylene response genes such as, senescence-associated genes, chitinases, and glucanases as late wound-response genes, was observed (Cheong et al., 2002). Second, many of the ethylene response transcription factors such as EREBPs are rapidly induced by wounding. These transcription factors may directly participate in the activation of ethylene-responsive genes. Ethylene has been shown to potentiate JA action in the wound response. The wound induction of JA accumulation is reduced by the addition of inhibitors of ethylene biosynthesis. Also, ethylene has been shown to positively regulate the induction of AOS, which catalyzes the first step in the biosynthesis of JA, in tomato and *Arabidopsis*. On the other hand, ROS and JA stimulate ethylene production by activating ACS gene expression in winter squash. Diphenylene iodonium (DPI), an inhibitor of ROS generation, blocks ethylene production but not JA accumulation.

Protein Ser/Thr phosphatase AP2C1 was shown to regulate the biosynthesis of wounded-induced ethylene and jasmonic acid in *Arabidopsis* (Schweighofer and Meskiene, 2008). Its regulation might be via dephosphorylation and inactivation of wounded-activated MAPKs involved in the pathways of ethylene and jasmonic acid biosynthesis. It was found that leaf of *ap2c1* mutant plants accumulated higher levels of JA after wounding. Consequently, *ap2c1* mutant plants demonstrated upregulated expression of the stress marker gene *PDF1.2* and were more resistant to phytophagous mites (*Tetranychus urticae*). At the same time, plants with an increased AP2C1 level displayed suppressed

wound activation of MAPKs, reduced ethylene production and compromised innate immunity against the necrotrophic fungal pathogen *Botrytis cinerea* (Figure 1.26.).

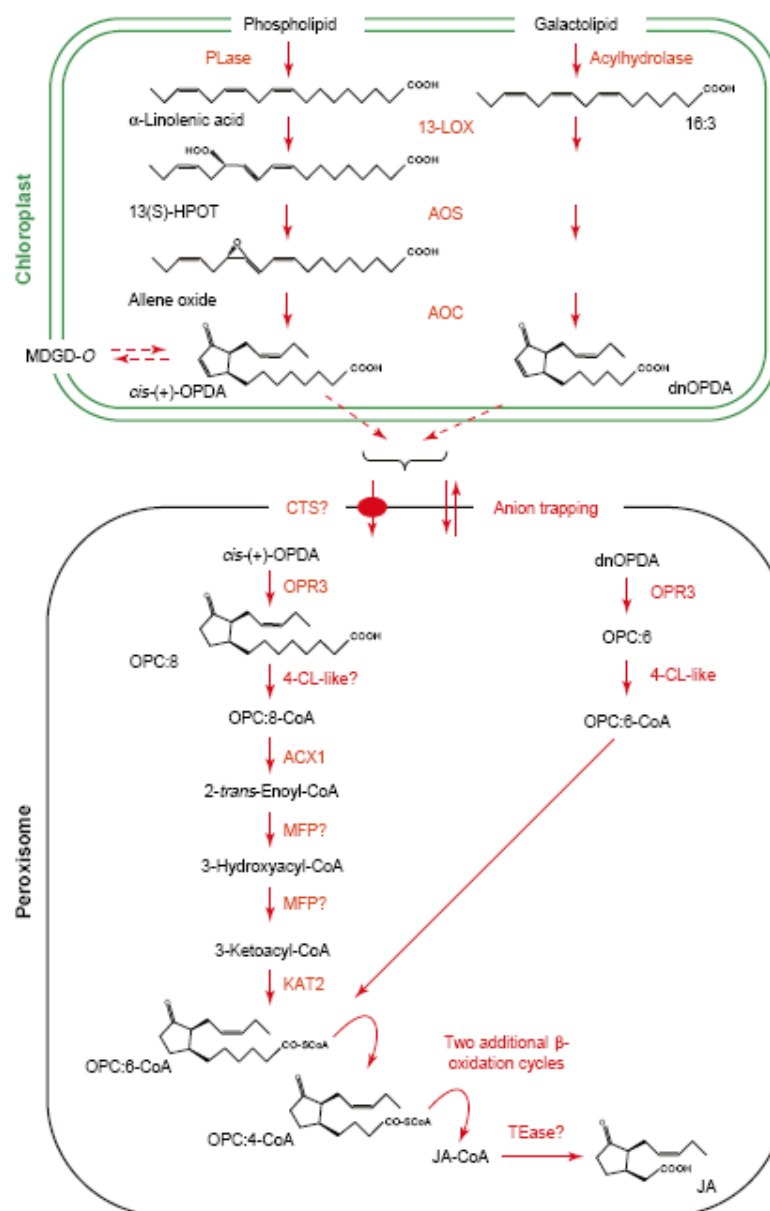


Figure 1.25. Model for the biosynthesis of JAs. JAs are derived from α -linolenic acid liberated from membrane phospholipids by the action of phospholipase A. α -Linolenic acid is first converted to 13-hydroperoxy linolenic acid (13-HPOT) and then to 12-OPDA in the chloroplasts in a series of reactions catalyzed by 13-lipoxygenase (LOX), allene oxide synthase (AOS), and allene oxide cyclase (AOC), respectively. 12-OPDA is then transported to peroxisomes and subsequently reduced by 12-oxophytodienoate reductase 3 (OPR3) to 3-oxo-2-(2'-pentenyl)-cyclopentane-1-octanoic acid (OPC), which then undergoes three cycles of β -oxidation in the peroxisomes to produce jasmonic acid (Baker et al., 2006)

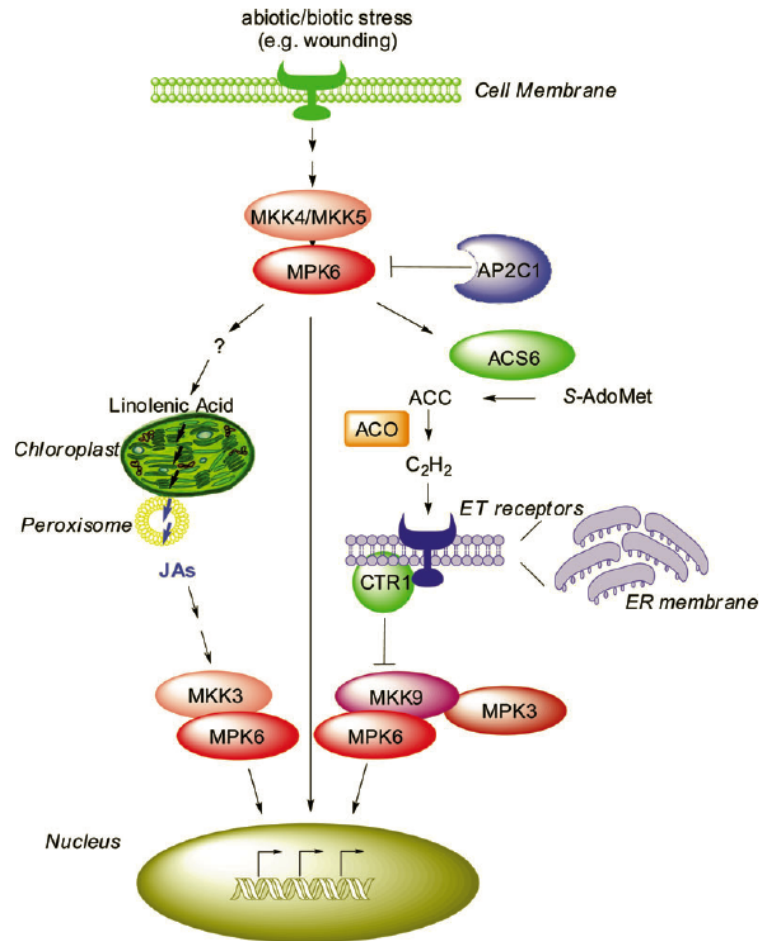


Figure 1.26. Summary of JA and ET biosynthesis and their signalling pathways in *Arabidopsis*. After stress perception plant cells activate protein phosphorylation cascades mediated by kinases. MAP kinase MPK6 phosphorylates target proteins, leading to cell responses. One of the targets is the enzyme responsible for ethylene production, ACS. ACS is stabilized by phosphorylation leading to enhanced ET production. ET receptors localized inside the cell at the endoplasmic membranes, bind ET and transmit the signal downstream to a specific kinase cascade that includes CTR1–MKK9–MPK3/MPK6, which conveys the signal to the nucleus to generate ET responses. At the same time MPK6 may modify other target(s) thereby leading to an enhancement of JA production (JA biosynthesis involves chloroplasts and peroxisomes). JA activates a specific MAPK pathway, which includes the MPK6 kinase. This signal is transferred to the nucleus and responses to JA are generated. Both pathways lead to activation of cell defence (Schweighofer and Meskiene, 2008).

1.9.3. Hormone-mediated signalling in *Arabidopsis* mutant plants

Microarray analysis of gene expression in wild-type and mutant plants indicates the existence of a substantial network of regulatory interaction and coordination among different plant defence pathways.

The *Arabidopsis* mutant *nonexpression of PR1 (npr1)* is insensitive to SA, fails to express SA-induced PR genes, and has reduced SAR. A screen for suppressor mutations of *npr1*

yielded a dominant mutation named *suppressor of SA insensitivity (ssi1)*, which has constitutive expression of PR genes and restored resistance to *P. syringae*.

Another *Arabidopsis* mutant with constitutive expression of PR genes, named *constitutive PR 5 (cpr5)*, has some similarity to *ssi1*. The *cpr5* phenotype is suppressed in the SA-deficient *eds5* mutant, but is only partially affected by the SA-insensitive *npr1* mutant. The *eds5* mutant suppresses the SA-accumulating phenotype of the *cpr* mutants, whereas *npr1* enhances it, indicating that *cpr5* has an SA-mediated, NPR1-independent resistance response. However, the *cpr5* phenotype is also suppressed by the ethylene-insensitive mutation *ein2* and by the JA-insensitive mutation *jar1*, suggesting SA-mediated, NPR1-independent resistance in *cpr5* requires components of the JA and the ethylene signal pathways.

cpr5 and *cpr6*, two *Arabidopsis* mutants that constitutively express PR genes, express both PR-1 and PDF1.2 genes in the absence of pathogen infection. Although the constitutive expression of PR-1 is dependent on SA, it is only partially suppressed by the *npr1* mutation, indicating the existence of a SA-mediated, NPR1-independent response. Only when ethylene signalling is blocked by *ein2* in addition to *npr1* mutation in *cpr5* and *cpr6* mutants is PR-1 gene expression abolished completely. Furthermore, *ein2* potentiates SA accumulation in *cpr5* and decreases SA accumulation in *cpr6*. These results suggest the existence of interactions between ethylene- and SA-dependent signalling through an NPR1-independent pathway. Interestingly, a suppressor of *npr1*, *ssi1*, which completely bypasses NPR1 function, constitutively expresses the JA/ethylene-dependent marker PDF1.2 gene in an SA-dependent manner, suggesting that SSI1, together with CPR5 and CPR6, may participate in the interactions between the SA- and JA/ethylene-dependent pathways (Figure 1.27).

The *Arabidopsis* mutant *constitutive expression of vegetative storage protein (cev1)* has constitutive production of JA and ethylene, constitutive expression of PDF1.2, Thi2.1, and chitinase CHI, and has enhanced defences against fungal pathogens (Ellis and Turner, 2001) and insect pests. The mutant *ethylene resistant 1 (etr1)* was used to make the double mutant *cev1etr1*, in which PDF1.2 expression was absent, confirming a requirement for an ethylene signal for PDF1.2 transcription (Ellis and Turner, 2001). Interestingly, *Thi2.1* is constitutively expressed in this double mutant, indicating that ethylene signalling suppresses the transcription of *Thi2.1*. The *cev1* mutant phenotype is partially suppressed in the *coronatine insensitive 1 (coi1)* and in the *ethylene resistant 1 (etr1)* mutant

backgrounds, and the triple mutant, *cevl;coi1;etr1* is wild type except for slightly shorter roots (Ellis et al., 2002). This indicates that *cevl* induces biosynthesis of JA and ethylene, and its mutant phenotype is largely determined by responses to these signalling molecules. *cevl*, therefore, acts at an early step in the perception/transduction pathway, before JA and ethylene biosynthesis.

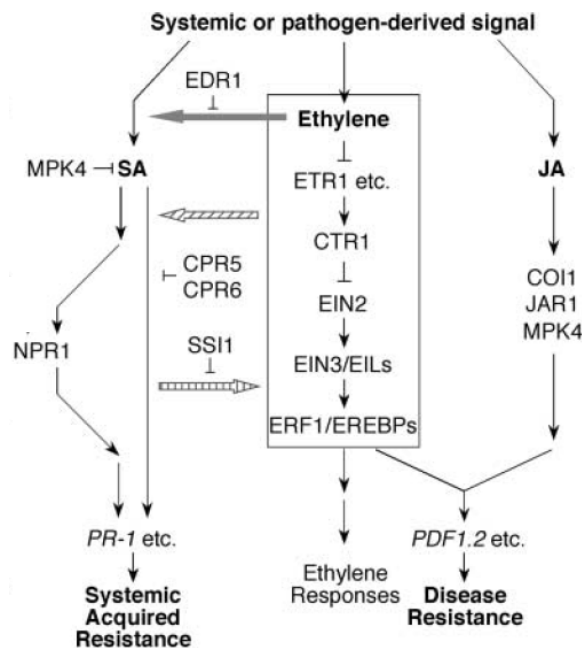


Figure 1.27. There are considerable interactions between JA/ethylene- and SA-dependent pathways in systemic acquired resistance. Ethylene potentiates SA-mediated *PR-1* gene expression. In the absence of CPR5 and CPR6, the ethylene pathway can also activate SA-dependent *PR-1* gene expression independent of NPR1 to promote systemic acquired resistance. In the *ssi1* mutant, the JA/ethylene-dependent *PDF1.2* gene is constitutively expressed. Arrows indicate positive regulation, and open blocks indicate negative regulation (Wang et al., 2002).

The antagonistic interaction between SA and JA signalling

The antagonistic interactions between salicylic acid (SA) and JA pathways first became evident from the analysis of SA- and JA-marker gene expression in SA and JA signalling mutants in *Arabidopsis*. Indeed, *coi1* mutations that disrupt JA signalling enhance basal and inducible expression of the SA marker gene *PR1*, while *npr1* mutations that disrupt SA signalling increases in the basal or induced levels of the JA marker gene *PDF1.2*. Interestingly, exogenous SA promotes the JA-dependent induction of the defence gene *PDF1.2* when applied at low concentrations. However, the induction of *PDF1.2* by JA is reduced at higher SA concentrations, leading to the proposal that the interaction between

these two pathways might be dose dependent (Mur et al., 2006). Plants treated with SA or inoculated with virulent strains of *P. syringae* pv. *tomato* show compromised resistance to *Alternaria brassicicola*, a necrotrophic pathogen sensitive to JA-dependent defenses, possibly due to the suppression of JA-dependent defences known to be effective against necrotrophic pathogens (Spoel et al., 2007).

The antagonistic interaction between SA and JA signalling is mainly mediated by NPR-independent and partly by NPR1-dependent pathway. Acting downstream from NPR1, WRKY70 is a versatile transcription factor with roles in multiple signalling pathways and physiological processes. WRKY70 regulates the antagonistic interactions between SA and JA pathways (Li et al., 2004). The *Arabidopsis mpk4* mutant exhibits constitutively active SA-dependent defence responses (increased SA levels, constitutive expression of PR1, and increased resistance to *P. syringae*) in the absence of pathogen attack. In contrast, the JA-dependent induction of the PDF1.2 gene was abolished in the *mpk4* mutant plants (Petersen et al., 2000). Hence, MPK4 is suggested to be a positive regulator of JA-dependent responses while a negative regulator of SA biosynthesis and signalling. SA-JA interaction in *Arabidopsis* is also regulated by an SA-inducible glutaredoxin 480 (GRX480) which interacts with the TGA-type transcription factors involved in the regulation of SA-inducible PR genes and suppresses the JA-responsive expression of *PDF1.2* (Ndamukong et al., 2007). In addition to COI1, the transcriptional regulator JIN1/MYC2 also has a role in antagonizing SA signalling in plants during infection by *P. syringae* (Laurie-Berry et al., 2006).

The synergistic interaction between JA and ET signalling

JA and ethylene synergistically induce a subset of defence genes following pathogen inoculation in *Arabidopsis*. For instance, induction of PDF1.2 by *A. brassicicola* requires both JA and ethylene signalling pathways (Penninckx et al., 1998). The cellulose synthase gene CeSA3/CEV1 controls a point of convergence between these two pathways as a negative regulator of both pathways, as deduced from the analysis of the *cev1* mutant that displays constitutively active JA and ET responses (Ellis et al., 2002). The ETHYLENE RESPONSE FACTOR1 transcription factor also functions at the crossroad of JA and ethylene signalling as a positive regulator of both pathways (Lorenzo et al., 2003).

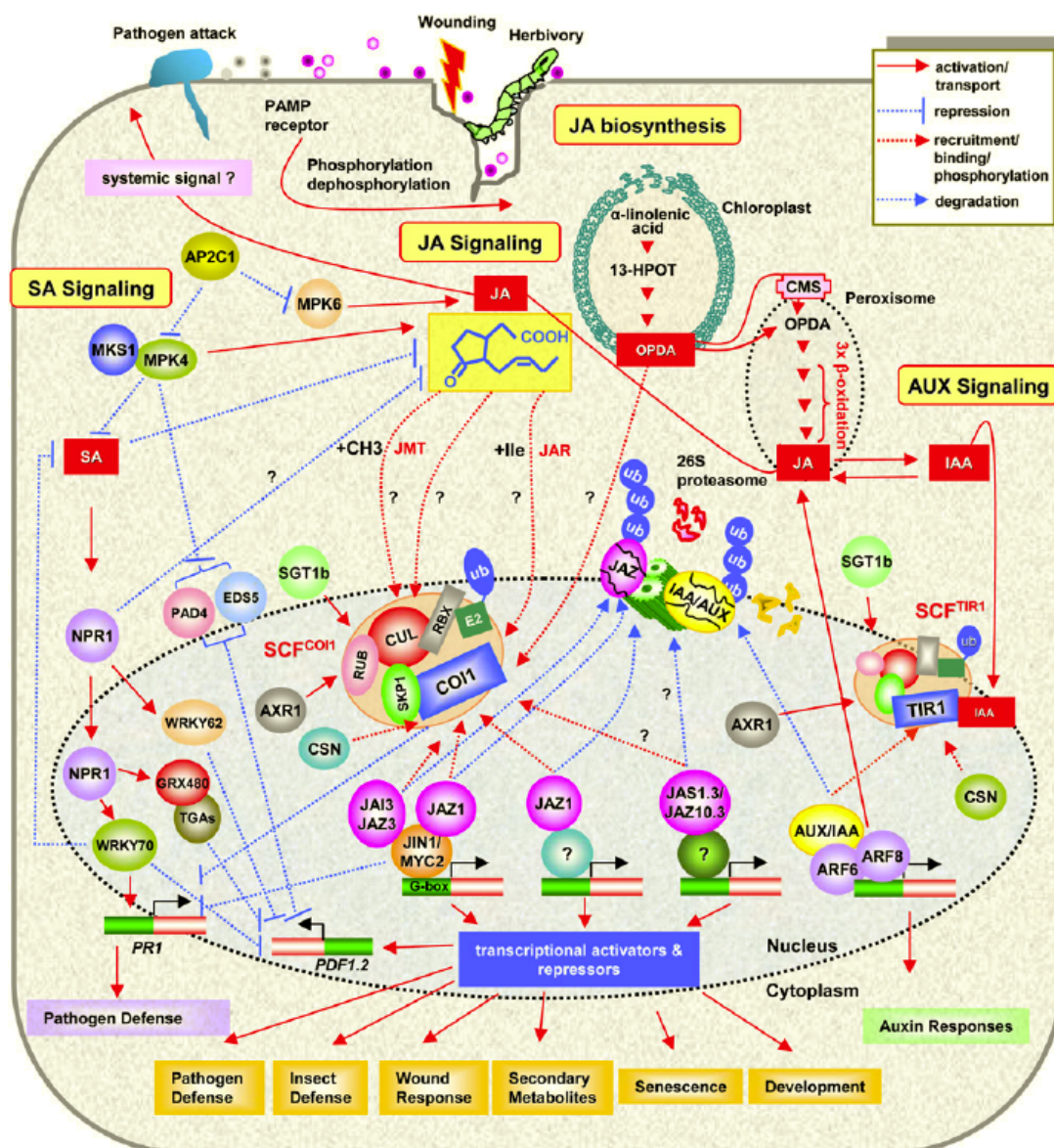


Figure 1.28. An integrated view of JA biosynthesis and signalling, including signalling interactions between JA and SA and JA and auxin (IAA) in *Arabidopsis*. Biotic and abiotic stresses, such as pathogen and insect attack and wounding, generate signals/elicitors that activate a phosphorylation cascade that regulates JA biosynthesis and signalling. JAZ proteins act as negative regulators of the transcriptional regulator JIN1/MYC2, and their JA- and SCF^{COI1}-dependent degradation liberates JIN1/MYC2 from repression. JIN1/MYC2, by possibly binding to the conserved G-box element found in the promoters, coordinates a transcriptional cascade that involves other transcriptional activators and repressors from AP2/ERF, WRKY, and MYBs to modulate distinct JA-dependent functions. The cross talk between JA and SA and JA and auxin signalling occurs at multiple points. As explained in the text, NPR1, MPK4, WRKY70, SCF^{COI1}, and JIN1/MYC2 are some of the major players involved in these interactions. Similarly, the JA-auxin cross talk is modulated by CSN, SGT1b, AXR1, and ARFs as explained in text (Kazan and Manners, 2008).

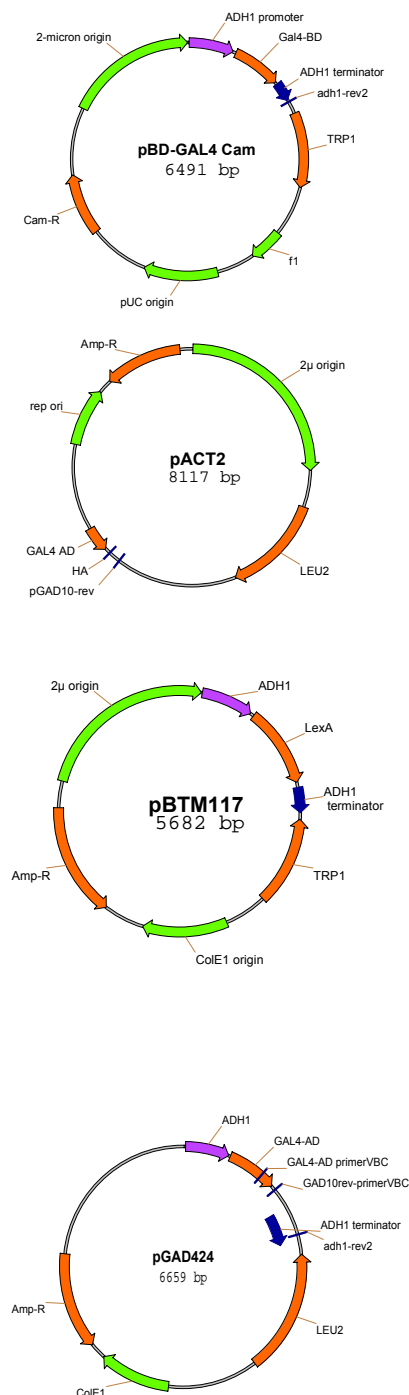
The synergistic interaction between JA and Auxin signalling

JA activates expression from auxin biosynthesis genes (Dombrecht et al., 2007), while auxin activates expression of JA biosynthesis genes. These examples clearly illustrate that auxin and JA signalling are intimately interlinked. Protein degradation pathways via SCF E3 ubiquitin ligase and the COP9 signalosome (CSN) complexes play essential roles not only in JA but also in auxin signalling. AXR1, which encodes a subunit of the RUB1-activating enzyme that regulates the protein degradation activity of SCF complexes, regulates both SCFTIR1 and SCFCOI1 involved in auxin and JA signalling, respectively. SUPPRESSOR OF THE G2 ALLELE OF *skp1-4b* (SGT1b) is required for both SCFTIR-mediated auxin and SCFCOI1-mediated JA responses (Gray et al., 2003). Auxin and JA pathways are also interlinked at the level of ARFs. At least two ARFs, ARF6 and ARF8, are required for JA biosynthesis (Figure 1.28.).

2. MATERIALS AND METHODS

2.1. Plasmid constructs

2.1.1. Vectors

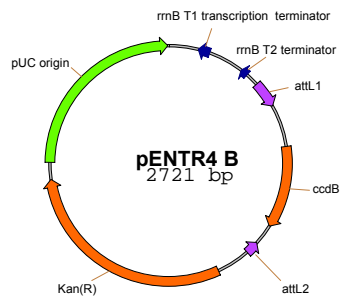


pBDcam : GAL4 DNA-binding domain (BD) yeast two-hybrid vector, confers chloramphenicol resistance to *E. coli* transformants, selected in yeast by tryptophan marker (Stratagene).

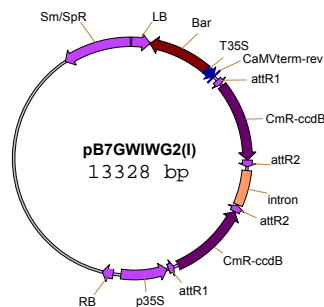
pACT2 : yeast two-hybrid vector. Contains the LEU2 gene for selection in Leucine- auxotrophic yeast strains and GAL4 activation domain (Clontech)

pBTM117 : yeast two-hybrid vector that contains the TRP1 gene for selection in Trptophan- auxotrophic yeast strain and lexA binding domain. This vector is lacking the EcoRI restriction site compared to pBTM116 (constructed by Markus Teige from pBTM116). A new reading frame was created in the multiple cloning sites.

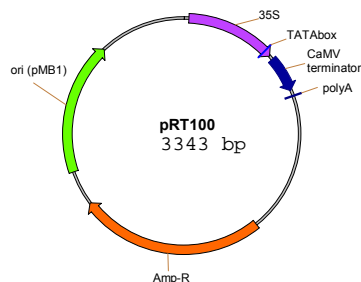
pGAD425 : contains the LEU2 gene for selection in Leucine- auxotrophic yeast strains and GAL4 activation domain. The vector was constructed from pGAD424 (Clontech, USA) by cutting at the EcoRI site, subsequently digested with mung bean nuclease and religated. This vector is lacking the EcoRI restriction site compared to pGAD424. A new reading frame was created in the multiple cloning sites.



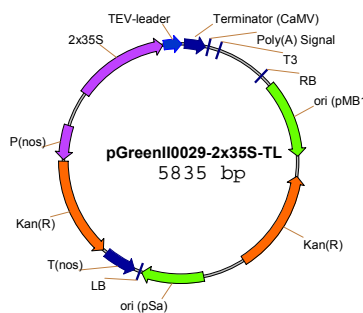
pENTR4 B : Modified pENTR Gateway[®] entry vectors are designed to clone DNA sequences using restriction endonucleases and ligase to create a Gateway[®] entry clone. The resulting entry clone is ready for recombination with a destination vector to create an expression clone (Invitrogen).



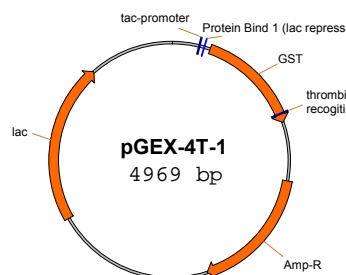
pB7GWIWG2(I) : Binary gateway destination vectors for *Agrobacterium*-mediated plant transformation contains hairpin RNA expression cassette and bar marker (provided by Dirk Inze, Belgium) .



pRT100 : Plant expression vector for transient expression under the control of CaMV 35S promoter (Topfer et al., 1987). The vector is used for localization experiment in protoplasts



pGreenII0029 : Binary vector for stable and transient expression in plants (Hellens et al., 2000). Information at www.pgreen.ac.uk



pGEX-4T-1 : *E.coli* expression vector, purchased from Amersham Pharmacia. Protein expression is under the control of the tac promoter, which is induced using the lactose analog IPTG.

2.1.2. Plasmids used in this study

No.	Name	creator
#476	pGEX-MEK4	Stefan Kiegerl
#586	pRT-AtMKK2-gof-myc	Markus Teige
#634	pJS-delta ANP1-HA	Jen Scheen (Boston)
#724	pGEX-AtMPK6 lof (K/M)	Markus Teige
#727	pSP72-2x35S-TL-gAP2C2wt-MYC	Vaiva Kazanaviciute
#790	pGEX-AP2Cwt	Alois Schweighofer
#792	pGEX-AP2C-G178D (lof2)	Alois Schweighofer
#794	pGreenII-2x35S-TL-gAP2C2wt-HA	Vaiva Kazanaviciute
#799	pGreenII-AP2C2prom-GUSint	Vaiva Kazanaviciute
#804	pGreenII-2x35S-TL-gAP2C2wt-GFP	Vaiva Kazanaviciute
#805	pGreenII-2x35S-TL-gAP2C2wt-MYC	Vaiva Kazanaviciute
#808	pGAD425-AtMPK1wt	Markus Teige
#809	pGAD425-AtMPK2wt	Markus Teige
#810	pGAD425-AtMPK3wt	Markus Teige
#811	pGAD425-AtMPK4wt	Markus Teige
#812	pGAD425-AtMPK5wt	Markus Teige
#813	pGAD425-AtMPK6wt	Markus Teige
#814	pGAD425-AtMPK7wt	Markus Teige
#815	pGAD425-AtMPK8wt	Robert Doczi
#816	pGAD425-AtMPK9wt	Robert Doczi
#817	pGAD425-AtMPK11wt	Robert Doczi
#818	pGAD425-AtMPK12wt	Robert Doczi
#819	pGAD425-AtMPK13wt	Robert Doczi
#820	pGAD425-AtMPK14wt	Robert Doczi
#821	pGAD425-AtMPK15wt	Robert Doczi
#822	pGAD425-AtMPK16wt	Robert Doczi
#823	pGAD425-AtMPK17wt	Robert Doczi
#824	pGAD425-AtMPK19wt	Robert Doczi
#825	pGAD10-AtMPK20wt	Robert Doczi
#847	pGAD425-cAP2C2wt	Julija Umbrasaitė
#854	pGreenII-AP2C2prom-GFP	Alois Schweighofer
#855	pBDcam-cAP2C2wt	Alois Schweighofer
#856	pBTM117-cAP2C2wt	Alois Schweighofer
#895	pGEX-AP2C2wt	Chonnanit Choopayak
#982	pGreenII0229-2x35S-TL-AtMPK4wt-YFPn	Vaiva Kazanaviciute
#983	pGreenII0229-2x35S-TL-AtMPK4wt-YFPc	Vaiva Kazanaviciute
#984	pGreenII0229-2x35S-TL-YFPn-AtMPK4wt	Vaiva Kazanaviciute
#985	pGreenII0229-2x35S-TL-YFPc-AtMPK4wt	Vaiva Kazanaviciute
#986	pGreenII0229-2x35S-TL-AtMPK6wt-YFPn	Vaiva Kazanaviciute
#987	pGreenII0229-2x35S-TL-AtMPK6wt-YFPc	Vaiva Kazanaviciute
#1002	pGreenII0229-2x35S-TL-YFPc-AtMPK6wt	Armin Djamei
#1003	pGreenII0229-2x35S-TL-YFPn-AtMPK6wt	Armin Djamei
#1004	pGreenII0229-2x35S-TL-AtMPK3wt-HA	Julija Umbrasaitė
#1005	pBTM117-AtMPK4wt	Julija Umbrasaitė
#1011	pGreenII0029-2x35S-TL-YFPctd-gAP2C2wt	Chonnanit Choopayak
#1012	pGreenII0029-2x35S-TL-YFPntd-gAP2C2wt	Chonnanit Choopayak
#1013	pGreenII0029-2x35S-TL-gAP2C2wt-YFPctd	Chonnanit Choopayak
#1014	pGreenII0029-2x35S-TL-gAP2C2wt-YFPntd	Chonnanit Choopayak
#1015	pBTM117-AtMPK3wt	Chonnanit Choopayak

No.	Name	creator
#1016	pBTM117-AtMPK6wt	Chonnanit Choopayak
#1024	pGEM-Importin alpha	Chonnanit Choopayak
#1031	pGEM-AP2C2-RNAi	Chonnanit Choopayak
#1038	pENTRY4B-AP2C2-RNAi	Chonnanit Choopayak
#1050	pB7GWIWG2(I)-AP2C2-RNAi	Chonnanit Choopayak
#1055	pGreenII0029-2x35S-TL-IMP-YFPwt	Chonnanit Choopayak
#1066	pGreenII0029-2x35S-TL-YFPctd-IMP	Chonnanit Choopayak
#1067	pGreenII0029-2x35S-TL-YFPntd-IMP	Chonnanit Choopayak
#1081	pRT100-35S-YFPctd	Alois Schweighofer
#1082	pRT100-35S-YFPctd	Alois Schweighofer
#1090	pGreenII0029-AP2C2prom-gAP2C2wt-YFPwt	Chonnanit Choopayak
#1091	pRT100-35S-YFPctd-AtMPK3wt	Alois Schweighofer
#1092	pRT100-35S-YFPctd-AtMPK4wt	Alois Schweighofer
#1093	pRT100-35S-YFPctd-AtMPK6wt	Alois Schweighofer
#1107	pRT100-35S-YFPntd-AP2C2wt	Chonnanit Choopayak
#1108	pRT100-35S-YFPntd-IMP	Chonnanit Choopayak
#1109	pRT100-35S-YFPctd-IMP	Chonnanit Choopayak
#1148	pGreenII0029-2x35S-TL-gAP2C2wt-CFP	Chonnanit Choopayak
#1149	pGreenII0029-2x35S-TL-IMP-CFP	Chonnanit Choopayak
#1156	pBTM117-IMP	Chonnanit Choopayak
#1316	pGEX-AtMPK6 K/M (lof)	Markus Teige
#1338	pGEX-HAB1	Zahra Ayatollahi
#1342	pGEX-ABI2	Zahra Ayatollahi
#1392	pFGC19-35S-px-CFP (px-cb)	Andreas Nebenführ, USA
#1396	pFGC19-35S-pt-CFP (pt-cb)	Andreas Nebenführ, USA
#1400	pGEX-cAP2C2-lof1(G155D)	Chonnanit Choopayak
#1401	pGEX-cAP2C2-lof2(G155R)	Chonnanit Choopayak
#1402	pGEX-cAP2C2-lof3(R287A)	Chonnanit Choopayak

2.2. Oligonucleotides

2.2.1. PCR primers

Oligonucleotides for PCR were purchased from VBC Genomics (Vienna, Austria).

AP2C2	#179	fwd: CCATGGCGTCTTCAGTTGCCGTTTGCA
	#180	rev: GCGGCCGCAGAAGAGGTGGCACAACCTG
AP2C1	#210	rev: CATCAGACGAGCCTCGTGAAGCAGATAAATCG
	#244	fwd: TCGGCCGCTGTGGCTGCG
IMP	#353	fwd: AACCATGGCACTGAGACCCAAC
	#354	rev: TTGCGGCCGCAGCTGAAGTTGAAT
IMP internal	#357	fwd: GCTTCCGCTGCTCAATCAGCTT
	#361	rev: GCAATGTTTGTAGAGCCCAAGCTGCCTC
ACX1	#479	fwd: GTGGTGGACATGGATACTTGTGGTG
	#480	rev: GCAGACAGGAAGAATTTGTGAGAGTTTGG
ACX5	#481	fwd: CTGGAAAGGCTCCTTCTGGGA
	#482	rev: CCGAGTCATTGAGTGGATCCT
MKP1	#177	fwd: CCATGGTGGGAAGAGAGGATGCGATG
	#320	rev: TGTCTTTCGCCACAGCATCT

Primer names	No.	Sequences (5'--3')
LB-GABI-Kat	#398	CCCATTGGACGTGAATGTAGACA
RB-GABI-Kat	#393	GTGGATTGATGTGATATCTCC
LBa1-SALK	#319	TGGTTCACGTAGTGGGCCATCG
LBb1-SALK	#206	GCGTGGACCGCTTGCTGCAACT
RB-SALK	#379	CTTCAACGTTGCGGTTCTGTCAGTT
pGKB5-Gus/Rb	#321	rev: ACGCAGCACGATACGCTGG

2.2.2. RT-PCR primers

Primer names	No.	Sequences (5'--3')
AP2C2	#406	fwd: AGGAGATCCCAAACAGGCAATA
At1g07160	#407	rev: TATCCACATAACCGCCCGAGCTC
AP2C1	#244	fwd: TCGGCCGCTGTGGCTGCG
At2g30020	#210	rev: CATCAGACGAGCCTCGTGAAGCAGATAAATCG
IMP	#353	fwd: AACCATGGCACTGAGACCCAAC
At3g06720	#361	rev: GCAATGTTTGTAGAGCCCAAGCTGCCTC
ACX1	#479	fwd: GTGGTGGACATGGATACTTGTGGTG
At4g16760	#455	rev: TATCCCACATATCCTTCTCAGAGTAG
ACX5	#481	fwd: CTGGAAAGGCTCCTTCTGGGA
At2g35690	#482	rev: CCGAGTCATTGAGTGGATCCT
MKP1	#177	fwd: CCATGGTGGGAAGAGAGGATGCGATG
At2g30020	#320	rev: TGTCTTTCGCCACAGCATCT
ACT3	#260	fwd: ATGGTTAAGGCTGGTTTTGC
At2g37620	#261	rev: AGCACAATACCGGTAGTACG
THI2.1	#274	fwd: TCCAACCAAGCTAGAAATGGC
At1g72260	#275	rev: CGACGCTCCATTACAAATTC

2.2.3. Primers for construction of site directed mutagenesis

Primer names	No.	Sequences (5'--3')
AP2C2lof-155 (G-D)	#473	fwd: CAGGCAATATTCGACGTCTATGATGGTCACGGAGG
	#474	rev: CCTCCGTGACCATCATAGACGTCGAAGATTGCCTG
AP2C2lof-155 (G-R)	#475	fwd: CAGGCAATATTCGGGTCTATGATGGTCACGGAGG
	#476	rev: CCTCCGTGACCATCATAGACCCGGAATATTGCCTG
AP2C2lof-287 (R-A)	#477	fwd: CAAGGATCATTAGCGGTATCTGCTGGAATAGGAGATGC
	#478	rev: GCATCTCCTATTCCAGCAGATACCGCTAATGATCCTTG

2.2.4. Primers for construction of AP2C2-RNAi

Primer names	No.	Sequences 5'--3'
AP2C2-Catma	#351	TTGCGGCCGCTGCATTTCGATATAGGAGCTGCAA
	#352	AACCATGGGTCTCCACATCTCCGTTCTGCCT

2.3. Antibodies

2.3.1. Primary antibodies

AtMPK3: Polyclonal antibody from rabbit, raised against N-terminal sequence NTGGGQYTDFPAVD from *Arabidopsis* MPK3. (Davids Biotechnologie, Germany)

AtMPK4: Polyclonal antibody from rabbit, raised against the C-terminal sequence ELIYRETVKFNPQDSV of *Arabidopsis* MPK4 (Davids Biotechnologie, Germany)

AtMPK6: Polyclonal antibody from rabbit, raised against C-terminal sequence FNPEYQQ of the Medicago SIMK (Davids Biotechnologie, Germany), recognizes specifically the *Arabidopsis* MPK6 (Davids Biotechnologie, Germany)

Anti-GFP: Monoclonal antibody was obtained by immunizing mice with partially purified recombinant *Aequorea victoria* GFP as immunogen. Anti-GFP recognizes both wild-type and mutant forms of GFP (Roche, Cat. No. 1814460).

Anti-Myc: Polyclonal antibody from rabbit, raised against sequence within the carboxy terminal domain of human c-Myc (Santa Cruz Biotechnology, USA)

Anti-HA (16B12): Monoclonal antibody from mouse, raised against sequence CYPYDVPDYASL specifically recognizes the influenza hemagglutinin epitope (YPYDVPDVA) (Covance Inc., USA).

Anti-Phospho-p44/42 MAP Kinase (Thr202/Tyr204) (E10): Monoclonal antibody is produced by immunizing mouse with a synthetic phospho-peptide (KLH-coupled) corresponding to residues surrounding Thr202/Tyr204 of human p44 MAP kinase. It detects endogenous levels of p44 and p42 MAP kinase (Cell Signaling Technology®).

2.3.2. Secondary antibodies

Anti-mouse IgG: Alkaline phosphatase conjugate (whole molecule), antibody developed in goat (polyclonal, Sigma).

Anti-rabbit IgG: Alkaline phosphatase conjugate (whole molecule), antibody developed in goat (polyclonal, Sigma).

2.4. DNA work

2.4.1. Southern blotting

Genomic DNA was extracted from young plant leaves using a DNeasy[®] plant mini kit (Qiagen) according to the manufacturer's protocol. Approximately 4 µg of DNA was digested with specific restriction endonucleases in 50 µl of restriction reaction at 37°C overnight. The digested DNA was precipitated with 1/10 volume of 3 M sodium acetate (pH 5.2) and 2 volumes of 96% ethanol at -20°C for one hour followed by centrifugation for 5 min 13,000 rpm at 4°C. The precipitated DNA was dissolved in 10 µl TE (10mM Tris-HCl, pH8.0, 1mM EDTA, pH8.0) combined with 1 µl BlueJuice[™] Gel Loading Buffer (65% [w/v] sucrose, 10mM Tris-HCl pH7.5), 10mM EDTA, 0.3% [w/v] Bromophenol Blue) and loaded on 0.8% agarose gel containing 0.5 µg/ml ethidium bromide in 1x TBE buffer (89mM Tris base, 89mM boric acid, 2 mM EDTA). The gel was run at 5 volts per cm until the dye ran off the gel. After electrophoresis the gel was photographed and the DNA was denatured by incubating it in the following solutions with gentle agitation at RT: 10 min 0.25N HCl, 1 min sterile deionised water, 3x10 min denaturation solution (1.5M NaCl, 0.5M NaOH), 1 min sterile deionised water, 2x15 min neutralization solution (1.5M NaCl, 1M Tris base, 1mM EDTA, pH 7.4), 5 min sterile deionised water. DNA fragments, separated by electrophoresis, were transferred to Hybond[™]-N⁺ nitrocellulose membrane (Amersham Biosciences) by capillary action in 10xSSC buffer (1.5M NaCl, 0.15M sodium citrate (C₆H₈O₇Na₃ x 2H₂O), pH 7.0) overnight. The transferred DNA was cross-linked to the membrane by irradiation to 245 nm ultraviolet light. The membrane was prehybridized in a solution containing 5xSSC, 0.1% [w/v] SDS, 5% [w/v] Dex.SO₄ ((C₆H₉O₅SO₃Na)_{n+1}), 1/20 volume Liquid Blocking agent (Amersham Biosciences) at 62°C rotating for 2 hours and hybridised in the same solution containing the denatured labelled probe at 63°C rotating overnight. Afterwards the membrane was washed with first wash solution (1xSSC, 0.1% [w/v] SDS) at 60°C rotating for 15 min, followed by the second wash with a buffer containing 0.5xSSC and 0.1% [w/v] SDS in the same conditions. Next, the membrane was incubated in 1/10 volume Liquid Blocking agent in diluent buffer (0.1M Tris-base, 0.3M NaCl, pH 7.5) with gentle agitation at room temperature for one hour. Antibody incubation and detection was performed using

a Gene Images™ CDP-Star™ Detection Kit and Hyperfilm™-ECL™ (Amersham Biosciences) according to the manufacturer's manuals.

To generate a probe specific to LB for pAC161 T-DNA (GABI-Kat), pCR21-GABI-Kat vector (created by Wilfried Rozhon) was digested with *EcoRI* restriction endonucleases. The 419 bp DNA fragment was isolated and labelled using a Gene Images™ Random-Prime DNA Labelling Kit (Amersham Biosciences) according to the manufacturer's protocol.

2.4.2. DNA extraction from leaf tissues

Genomic DNA was extracted from young leaves or cotyledons using the PRECELLYS®24 homogeniser (Peqlab Biotechnologie GmbH, France). The fresh or treated tissues were put in 2ml tube containing 1.4 mm Ø ceramic beads and frozen immediately. The frozen leaves were vigorously homogenised at 5000 rpm for 5 seconds at room temperature. After becoming fine green powder, the tubes were immediately put on ice and added with 200 µl CTAB buffer (2%CTAB, 1.4M NaCl, 20mM EDTA, 100mM Tris-HCl pH8.0, 10µl/ml β-ME). The homogenate was transferred to a new 1.5 ml appendorf tube and incubated in a Thermomixer, eppendorf AG, Germany and shaken at 500 rpm 60°C for 30 min. The purification step was done twice by adding 150 µl chloroform/isoamyl alcohol (24:1). The tubes were vigorously vortexed and spun in a Sigma3K30 centrifuge instrument at 10,000 rpm at 4°C for 10 min. The clear upper phase containing gDNA was transferred to new 1.5 appendorf tubes. Genomic DNA was precipitated in 2/3 volume of isopropanol, washed with 70% ethanol and dissolved in RNase-water.

2.4.3. Creation of loss-of-function mutations of AP2C2

2.4.3.1. Site directed mutagenesis

cDNA of AP2C2 was mutated using the QuikChange Site II - Directed Mutagenesis kit (Stratagene) to introduce the single amino acid exchange glycine (G) to aspartic acid (D) at position 155 (lof1), glycine (G) to arginine (R) at position 155 (lof2) or arginine (R) to alanine (A) at position 287 (lof3). The basic procedure utilizes a supercoiled dsDNA vector (pGEM-Teasy) with an insert of interest (cAP2C2) and two synthetic oligonucleotide primers containing the desired mutation (see 2.2.3.). PCR using PfuTurbo DNA polymerase (Stratagene) was performed with 18 cycles of denaturation at 95°C 30 second, annealing at 55°C for 1 min, polymerization at 68°C for 5 min and 68°C for 10 min.

Following temperature cycling, the product was treated at 37°C for 1 hour with DpnI endonuclease (target sequence: 5'-Gm6ATC-3'), which is used to digest the parental DNA template and consequently selected for mutation-containing synthesized DNA. The nicked PCR product was then transformed into XL1-Blue Supercompetent *E.coli* cells (cat.no.200236, Stratagene) according to the instruction. The mutated constructs were verified by sequencing and cloned into pGEX-4T-1 vector.

2.4.3.2. AP2C2-RNAi plasmid construction

AP2C2-RNAi plasmid was created according to the Catma1a06210 DNA fragment designed by the Complete *Arabidopsis* Transcriptome MicroArray (CATMA) database of the AGRIKOLA project (*Arabidopsis* Genomic RNAi Knock-out Line Analysis). The 160 bp DNA fragment, amplified from pGEM-cAP2C2 using primers 5' AACCATGGGTCTCCCAC ATCTCCGTTCTGCCT 3' and 5' TTGCGGCCGCTGCATT CGATATAGGAGCTGCAA 3' (done by Julija Umbrasaitė), was cloned into pGEM-Teasy vector, sequenced and then cloned into pENTR4-B gateway entry vector. The resulting pENTR-AP2C2-RNAi entry plasmid was mixed with the destination vector for *Agrobacterium*-mediated plant transformation, pB7GWIWG2 (provided by Dirk Inze, Flanders Interuniversity, Gent, Belgium) (Karimi et al., 2002) in the presence of Gateway®LR Clonase Enzyme mix (Invitrogen) according to the instruction of the kit. The reaction was placed at RT overnight and then treated with 2 µl proteinase K at 37°C for 10 min. After enzyme inactivation at 65°C for 10 min, all reaction was transformed into DH5α competent *E.coli* cell. The positive colonies were identified by bacterial growth on the medium containing spectinomycin. The DNA plasmid was extracted and analyzed by restriction enzyme analysis.

2.5. RNA work

2.5.1. RNA extraction

Total RNA from plant leaves was isolated using Tri®Reagent (Sigma, T9424). Approximately 25 mg of leaves were frozen in liquid nitrogen and then ground with a cold pestle and a mortar until becoming green powder. 500 µl Tri®Reagent was added and mixed using mortar until homogeneous and then incubated at 60°C for 5 min. The mixture was transferred to ice and centrifuged using a Sigma3K30 centrifuge at 12,000 rpm, at 4°C, for

10 min. 400 µl of clear brown supernatant was transferred to a new tube and was cleaned by vigorous vortexing in 100 µl of chloroform. After standing at RT for 3 min, the tubes were centrifuged at 10,000 rpm, for 15 min, at 4°C. 220 µl of clear colourless upper phase was transferred to a new tube. Total RNA was precipitated with ½ volumes (110 µl) of isopropanol and ½ volumes (110 µl) of 0.8M Sodium citrate/1.2M NaCl. After centrifugation, pellets were washed and dissolved in 40 µl DEPC water.

2.5.2. Reverse transcription

Complementary DNA (cDNA) was produced from total RNA solution. The RNA solution was incubated at 55°C for 10 min and mixed well prior use. In each reaction, 9 µl of RNA solution containing 1µg RNA was mixed with 1.5µl 400µM oligoT and incubated at 65°C for 10 min. After adding 9.5 µl of the master mix containing, 1xbuffer (supplied with transcriptase), 1unit Ribulock™ RNase inhibitor (Fermantas), 10mM DTT (supplied with transcriptase), 25mM dNTP and 1unit of Expand Reverse transcriptase (Roche), the reaction was incubated at 42°C for 90 min. Then 1 µl of the cDNA reactant was used for PCR with the specific primers.

2.6. Protein work

2.6.1. Protein extraction from plants and protoplasts

Proteins were extracted from *Arabidopsis* leaves. 100 mg of plant tissue was frozen in liquid nitrogen and stored at -80°C. All the extraction steps were carried out at 0°C or 4°C. The frozen samples were disrupted by grinding using a pre-chilled mortar and pestle in 400 µl extraction buffer (25mM Tris-HCl, pH 7.8, 10mM MgCl₂, 15mM EGTA, 75mM NaCl, 1mM dithiothreitol, 1mM NaF, 0.5mM NaVO₃, 15mM β-glycerophosphate, 0.1% [v/v] Tween-20, 15mM *p*-nitrophenylphosphate, 0.5mM PMSF, leupeptine (5 µg/ml), aprotinin (5 µg/ml)). The homogenate was transferred into a microcentrifuge tube and centrifuged in a Sigma3K30 instrument for 35 min. for 18,000 rpm at 4°C. The supernatant was transferred into a new microcentrifuge tube and protein concentration was estimated by Bradford assay (§ 2.6.2.). Protein extract was diluted to an appropriate concentration (1-2 mg/ml). Protein extracts were stored at -20°C combined with 4xSDS buffer (200mM Tris-HCl pH6.8, 400mM DTT, 8% [w/v] SDS, 40% [v/v] glycerol, 0.1% [w/v] bromphenol blue).

2.6.2. Determination of protein concentration

Protein concentration was quantified by Bradford assay. Bradford assay dye reagent (Bio-Rad Protein Assay Dye Reagent Concentrate, cat. no. 500-0006) was diluted with deionised water 1:5. 2-10 μ l of protein extract was mixed with 1 ml diluted dye reagent in a plastic cuvette by vortexing, and incubated at room temperature for 15-20 min. The optical density was measured at 595 nm. Protein concentration was calculated by comparing the A_{595} with the BSA standard curve.

2.6.3. SDS-PAGE

SDS PAGE was performed using a Hoefer Mighty Small gel running system. Protein extracts combined with 4xSDS buffer (§ 2.6.1.) were heated at 95°C for 2 min. Equal amounts of protein extract were loaded on a 10% SDS PAA separating gel (0.375 M Tris-HCl, pH 8.8, 0.1% [w/v] SDS, 10% [v/v] acryl-bisacrylamide mix, 0.04% [v/v] N,N,N',N'-Tetramethyl-1-, 2-diaminomethane (TEMED), 0.1% [w/v] ammonium persulfate) with a 5% stacking gel (0.125 M Tris-HCl, pH 6.8, 0.1% [w/v] SDS, 5% [v/v] acryl-bisacrylamide mix, 0.1% [v/v] TEMED, 0.1% [w/v] ammonium persulfate). For western blotting 10-15 μ g of protein extract was loaded per lane. 0.75 mm thickness gels were run at 15 mA, and 1.5 mm gels were run at 20 mA in a running buffer containing 0.1 M Tris base, 0.384 M glycine, 0.1% [w/v] SDS, pH 8.8, until the dye ran out of the gel.

2.6.4. Western blotting

Following electrophoresis, proteins in a polyacrylamide gel were transferred to polyvinylidene difluoride membranes (Millipore) in a buffer-tank-blotting apparatus. The transfer was carried out at 75V for 2.5 hours. Transfer efficiency was checked by staining proteins on the membrane in Ponceau S (0.5% [w/v] Ponceau S, 1% [v/v] glacial acetic acid) for 30 s with gentle agitation, and destaining in water for 30 s. Membranes with transferred proteins were incubated in blocking solution (TBS-T buffer (50mM Tris base, 150mM NaCl, 0.1% [v/v] Tween 20) with 5% nonfat dried milk (obtained from a local manufacturer) for 2 hours at room temperature with gentle agitation. Afterwards they were probed with monoclonal 1:5,000 antiGFP antibody or polyclonal antiMPK3, antiMPK4, and antiMPK4 diluted 1:10000 in TBS-T buffer containing 5% [w/v] nonfat dried milk for 12-16 h at 4°C with gentle agitation. The membranes were washed in TBS-T buffer containing 5% [w/v] nonfat dried milk by changing the washing solution four times every

15 minutes. Secondary anti mouse IgG developed in goat (Sigma, A-5153) and anti rabbit IgG (Sigma) diluted 1:5000 in TBS-T containing 1% [w/v] nonfat dried milk were used to locate antiGFP and antiMPK's, respectively. The probing with secondary antibody was carried out for 1 hour at room temperature. Afterwards the membranes were washed in TBS-T buffer by changing the buffer eight times every 20 minutes. Chemiluminescent detection reaction was performed using CDP-star detection reagent (Amersham Biosciences) according to manufacturer's recommendations. Membranes were exposed to HyperfilmTM-ECL filmTM (Amersham Biosciences).

2.6.5. Expression and purification of GST-fusion proteins

GST-fusion proteins were extracted from *E.coli* strain DH5 α containing the gene of interest in pGEX-4T-1 plasmid. The single colony was inoculated in 100 ml LB containing ampicillin (50 mg/ml in H₂O) and then shaken O/N at 37°C. The overnight inoculum was diluted to A₆₀₀ 0.2 in 300 ml LB + ampicillin and further shaken at 28°C until A₆₀₀ 0.8 before induction by 1mM IPTG at 28°C for 2 hours. The induction culture was transfer to 50ml Falcon tubes and centrifuged in an Eppendorf 5810R centrifuge instrument at 4°C at 4,000 rpm for 10 min. The supernatant was completely removed before adding 10 ml lysis buffer (50mM Tris-HCl pH 8.0, 10mM MgCl₂, 150mM NaCl, 1% NP-40, 1 tab protease inhibitor). The homogenous pellets were sonicated at 50/50 cycle 10 sec 3 times on ice and then centrifuged in pre-cooled SS34 centrifuge tubes in Sorvall[®] RC5C instruments Dupont at 14,000 rpm 4°C for 20 min. Supernatant was mixed with 200 μ l 50% slurry GST-sepharose beads (Amersham Biosciences) and rotated 30 min in a cold room before being applied into Poly-Prep Chromatography Columns (BioRad). The column then was washed with ice-cold washing buffer (50mM Tris-HCl pH8.0, 10mM MgCl₂, 1% NP-40) and then eluted with freshly prepared 10mM reduced glutathione. 5-6 fractionates were kept and the protein amount was checked by Bradford assay and in 10%SDS PAGE.

2.6.6. *In vitro* kinase assay

Kinase assays were performed according to (Meskiene et al., 2003). Protein extracts were prepared as described in § 2.6.1. For immunoprecipitation of AtMPK3, AtMPK4, and AtMPK6, crude anti-MPK3 (1:5,000), anti-MPK4 (1:5,000), and anti-MPK6 (1:10,000) antibodies were used, respectively. 100 μ l (1 μ g/ μ l) of cleared supernatant was incubated with 20 μ l of protein A Sepharose CL-4B beads (GE Healthcare) and 3-5 μ l of an

appropriate antibody for 12-16 h rotating at 4°C. The beads were washed three times with wash buffer (50 mM Tris, pH7.4, 250mM NaCl, 5mM EGTA, 5mM EDTA, 0.1% [v/v] Tween-20, 5mM NaF, 0.1% [v/v] Nonidet P-40, 0.5mM PMSF) and once with kinase buffer (20mM Hepes, pH 7.5, 15mM MgCl₂, 5mM EGTA, 1mM DTT). Kinase reactions with the immunoprecipitated MAPKs were performed for 30 min at RT in 15 µl of kinase buffer containing 1.5 µg of MBP and 3 µCi of [γ -³²P]ATP. The reaction was stopped by adding 4xSDS. SDS-PAGE was performed as described § 2.6.3. Afterwards gels were stained in Coomassie Blue staining solution (0.25% [w/v] Coomassie Brilliant Blue R-250, 45% [v/v] methanol, 10% [v/v] acetic acid) for 5 min, and destained with regular changes of destaining solution (45% [v/v] methanol, 10% [v/v] acetic acid) for 1.5 h. The gels were placed on 3 mm Whatman paper and dried at 80°C for 45 min. The phosphorylation of MBP was analysed by autoradiography.

2.6.7. In gel kinase assay

In gel kinase assay was performed as described (Shibuya et al., 1992) with some modifications. A 12.5% separating SDS PAGE (0.375M Tris-HCl pH8.8, 0.1% [w/v] ammonium persulfate) containing 0.5 mg/ml of myelin basic protein with 5% stacking gel was poured in a Hoeffer minigel cast using 0.75 mm spacers. Protein extracts were prepared as described §2.6.1. Samples (15 µg of total protein extract/lane) and a prestained molecular weight marker were loaded on a polymerised gel and run at 10 mA/gel in running buffer (§2.6.3). After electrophoresis, SDS was removed from the gel by washing it with 100 ml 20% isopropanol in 50mM Tris-HCl pH8.0 for 1 hour at room temperature with continuous agitation, and changing the wash buffer two times. Afterwards the gel was incubated for 1 hour in 200 ml buffer containing 50mM Tris-HCl pH8.0 and 5mM DTT with continuous agitation. The denaturation was performed by incubating the gel in 50 ml denaturation solution (6M guanidine-HCl, 20mM DTT, 2mM EDTA, 50mM Tris-HCl pH8.0) at RT with continuous agitation and changing the solution twice with 30 min interval. The proteins were renatured by incubating the gel in a buffer containing 50mM Tris-HCl pH8.0, 5mM DTT, 0.04% [v/v] Tween-40 for 12-18 hours at 4°C and with 7 buffer changes 200 ml each without agitation. Afterwards the gel was pre-incubated in 10 ml of kinase assay buffer (50mM Hepes-HCl pH8.0, 2mM DTT, 0.1mM EGTA, 20mM MgCl₂) at RT with continuous agitation for 30 min.

The kinase reaction was performed by incubating the gel in 20 ml of kinase assay buffer containing 30 μ M ATP and 50 μ Ci [γ - 32 P] ATP (3000 ci/mmol) for 1 hour at RT with continuous agitation. After that the gel was washed 6 times with 10% [w/v] TCA containing 1% [w/v] sodium pyrophosphate. The washes were performed repeatedly for about 1.5 hours to reduce the background. The gel was dried under vacuum on 3 mm paper and exposed to X-ray sensitive film at -80°C overnight.

2.6.8. *In vitro* phosphatase assay

2.6.8.1. Casein substrate labelling

1 mg of hydrolyzed and partially dephosphorylated casein (Sigma, C4765) was labeled by using ~100 μ Ci γ - 32 P ATP and ~25 units of catalytic subunit of protein kinase A (Sigma, P2645) in a buffer containing 50mM Tris-HCl pH7.0 and 5mM MgCl₂. After incubation for 30 min at 30°C the reaction was stopped by adding 5x volume of 20% TCA in 20 μ M NaH₂PO₄. The precipitated casein was pelleted by centrifuging for 1 min 10000g and washed 8-10 times with 20% TCA/20 μ M NaH₂PO₄. Finally, the casein was dissolved in 0.4 ml of 0.2M Tris-HCl pH8.0. The efficiency of γ - 32 P incorporation was determined by measuring with a scintillation counter. 5 μ l of labelled casein (~2.5 mg/ml) were mixed with 750 μ l acidic charcoal mixture (0.9M HCl, 90mM Na-pyrophosphate, 2mM NaH₂PO₄, 4% v/v NoritA) in a microcentrifuge tube and incubated for 10 min at room temperature. Afterwards the tube was centrifuged for 5 min 10,000g. The β emissions of pellet (labelled casein) and supernatant (unincorporated γ - 32 P, i.e. background) was quantitated as counts per minute (cpm) in a Tri-carb 1600 TR Liquid scintillation counter (Packard). The background was ~0.1%, i.e. the labelled casein gave ~200,000 cpm, whereas the background gave ~200 cpm.

2.6.8.2. MPK6 substrate labelling

The pGEX-MPK6-lof (K/M) plasmid provided by Markus Teige was used as the substrate. The MPK6-lof protein lost the phosphorylation ability and was suitable for phosphatase activity assay. The GST-MPK6-lof protein was isolated and purified from *E.coli* and then was phosphorylated by GST-MKK4 with a ratio of 10:1 using ~100 μ Ci γ - 32 P ATP in a buffer containing 50mM Tris-HCl pH7 and 5mM MgCl₂. After incubating for 1 hour at 30°C the reaction was stopped by passing the reaction through a PD-10 Desalting column (GE Healthcare) containing Sephadex G-25 medium. 10 fractions of 500 μ l elution buffer

(50mM Tris-Cl pH8.0, 1mM DTT, 10mM MgCl₂) were collected. The efficiency of the $\gamma^{32}\text{P}$ incorporation was determined by measuring with a scintillation counter. 5 μl of labelled MPK6 were mixed with 750 μl acidic charcoal mixture (0.9M HCl, 90mM Na-pyrophosphate, 2mM NaH₂PO₄, 4% v/v NoritA) in a microcentrifuge tube and incubated for 10 min at RT. Afterwards the tube was centrifuged for 5 min 10,000g. The β emissions of pellet (labelled MPK6) and supernatant (unincorporated $\gamma^{32}\text{P}$, i.e. background) was quantitated as counts per minute (cpm) in a Tri-carb 1600 TR Liquid scintillation counter (Packard).

2.6.8.3. Substrates dephosphorylation

The phosphatase assay was carried out in a total volume of 50 μl containing 50 mM Tris-HCl pH 8.0, 0.1mM EGTA, 1mM DTT, 10mM MgCl₂, 0.1 μM okadaic acid, and radio-labelled substrate in the presence of GST-protein phosphatases (extraction and purification method according to § 2.6.5). Approximately 0.1 or 1 μg of GST-phosphatase protein was incubated with the reaction mixture at 28°C for 30/60 min. The reaction was terminated by the addition of 0.75 ml of acidic charcoal mixture (0.9N HCl, 90mM Na-pyrophosphate, 2mM NaH₂PO₄, 4% (w/v) NoritA. Samples were centrifuged, and the amount of radioactivity in 0.5 ml of supernatant was determined by scintillation counting. The phosphatase activity was expressed as free phosphate released per minute per milligram of protein (CPM/mg).

2.6.9. Catalase activity measurement

1-month-old whole plants were exposed to high-light for 3 hours before leaf collection. The 25 mg frozen leaves were ground in 200 μl extraction buffer (60mM Tris pH7, 1mM PMSF, 10mM DTT) till homogeneity. After centrifugation at 13,000 g for 10 min at 4°C, the supernatant was kept for catalase activity measurement. The catalase activity measurement method was modified from Beer and Sizer (Beers and Sizer, 1952) that the disappearance of peroxide is followed spectrophotometrically at OD₂₄₀ nm. One unit decomposes one micromole of H₂O₂ per minute at 25°C and pH7.0. The reaction was made in 1 ml of H₂O composed of 20 μg protein extracts, and 20 μl 3.26M H₂O₂ (or 10%) at RT. A₂₄₀ was recorded at 0 and 10 min after adding protein extracts. The decrease of A₂₄₀ corresponded for the disappearance of H₂O₂ by catalase activity. The enzymatic activity

was expressed as percentage of units per milligram of protein:

$$\text{Units / mg protein} = \frac{(A_{240} - 0.0192) \times 1000}{0.02 \times 10 \text{ min} \times \text{Protein (mg/ml)}}$$

2.7. Bacterial work

2.7.1. *Escherichia coli*

2.7.1.1. Production of competent *E.coli* (Inoue et al., 1990)

Overnight culture from a fresh single colony of *E.coli* DH5 α was inoculated in 10ml LB medium and cultivated at 37°C on the shaker at 180-200 rpm for overnight. The overnight culture again was diluted to $A_{600} \sim 0.3$ in 80 ml SOB medium (2%(w/v) Trypton, 0.5% Yeast Extract, 10mM NaCl, 2.5mM KCl, 10mM MgCl₂, 10mM MgSO₄) in 1 liter flask and grown at 30°C ~200 rpm till $A_{600} \sim 0.6$. After the culture was cool on ice for 10 min, it was transfer to two sterile SS34 tubes and centrifuged at 1500g (3,500rpm) for 10min at +4°C. Supernatant was removed carefully. The cells were kept on ice and then were resuspended in 22 ml of ice-cold TB buffer (10mM Pipes, 15mM CaCl₂, 250mM KCl, 55mM MnCl₂ pH 6.7) and further kept on ice for 10min. The cells were precipitated again by centrifugation at +4°C 3500 rpm for 10min and were resuspended in 4 ml of ice-cold TB buffer. After adding 7% DMSO, the cells were kept on ice for 10 min and then were aliquoted into sterile appendorf tubes with a cut yellow tip and frozen immediately in liquid nitrogen. The competent cells could be stored at -80°C for long.

2.7.1.2. Transformation of *E.coli*

Plasmid DNA (~ 0.5-1 μ g) or ligation reaction was added into competent cells on ice. The cells were put on ice for 30 min, followed by heat shock at 42°C for 1 min and then put back again on ice for 10 min. After adding 1ml LB medium, the suspension cells were incubated at 37°C for 1 hour on a shaker. The cell pellets after centrifugation were plated on LB plate containing the appropriate antibiotic.

2.7.2. *Agrobacterium tumefaciens*

2.7.2.1. *Agrobacterium tumefaciens* strains

A. tumefaciens strain GV3101 containing Ti-plasmid pMP90 and helper plasmid pSOUP was used (Table. 2.1.).

2.7.2.2. Cultivation of *A. tumefaciens*

Agrobacterium tumefaciens was grown at 28°C with a generation time of 1-2 hours. Colonies on solid media were visible only after 2 days of incubation. For selection of *Agrobacterium tumefaciens* GV3101/pSOUP, the rifampicin, gentamycin and tetracycline antibiotics were used.

2.7.2.3. Preparation of *A. tumefaciens* electrocompetent cells

A starter culture was initiated by inoculation with a single colony in 5 ml LB broth (1% [w/v] trypton, 0.5% [w/v] yeast extract, 1% [w/v] NaCl, pH7.5) with the appropriate antibiotics and grown overnight at 28°C with vigorous shaking. The overnight culture was diluted to A₆₀₀ 0.04 - 0.08 in 100 ml of the same medium and grown until A₆₀₀ had reached 0.5 (normally ≥ 4 hours). The cells were collected by centrifugation for 10 min 4000 rpm at 4°C and resuspended in 40 ml 1mM Hepes pH7.0. The cells were collected by centrifuging for 10 min at 4000 rpm 4°C and resuspended in 40ml 1 mM Hepes/10% [v/v] glycerol. The cells were spun down for 10 min at 4000 rpm 4°C and resuspended in 2 ml 1mM Hepes/10% [v/v] glycerol. The cells were split into two microcentrifuge tubes and spun down 2 min 6000 rpm. Finally, the cells were resuspended in 200µl of 1mM Hepes/10% [v/v] glycerol, aliquoted into 40 µl, frozen in liquid nitrogen and stored at -80°C.

Table 2.1. Antibiotics for selection of *A. tumefaciens* GV3101 strain

Selection	Antibiotic	Concentration	Solvent
Chromosome	Rifampicin	50 µg/ml	Methanol
Ti-plasmid pMP90	Gentamycin	50 µg/ml	Water
Helper plasmid pSoup	Tetracycline	2 µg/ml	Ethanol

2.7.2.4. *Agrobacterium* transformation by electroporation

Electroporation was performed using BioRad Gene PulserTM with capacitance 25 µF, voltage 2,5 kV, and resistance 400 Ω. Electrocompetent *Agrobacterium* cells were thawed on ice, mixed with 1-2 µl DNA (~200 ng). The DNA/cell mixture was transferred to a chilled cuvette on ice avoiding air bubbles. The cuvette was cleaned with tissue paper and

inserted into the cuvette chamber. After the pulse (followed by 8-9 ms delay) the cuvette was removed and 1 ml cold LB (without antibiotics) was added. The solution was mixed gently by pipetting up and down. The cells were transferred to a microcentrifuge tube and incubated at 28°C for 2-4 hours with vigorous agitation. The cells were collected by centrifugation for 2 min at 6,000 rpm, resuspended in 100 µl LB. 1/10 volume was plated on the LB with antibiotics plate and then the rest on the LB with antibiotics plate. The plates were incubated at 28°C until colonies appeared (2-3 days).

2.7.2.5. Selection of transformants

Agrobacterium colonies that were able to grow on selection medium were examined by PCR to confirm the presence of plasmid of interest. Briefly, *Agrobacterium* overnight cultures were inoculated with single colonies, and DNA was isolated by standard miniprep procedure. Isolated DNA was used as a template for PCR reaction. The PCR reaction was performed with Taq polymerase according to manufacturer's protocol using the gene specific primers.

2.7.2.6. Preparation of *Agrobacterium* frozen stocks

Positive *Agrobacterium* colonies selected by PCR were used to inoculate 1.5 ml liquid culture. The culture was incubated at 28°C with vigorous agitation. 1,240 µl of saturated overnight culture was combined with 260 µl sterile 87% [v/v] glycerol in a cryotube and was frozen in liquid nitrogen and stored at -80°C.

2.8. Yeast work

2.8.1. Yeast strains

LexA-system : L40 (MATa trp1 leu2 his3 LYS2 lexA-HIS3 URA3 LexA-lacZ)

GAL4-system : PJ69-4A (MATa trp1-901 leu2-3112 ura3-52 his3-200 gal4. Δ. gal80.

Δ. LYS2 GAL1-HIS3 GAL2-ADE2. met2GAL7-lacZ).

2.8.2. Yeast one-step transformation

Yeast was transformed using lithium acetate (LiAc)/single-stranded DNA (ssDNA)/polyethylene glycol (PEG) protocol. 2-6 day-old yeast colonies were transformed. 10-15 µl volume of yeast cells was removed from the plate with a sterile

toothpick into a sterile 1.5 ml microcentrifuge tube. 2 μ l (~500 ng) of plasmid DNA was added to yeast and mixed by vortexing. 150 μ l of transformation mixture (39% [w/v] PEG4000, 0.2 M LiAc, 0.1 M DTT, and 375 ng/ μ l ssDNA) was combined with the yeast, and incubated for 30 min at 42°C. PEG was washed by 1 ml sterile synthetic dropout (SD) medium (0.67% [w/v] yeast nitrogen base, 2% [w/v] glucose) and centrifuged for 2 min at 3000 rpm. Finally, the yeast was resuspended in 50-100 μ l sterile SD medium, plated on selective SD plates and incubated at 28°C until colonies appeared. Yeast clones with active both *HIS3* and *lacZ* (β -galactosidase liquid assay § 2.8.3) reporter genes were subjected for further analysis. The protein-protein interaction was evaluated by the growth of yeast on SD media without tryptophan, leucine and histidine supplemented with 6mM 3-aminotriazole (3AT; a competitive inhibitor of His3p) (SD-W-L-H+AT) and quantitative β -galactosidase assay.

2.8.3. β -galactosidase assay

Fresh yeast cultures were assayed to ensure that the GAL-*lacZ* reporter was induced to optimal levels. Yeast cells were scraped from a plate, resuspended in 1 ml SD medium, and the optical density was measured at 600 nm. The suspension was diluted in 9 ml SD-W-L to have $A_{600} \sim 0.3$ ($\sim 3 \times 10^6$ cells/ml), divided into three tubes 3 ml each, and grown at 30°C with vigorous agitation until A_{600} had reached ~ 0.8 -1.0. The cells were collected by centrifugation for 2 min at 13000 rpm. The supernatant was removed and the cells were resuspended in 200 μ l lysis buffer (25 mM Tris-HCl pH 7.5, 20 mM NaCl, 8 mM MgCl₂, 5 mM DTT, 0.1% [v/v] NP-40). The Microcentrifuge tubes with the cells were frozen in liquid nitrogen and stored at -80°C. Yeast cells were disrupted by vortexing with ~ 300 μ l glass beads (425-600 nm diameter) for 20 min at 4°C. The tubes were centrifuged for 10 min at 14,000 rpm. The supernatant was transferred to a fresh tube and protein concentration was determined by Bradford assay (§ 2.6.2). For ONPG assay 50 μ l protein extract was mixed with 650 μ l Z-buffer containing β -ME (16.1 g/l Na₂HPO₄ x 7 H₂O, 5.5 g/l NaH₂PO₄ x H₂O, 0.75 g/l KCl, 0.246 g/l MgSO₄ x 7 H₂O, 0.5 % [v/v] β -mercaptoethanol) and 150 μ l o-nitrophenyl- β -D-galacto-pyranoside (ONPG, dissolved in Z-buffer to concentration 4 mg/ml). The reaction was incubated at 37°C till yellow colour developed and stopped by adding 400 μ l of 1.0 M NaCO₃. 1 ml of the reaction was transferred to a plastic cuvette and extinction at 420 nm was measured. The enzymatic

activity was expressed as β -galactosidase units per milligram of protein:

$$\text{Units } \beta\text{-galactosidase / mg protein} = \frac{A_{420} \times 25 \times 1000}{45 \times \text{Minutes} \times \text{Protein (mg/ml)}}$$

2.8.4. cDNA library screening:

2.8.4.1. Two-hybrid library and yeast vectors

Arabidopsis two-hybrid library (consisting of a 1:1 mix of auxin induced and uninduced seedling roots) provided by Dr. Bert van der Zaal, Institute of Molecular Plant Sciences, Leiden University, The Netherlands. cDNA was inserted in the multiple cloning site of the pACT2 vector (EcoRI/XhoI). *AP2C2* cDNA fused to GAL4 binding domain in pBDcam vector (Stratagene) was used as bait for the screening.

2.8.4.2. Yeast transformation

Yeast containing *AP2C2* in pBDcam vector was inoculated in 100 ml SD liquid medium without tryptophan (SD-W) and grown at 30°C with vigorous agitation until culture was in mid-logarithmic phase. The cells were harvested by centrifugation at 3000 rpm for 5 min and washed with 20 ml sterile water. The pellet was resuspended in 10 ml 100mM LiCl. The yeast suspension was divided out into ten microcentrifuge tubes and centrifuged at 3000 rpm for 5 min. The following components were added in the order indicated and mixed thoroughly by vortexing: 10 μ l ssDNA (10 mg/ml), 1 μ g plasmid DNA (in pACT vector) and 290 μ l transformation mix, consisting of 240 μ l 50% [w/v] PEG 3500, 18 μ l 2M LiAc, 33 μ l sterile water. The yeast was incubated 30 min at 42°C, washed as described § 2.8.2 and plated on SD -L-W-adenine plates.

2.8.4.3. Characterization of putative interacting proteins

Yeast clones with active both *ADE2* and *lacZ* (β -galactosidase liquid assay § 2.8.3) reporter genes were subjected to further analysis. *AD:cDNA* plasmids were isolated from yeast, amplified by transforming into *E. coli* and analysed by restriction enzyme digestion. Plasmid DNA isolated from *E. coli* was transformed back into the yeast strain containing the *BD:AP2C2* and tested for activation of both the *ADE2* and *lacZ* reporter genes. The positive clones were sequenced.

2.8.4.3.1. Plasmid rescue from yeast

Individual positive clones were inoculated into 2 ml SD-L-W medium and grown overnight. The cells were collected by centrifugation for 3 min at 6000 rpm. The pellet was resuspended in 100 µl STET (8% [w/v] sucrose, 50mM Tris-HCl pH 8.0, 50mM EDTA, 5% [v/v] Triton X-100). Approximately 200 µl volume of glass beads (425-600 nm diameter) was added and vortexed for 5 min to disrupt the cells. The tube was heated at 95°C for 3 min, then placed briefly on ice, and then centrifuged for 10 min at 13,000 rpm 4°C. 100 µl of supernatant was transferred into a new microcentrifuge tube containing 50 µl 7.5M ammonium acetate. The mixture was centrifuged for 10 min at 13,000 rpm 4°C following 1 hour incubation at -20°C. 100 µl supernatant was combined with 200 µl 96% ethanol in a new microcentrifuge tube and centrifuged for 15 min at 15,000 rpm 4°C. The DNA pellet was washed with 70% ethanol, dried at room temperature and dissolved with 20 µl sterile water.

2.8.4.3.2. Sequencing of interacting clones

cDNA library plasmids were sequenced with a fwd: 5'-GAAGATACCCACCAAACCCA-3' primer that anneals 31 nucleotide upstream the end of GAL4 activation domain. The sequences were analysed using the BLAST 2.0 algorithm (<http://mips.gsf.de/proj/thal/dl/> and <http://www.ncbi.nlm.nih.gov/BLAST/>).

2.9. Plant work

2.9.1. Plant lines

Transgenic *Arabidopsis thaliana* plants were generated by *Agrobacterium* - mediated transformation. T-DNA insertional knockout lines were obtained from *Arabidopsis* Biological Resource Centre (ABRC) or from The Nottingham *Arabidopsis* Stock Centre (NASC). Double or Triple knockout lines were created by crossing over between single knockout lines (Table 2.2).

2.9.2. Plant growth conditions

Arabidopsis plants were grown aseptically or under non-sterile conditions. In both cases seeds were kept at 4°C for 3 days to break the dormancy and grown at 22°C and 60% relative humidity. Plants were grown in a short-day (8h light/16h dark) or a long-day (16 hours light/8 hours dark) photoperiod.

2.9.2.1. Non-sterile *Arabidopsis* growth

Seeds were sown on the mixture of soil, sand and vermiculite (10:6:1), covered to contain the humidity and put in cold room (+4°C) for 3 days. The cover was removed when cotyledons had fully expanded. Plants were grown under short-days for the first five-six weeks. Later on plants were moved to the long-day photoperiod to induce flowering. The seeds were collected when the siliques were dried and started opening. The collected seeds were stored at RT.

2.9.2.2. Sterile *Arabidopsis* growth

Surface sterilized *Arabidopsis* seeds were sown on plant medium consisted of half concentrated Murashige Skoog (MS) salts with Gamborg B5 vitamins (Duchefa), 1% [w/v] sucrose and 0.7% [w/v] plant agar, pH5.7 adjusted with 1M KOH. Plates with seeds were put in a cold room for 3 days before transferring to the growth chamber in long days at 22°C and 60% relative humidity.

Table 2.2. *Arabidopsis* plant lines used in this study

Plant lines	creator
<i>35S::AP2C2-GFP</i>	Vaiva Kazanaviciute
<i>35S::AP2C2-HA</i>	Vaiva Kazanaviciute
<i>35S::AP2C2-Myc</i>	Vaiva Kazanaviciute
<i>AP2C2::GUS/wt</i>	Vaiva Kazanaviciute/Chonnanit Choopayak
<i>AP2C2::GUS/CAT2HP1</i>	Chonnanit Choopayak
CAT2HP1, CAT2HP2 , PTHW	Dirk Inze (Ghent, Germany)
<i>AP2C2-RNAi</i>	Chonnanit Choopayak
<i>ap2c1</i> (SALK_065126)	Vaiva Kazanaviciute
<i>mpk6</i> (SALK_127507)	Vaiva Kazanaviciute
<i>ap2c2</i> (GK-361F11)	Chonnanit Choopayak
<i>ap2c1/2</i>	Chonnanit Choopayak
<i>mkp1</i>	Roman Ulm (Freiburg, Germany)
<i>ap2c2/mkp1</i>	Chonnanit Choopayak
<i>acx1</i> SALK_041464, <i>acx5</i> SALK_009998, <i>acx1/5</i>	Gregg A Howe (Michigan, USA)
<i>ap2c2/acx1/5</i>	Chonnanit Choopayak

2.9.3. Surface sterilization of *Arabidopsis* seeds

Arabidopsis seeds were surface sterilized with 6% [v/v] sodium hypochloride for 5 min followed by triple wash with sterile deionised water. Sterile seeds were spread on the medium using sterile 1 ml pipetman tip.

2.9.4. *A. tumefaciens* mediated transformation of *Arabidopsis* by floral dip

Arabidopsis plants were transformed using a floral dip method (Clough and Bent, 1998). *Arabidopsis* was grown in 10 cm pots at a density of 8-10 plants per pot in short days for 4 weeks. Afterwards plants were transferred to long days to induce flower development. The first inflorescence shoots were removed. Plants were transformed when secondary inflorescence were about 8-10 cm tall. *A. tumefaciens*, containing plasmid of interest, were inoculated in 2 ml LB medium with appropriate antibiotics. Next day 50 ml of selective LB medium was inoculated with the first preculture. On the third day the *Agrobacterium* culture was diluted to A_{600} 0.2 in 300 ml of the same medium and grown till A_{600} reached 0.8. Then the culture was spun down at 4000 rpm for 10 min at RT. The pellet was resuspended in 300 ml 5% [w/v] sucrose and transferred to a suitable beaker. SilvetL-77 (OSi Specialties Inc.) was added to the final concentration 0.05% [v/v]. Inflorescence shoots were dipped in *Agrobacterium* suspension for 10 s, covered with a transparent cover for 48 h and moved to low light conditions. The cover was slightly opened after 24 h. After additional 24 h the cover was removed and plants returned to their normal growth conditions. The dipping was repeated after a week.

2.9.5. Selection of transgenic plants

2.9.5.1. Segregation analysis

Selection of transformed plants was based on an introduced resistance marker, bacterial gene encoding the neomycin phosphotransferase. Transformed seeds/seedlings were selected on medium containing antibiotic kanamycin. Seeds were surface sterilised (§ 2.9.3.) and spread on plates containing selective plant medium with 50 mg/l kanamycin and put in cold room for 3 days before moving to a plant growth chamber. After 14 days, seedlings with green cotyledons, first true leaves and developed roots were transferred to soil.

2.9.5.2. Analysis of *ap2c2* knockout line

T2 *ap2c2* knockout seeds (GK-316F11) were obtained from GABI-Kat collection. T2 plants, which were able to survive and grown on 1/2 MS media containing 7.5 mg/ml sulfadiazin (Sulfadiazin: 4-amino-N-[2-pyrimidinyl] benzene-sulfonamide-Na, Sigma S-6387), were analysed. The position of T-DNA insertion in the *AP2C2* gene was verified by PCR using *AP2C2* specific primers (#179 and #180) and LB specific T-DNA primer (#398) or RB primer (#393). The copy number of T-DNA insertion was analysed by Southern blotting using DNA probed which prime at the near left end of T-DNA. The line with a homozygous single T-DNA insertion was selected. The *AP2C2* transcript was amplified by RT-PCR using *AP2C2* internal primers (#406 and #407).

2.9.6. Plant tissue culture methods:

2.9.6.1. Cultivation of *Arabidopsis* suspension culture

Arabidopsis suspension culture was cultivated in sterile, non-detergent washed Erlenmeyer flasks in darkness or in long days at 22°C shaken at 140 rpm/min. Every week the cultures were diluted with fresh medium in ratio 1:3. *Arabidopsis* suspension medium consisted of MS macrosalts (1650 mg/l NH_4NO_3 , 1900 mg/l KNO_3 , 440 mg/l $\text{CaCl}_2 \times 2 \text{H}_2\text{O}$, 370 mg/l $\text{MgSO}_4 \times 7 \text{H}_2\text{O}$, 170 mg/l KH_2PO_4), MS microsals (16.9 mg/l $\text{MnSO}_4 \times \text{H}_2\text{O}$, 8.6 mg/l $\text{ZnSO}_4 \times 7 \text{H}_2\text{O}$, 6.2 mg/l H_3BO_3 , 0.83 mg/l KI, 0.25 mg/l $\text{Na}_2\text{MoO}_4 \times 2 \text{H}_2\text{O}$, 0.025 mg/l $\text{CoCl}_2 \times 6 \text{H}_2\text{O}$, 0.025 mg/l $\text{CuSO}_4 \times 5 \text{H}_2\text{O}$), Fe-EDTA (11.5 mg/l $\text{FeSO}_4 \times 7 \text{H}_2\text{O}$, 37.25 mg/l $\text{Na}_2\text{-EDTA}$), B5 vitamins (100 mg/l myo-inositol, 1 mg/l nicotinic acid, 1 mg/l pyridoxin, 10 mg/l thiamine), 3% [w/v] sucrose and 1 mg/l 2,4-dichlorophenoxy acetic acid (2,4-D), pH adjusted to 5.7 with KOH.

2.9.6.2. Protoplast isolation

All the centrifugation steps were carried out in a swing-out centrifuge without a brake at room temperature. The enzyme solution was prepared in advance. 1% [w/v] cellulase (Serva), 0.2% [w/v] macerozyme (Yakult) were dissolved in B5-0.34M G/M (0.32% [w/v] B5 powder (Duchefa), 0.17 M glucose, 0.17 M mannitol, pH adjusted to 5.5 with KOH) medium by stirring slowly about 1 hour at room temperature. Afterwards the solution was filtered through Whatmann paper and sterilized by filtration through a 0.22 μm Millipore filter. The sterile enzyme solution was stored at -20°C. The 4-5 day old *Arabidopsis* suspension cells were collected in 50 ml Falcon tubes and spun for 5 min at 1500 rpm.

After discarding the supernatant, the tubes were filled with 25 ml B5-0.34 M G/M medium and gently mixed. 25 ml of enzyme solution was added, gently mixed and divided into two 15 cm diameter Petri plates, 25 ml each. The plates were covered with aluminium folia and placed on an orbital shaker for 2-4 hours at 50 rpm/min. The harvesting of cells was started when single round-shaped protoplasts appeared. The cells were transferred into 50 ml Falcon tubes, spun 5 min at 1000 rpm and resuspended in 25 ml B5-0.34M G/M, spun 5 min 1000 rpm, resuspended in 10 ml of B5-0.28 M Suc (0.32% [w/v] B5 powder (Duchefa), 0.28 M sucrose, pH adjusted to 5.5 with KOH). Protoplasts were transferred into 13 ml Falcon tubes and spun for 7 min at 800 rpm. The cells were collected with a wide-tip plastic pipette into a new tube. 50 μ l of protoplasts were diluted in 450 μ l B5-0.28 M Suc and counted in a Rosenthal chamber. The final concentration of protoplasts were approximately 4×10^6 cells/ml.

2.9.6.3. Protoplast transformation

Plasmid DNA used for transformation was isolated with JetStar (Genomed) or Qiagen DNA isolation kits according to manufacturers protocols and diluted to concentration 1 μ g/ μ l. Polyethylene glycol (PEG) solution was prepared in advance: 25% [w/v] PEG 6000 was dissolved in 0.45 M mannitol and 0.1 M $\text{Ca}(\text{NO}_3)_2$ by stirring, and pH adjusted to 9.0 with KOH. PEG solution was sterilized by filtration and stored at -20°C . Harvested protoplasts were incubated for at least 2 hours at 4°C prior to transformation. The 5-10 μ g plasmid DNA was mixed with 50 μ l protoplasts (~ 200000 cells) by ticking the tube. Then 150 μ l PEG solution was added and mixed immediately by ticking the tube 4-5 times and incubated 10 min at room temperature. PEG was washed out by adding 0.275 M $\text{Ca}(\text{NO}_3)_2$, in two steps of 0.5 ml, and mixing well by inverting the tubes several times. Protoplasts were sedimented by spinning for 7 min at 800 rpm. The supernatant was removed with a vacuum pump. Finally the protoplasts were resuspended in 0.25 ml of B5-0.34M G/M and cultivated 5-24 h at 24°C in the dark.

2.10. Expression analysis

2.10.1. Promoter-reporter analysis

Arabidopsis wild type and catalase-deficient plants (CAT2HP1) were floral dipped with *Agrobacterium* bearing plasmid pGreenII-AP2C2prom-GUSint (#799) (constructed by

Vaiva Kazanaviciute). Two lines of T2 plants, which were able to grow in 1/2MS media containing 50mg/ml kanamycin, were selected. T3 plants with high GUS activity were studied further.

2.10.2. Stress treatment

Seedlings grown in 1/2MS liquid media or 1/2 MS agar media or plants grown in soil in plant growth chambers with normal growth conditions (22°C and 60% relative humidity and light intensity approximately 70-100 $\mu\text{mol.m}^{-2}.\text{s}^{-1}$) were subjected to specific conditions for treatment as described bellowed.

2.10.2.1. Abiotic stress treatment

Cold: Plants/seedlings were moved to 4°C for 3 hours before sample collecting.

Heat: Plants/seedlings were moved to 37°C for 3 hours before sample collecting.

Strong light: Plants/seedlings were placed directly under medium light with a quantity of 200 $\mu\text{mol.m}^{-2}.\text{s}^{-1}$. The white light source consisted of two 18 watts cool white bulbs (OSRAM L, LUMILUX, Germany). Light intensity was measured using Light Meter (LI-250A, LI-COR® Biosciences, USA).

UVB: Plants/seedlings were placed directly under UVB light with a quantity of 0.5W m^{-2} for 30 min and recovery for 2.50 hours by moving back to growth chamber. The UV-B light source consisted of six of 8 watts UV bulbs 312 nm (cat no. 29 84 400, Hero lab GmbH).

UVC: Plants/seedlings were placed directly under UVC light with a quantity of 0.75 Wm^{-2} for 30 min and a recovery for 2.50 hours by moving them back to a growth chamber. The UVC light source consisted of five 15 watts UV bulbs, G15T18 GEMICIDAL 254 nm (cat no. 400078, Stratagene). Plants were grown in soil under UVC for 30 min and recovery for 3 hour.

Freezing: Plants/seedlings were moved to -10°C for 30 min and recovery for 2.50 hours by moving them back to a growth chamber before sample collecting.

Wounding: The attached leaves/seedlings were wounded by a sterile blade no.10 (Swann-Morton®) or wire brush. The plants/seedlings were continually kept in a growth chamber. After 3 hours the wounded leaves/seedlings were collected.

Salinity: adding 250mM NaCl to seedlings grown in 1/2MS liquid media for 1 hour

H₂O₂: adding 20mM H₂O₂ to seedlings grown in 1/2MS liquid media for 1 hour
catechin: adding 100µg/ml (in methanol) into 1/2MS liquid media for 3 hours

2.10.2.2. Biotic stress treatment

Flg22: adding 100nM flg22 to seedlings grown in 1/2MS liquid media for 1 hour
Cellulase: adding 0.1mg/ml cellulase to seedlings grown in 1/2MS media for 3 hours
Xylanase: adding 1mg/ml xylanase to seedlings grown in 1/2MS media for 1 hour

2.10.2.3. Hormone treatment

Abscicic acid: adding 50,200,1000 µM ABA to seedlings grown in 1/2MS media for 1 hr
Auxin: adding 5,50,500,1000 µM NAA to seedlings grown in 1/2MS media for 1 hr
Jasmonic acid: adding 10,20,50,100 µM MeJA to seedlings grown in 1/2MS media for 1 hr
Salicylic acid: adding 10,20,50,1000 µM SA to seedlings grown in 1/2MS media for 1 hr
Cytokinin: adding 1mM BAP to seedlings grown in 1/2MS media for 1 hr
Ethylene: adding 10µM ACC to seedlings grown in 1/2MS media for 1 hr

2.10.3. Histochemical staining and microscopy

Plant tissues were incubated for 12-18 h at 37°C in staining solution containing 100 mM sodium phosphate (pH 7.0), 0.5 mM K₄[Fe(CN)₆], 0.5 mM K₃[Fe(CN)₆], 0.01% [v/v] polyoxyethylene sorbitan monolaurate (Tween 20), and 0.5 mM 5-bromo-4-chloro-3-indolyl-β-D-glucuronic acid (X-Glc). Slight vacuum was applied for 5 min to facilitate substrate infiltration. Chlorophyll was cleared by incubation in 70% ethanol for 24 h. The cleared tissue was rehydrated for 15 min each in 60%, 40%, 20%, 10% ethanol, and 5% ethanol/ 50% [v/v] glycerol. Finally, the tissue was mounted in 50% glycerol on a glass microscope slide and observed under Zeiss Axioplan2 microscope or Zeiss Stem2000 binocular with Nikon Coolpix4500 camera. Histochemical GUS reporter assay was performed according to (Jefferson et al., 1986).

2.11. Bacterial pathogen resistance assays

2.11.1. Bacterial growth

Pseudomonas syringae pv. *tomato* strain DC3000 was grown in NYG(A) medium (0.5% [w/v] bacto-peptone, 0.3% [w/v] yeast extract, 1.74% [v/v] glycerol, 1.5% [w/v] bacto

agar, pH adjusted to 7.0 with NaOH). The bacteria were streaked out from -80°C reference stock and incubated at 28°C for two days, and then the Petri plate with bacteria was maintained at 4°C up to one month. Bacterial cultures were grown fresh for every experiment.

2.11.2. Plant inoculation with *Pseudomonas syringae* DC3000

Arabidopsis was grown under short days to prevent early bolting and to encourage sustained growth and health of vegetative leaf tissue. 5-6 weeks old plants were used for inoculation with *P. syringae*. 14-16 hours prior to infiltration plants were covered with a cover to keep high air humidity and stomata open. A small portion of bacteria was removed from a Petri plate and resuspended in 1 ml of 10 mM MgCl_2 . The bacterial titer in resuspension was estimated using a spectrophotometer. A_{600} of 0.1 = $\sim 1 \times 10^8$ colony-forming units per ml (cfu/ml). The resuspended culture was diluted to 5×10^5 cfu/ml in 10 mM MgCl_2 . The bacterial suspension was infiltrated into the abaxial side of leaves with a 1 ml syringe (without a needle). The bacteria were uniformly resuspended within a minute before being taken up into a syringe. For one experiment 5 plants (4 leaves each) were inoculated. After inoculation plants were incubated at $22-24^{\circ}\text{C}$ with a cover.

2.11.3. Scoring plant disease resistance to *P. syringae*

Arabidopsis resistance to *P. syringae* was evaluated by monitoring the extent of pathogen growth on a plant. Bacteria populations were quantified at 0, 2 and 3 days after inoculation. Sampling was done in triplicates. For each sample two leaf tissue disks from two leaves were removed with a 0.3 cm diameter cork borer, i.e. 4 disks into one 1.5 ml microcentrifuge tube. The tissue was disrupted by grinding with a grinder in 200 μl 10mM MgCl_2 (for day 0) or in 1000 μl 10mM MgCl_2 (for days 2 and 3). The suspension was diluted and plated on NYG(A) plates containing 100 mg/l rifampicin and 50 mg/l cyclohexamide. For day zero, 100 μl of suspension was plated, i.e. dilution 5×10^{-1} . For day two, the suspension was diluted 10^{-2} , 10^{-3} and 10^{-4} . For day three following dilutions were plated 10^{-3} , 10^{-4} and 10^{-5} (Table.2.3.).

The plates with bacteria were incubated at 28°C . Colonies were counted after two days. Data was reported as \log_{10} of colony forming units per cm^2 of leaf tissue (one disk was approximately 0.07 cm^2 , so four disks were 0.28 cm^2).

Table 2.3. Dilution concept for quantification of bacterial growth

Stock	Volume, μl	Dilution	Plating, μl	Final dilution
Nr 1	1000	undiluted	10	10^{-2}
Nr 2	1000	10^{-2}	100	10^{-3}
			10	10^{-4}
Nr 3	1000	10^{-3}	100	10^{-4}
			10	10^{-5}

2.12. Ethylene production measurements

Leaves from six week-old plants (quadruplet samples) grown in short day conditions were wounded with a wire brush, transferred into 21.5 ml headspace-vials air-tight sealed. After 24 hours, 100 μl of the gas-phase was taken from the headspaces of vials and analysed by gas chromatography model GC5890 Series II Plus (Hewlett-Packard, Bristol, UK) using an HP-PLOT Al_2O_3 Column (50m x 0.535mm x 15 μM) (Agilent Technologies) and a hydrogen flame-ionization detection (FID) system. Measurement was performed in collaboration with Manfred Schwanninger, University of Natural Resources and Applied Life Sciences, Vienna. Ethylene was identified via co-migration with an ethylene standard and quantified with reference to a standard curve for ethylene concentration. The amount of ethylene produced was calculated per hour and milligram of fresh tissue. Statistical significance was evaluated by the least significant difference method and significance attributed if $P < 0.05$.

3. RESULTS

3.1. Interaction of AP2C2 with other proteins

3.1.1. Yeast two hybrid screening of *Arabopsis* cDNA library for AP2C2 interacting proteins

To identify potential interacting partners of AP2C2, a 1:1 mix of auxin induced and uninduced seedling roots cDNA library in pACT vector was screened using full length cDNA AP2C2 in the pACT (pBD-Gal4 base) vector as bait in PJ69-4A yeast. Positive clones were selected by assaying the activity of *Ade2* and *lacZ* reporter genes. Eight yeast colonies that survived on SD medium lacking leucine, tryptophan and adenine were inoculated into liquid SD medium lacking leucine and tryptophan. Plasmids containing putative AP2C2-interacting partners were extracted from yeast and sequenced. Three proteins; Mitogen activated protein kinase 6 (MPK6), Importin alpha 1 (IMP α 1), Glyoxalase 1 (GLX1) were identified as interacting partners of AP2C2 (Table 3 .1.). However, after repeating the interaction assays and not being able to reproduce GLX1/AP2C2 interaction, see 3.1.3., GLX1 was excluded from the experiments as a false positive signal.

Table 3.1. Interacting partners of AP2C2 identified in yeast two-hybrid screening of *Arabidopsis* cDNA library.

AGI code	name	functions
At2g43790	Mitogen activated protein kinase 6, MPK6	response to osmotic stress, oxidative stress, salt stress, jasmonic acid mediated signalling pathway, reactive oxygen species, ethylene stimulus, defence response to bacteria
At3g06720	Importin alpha 1, IMP α 1	nuclear import receptor
At1g11840	Glyoxalase1, GLX1 <u>interaction not confirmed</u>	catalyses the first step of glyoxalase system

Database search suggested putative functions of AP2C2 according to its interacting partners. For instance, MPK6 functions in response to biotic and abiotic stress such as oxidative stress (Kovtun et al., 2000; Yuasa et al., 2001), salt stress, environmental stresses

(Ichimura et al., 2000), pathogens (Nuhse et al., 2000), osmotic stress, jasmonic acid (Takahashi et al., 2007) and ethylene (Ouaked et al., 2003). Importin alpha 1 (IMP α 1) functions as a nuclear import receptor (Smith et al., 1997). Glyoxalase1 (GLX1) catalyses the first step of glyoxalase system which is important for the glutathione (GSH)-based detoxification of methylglyoxal (MG). MG is formed primarily as a by-product of carbohydrate and lipid metabolism (Takatsume et al., 2006).

3.1.2. AP2C2 interacts with MPK3, MPK4, MPK6 in yeast.

To investigate the specificity of AP2C2 interaction with MAP kinases, yeast two hybrid interaction assay was also performed with other available 18 MAPKs. Whereas *cAP2C2* was cloned into lexA-base binding domain pBTM117 vector, cDNAs of 18 *Arabidopsis* MAPKs were fused to GAL4 activation domain in pGAD425 vector (Teige et al., 2004). Both plasmids were co-transformed into *Saccharomyces cerevisiae* yeast strain L40. The interaction between proteins (AP2C2 and MAPKs) was evaluated by the growth of yeast on SD media without tryptophan, leucine and histidine supplemented with 6mM 3-aminotriazole (SD-W-L-H+3AT). Quantitative β -galactosidase assay was performed to examine the strength of protein-protein interaction (Figure 3.1.A.). The results demonstrated that AP2C2 specifically interacted with only MPK3, MPK4 and MPK6 of 18 tested MAPKs (Figure 3.1.B.).

3.1.3. AP2C2 interacts with IMP α 1 but not GLX1 in yeast.

To validate IMP α 1 and GLX1 as potential interacting partners of AP2C2. The *cAP2C2*-fished cDNA from library, pACT-cIMP α 1 or pACT-cGLX1 was co-transformed with pBTM117-cAP2C2 in L40 yeast. The protein-protein interaction was evaluated by the growth of yeast on SD media without tryptophan, leucine and histidine supplemented with 6mM 3-aminotriazole (SD-W-L-H+3AT) and quantitative β -galactosidase assay. The results demonstrated that AP2C2 interacted with IMP α 1 but not with GLX1 (Figure 3.1.C.).

3.1.4. AP2C2 interacts with ACX1, the interacting partner of AP2C1.

Since AP2C1 is the close homolog of AP2C2, the substrate specificity of AP2C1 with AP2C2 was tested. The putative interacting proteins of AP2C1 (IPs-AP2C1), were isolated from cDNA library by screening with *cAP2C1* (Kazanaviciute, 2006) including: Acyl-coA oxidase 1 (ACX1); Copper chaperone for superoxide dismutase 1 (CCS1); S-

Adenosylmethionine decarboxylase (SAMDC); Guanine nucleotide-binding proteins (G proteins); Tubulin alpha 5 (TUA5), CAX interacting protein 1 (CXTP1); RNA binding 1/Glycine rich protein 8 (GRP8); Lower cell density 1 (LCD1); Responsive to dehydration 21 (RD21A) and RNA-binding protein (RBP37) (see Table 3.2.). All these proteins were studied for interaction with AP2C2 by Y2H in L40 yeast. Each of pACT-IPs-AP2C1 was co-transformed with pBTM117-AP2C2 into L40 yeast. The protein interaction identified by the growth of yeast on SD-W-L-H+3AT medium and quantitative β -galactosidase assay demonstrated that among interacting partners of AP2C1, only Acyl-coA oxidase 1 (ACX1) was interacting with AP2C2 (Figure 3.1.D.).

3.1.5. No interaction between AP2C1, AP2C2 or AP2C3 with CPK3 in yeast

Since MAPKs were identified as interacting partners of AP2C2, calcium dependent protein kinase protein 3 (CPK3, At4g23650) was tested for interaction with AP2Cs: AP2C1, AP2C2 and AP2C3. pBTM117-cCPK3 and each of pGAD425-cAP2Cs plasmids were co-transformed into L40 yeast. No interaction of any AP2Cs with a CDK protein was identified by yeast growth on SD-W-L-H+3AT medium and β -galactosidase assay (Figure 3.1.E.).

3.1.6. IMP α 1 interacts with AP2C1 and AP2C2 but not AP2C3 in yeast.

To investigate the specificity of IMP α 1 interaction with AP2C2, AP2C1, AP2C3, MPK3, MPK4 and MPK6 were checked for interaction with IMP α 1 in L40 yeast. The pACT-cIMP α 1 plasmid was co-transformed with pBTM117-cAP2Cs or pBTM117-cMAPKs plasmids. The yeast growth on SD-W-L-H+3AT medium and β -galactosidase assay demonstrated that AP2C1, MPK3, MPK4 and MPK6 were interacting partners of IMP α 1 but the interaction was not detected with AP2C3 (Figure 3.1.F.)

3.1.7. AP2C2 interacted with MPK4, MPK6 and IMP α 1 but not MPK3 in protoplasts.

To find out if and in which intracellular compartment AP2C2 and its interacting partners from Y2H (MPK3, MPK4, MPK6 and IMP α 1) are building associations in plant cells, a biomolecular fluorescence complementation (BiFC) assay based on split-yellow fluorescent protein (YFP) was applied. The N-terminal domain or C-terminal domain of YFP fused to AP2C2, MPK3, MPK4, MPK6 or IMP α 1 was cloned into pRT100 vector under control of 35S promoter without translational leader (TL). The pairs of N-terminal and C-terminal fusion plasmids were transiently co-expressed in *Arabidopsis* protoplasts.

Fluorescence from reconstituted YFP indicated interaction between AP2C2 and MPK4, MPK6 or IMP α 1 but not MPK3. The AP2C2/MPK4 complex was localised in the nucleus (Figure 3.2.C.), whereas the AP2C2/MPK6 complex was detectable both in cytoplasm and the nucleus (Figure 3.2.E.). The AP2C2/IMP α 1 complex fluorescence was detected in the nucleus (Figure 3.2.G.). The weak fluorescence was observed in the negative control by co-expression of pRT100-35S-YFPctd and pRT100-35S-YFPntd vectors (Figure 3.2.I.).

Table 3.2. Interacting proteins of AP2C 1 fished from *Arabidopsis* cDNA library (Kazanaviciute, 2006)

AGI code	name	functions
AT4G16760	Acyl-coA oxidase1 , ACX1	Encodes a medium to long-chain acyl-CoA oxidase. Catalyzing the first step of fatty acid beta-oxidation. Gene expression is induced by wounding, drought stress, abscisic acid, and jasmonate.
AT1G12520	Copper chaperone for superoxide dismutase 1, CCS1	Copper/zinc superoxide dismutase copper chaperone. Localized to the chloroplast. Expressed in roots and shoots. Up-regulated in response to copper and senescence. The AtACC activates all three CuZnSOD activities located in three different subcellular compartments. Contains three domains, central, ATX-1 like and C-terminal. ATX-1 like domain essential for the copper chaperone function of AtCCS in planta.
AT3G02470	S-Adenosylmethionine decarboxylase, SAMDC	Encodes a S-adenosylmethionine decarboxylase involved in polyamine biosynthesis
AT1G48630	Guanine nucleotide-binding proteins, G proteins	similar to guanine nucleotide-binding family protein / activated protein kinase C receptor
AT5G19780	Tubulin alpha-5 , TUA5	Encodes an isoform of alpha tubulin
AT3G54900	CAX interacting protein 1, CXIP1	It activates CAX1 (CALCIUM EXCHANGER 1) gene Calcium transport activity
AT4G39260	RNA binding 1, glycine rich protein 8, ATGRP8	Encodes a glycine-rich protein with RNA binding domain at the N-terminus. Protein is structurally similar to proteins induced by stress in other plants. Gene expression is induced by cold. Transcript undergoes circadian oscillations that is depressed by overexpression of AtGRP7.
AT2G37860	Lower cell density 1, LCD1	Encodes a protein of unknown function. Mutants have pale leaves, lower cell density in the palisade parenchyma and increased sensitivity to ozone and virulent <i>Pseudomonas syringae</i>
AT1G47128	Responsive to dehydration 21, RD21A	cysteine proteinase precursor-like protein/dehydration stress-responsive gene
AT3G49390	putative, RNA-binding protein, RBP37	RNA-binding protein

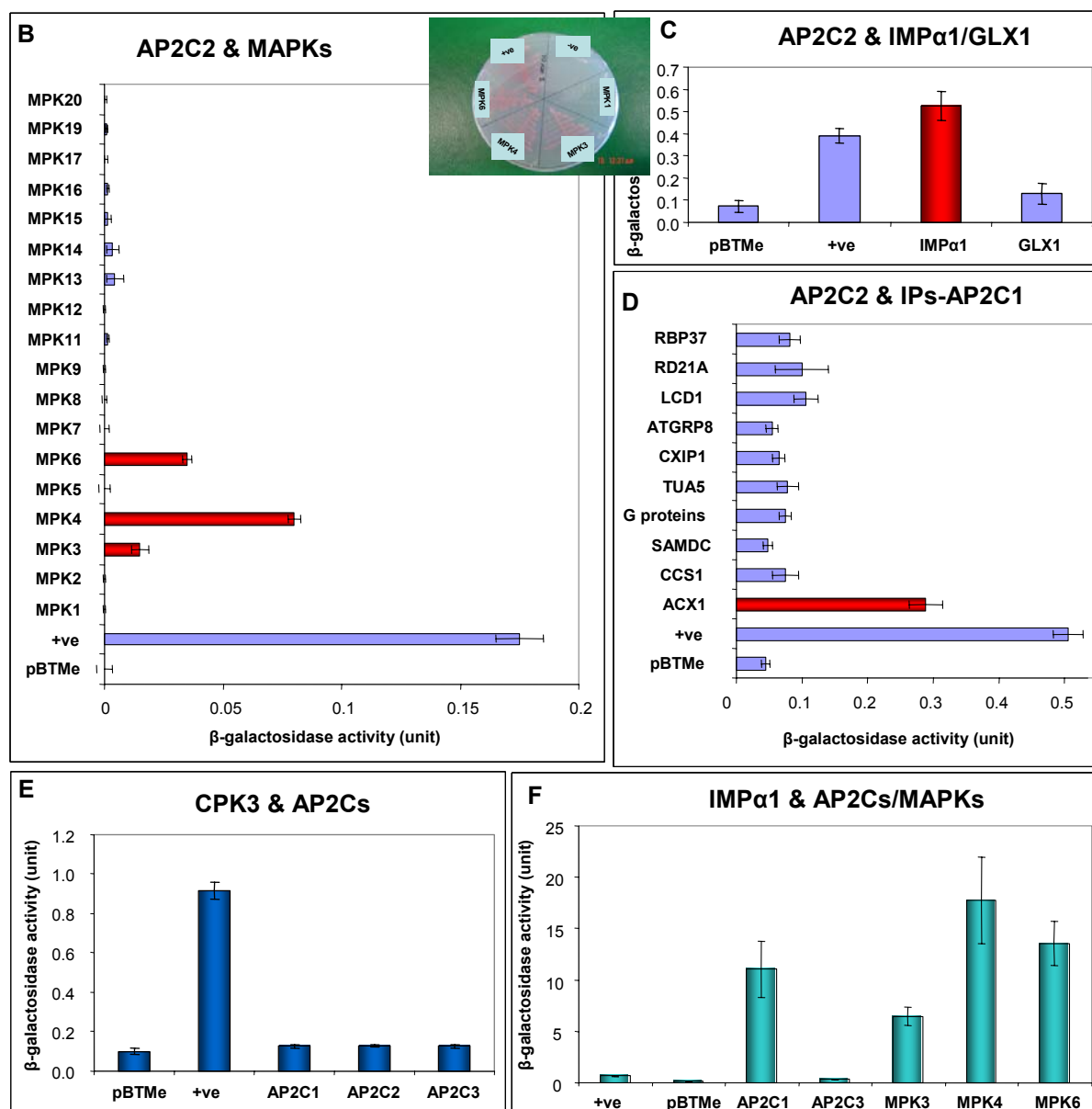


Figure 3.1. Identification of potential interacting partners of AP2C2 in Y2H. Y2H was performed in L40 yeast strain. Yeast was co-transformed with plasmid pBTM117 carrying cAP2C2-LexA BD and with pGAD425 plasmid carrying cMAPKs-GAL4 AD or pACT plasmid carrying cDNA-GAL4 AD. Among 18 MAPKs, MPK3, MPK4 and MPK6 showed interaction with AP2C2 identified by (A) yeast grown on SD media without tryptophan leucine and histidine and (B) β-galactosidase activities. (C) AP2C2 also showed interaction with Importinα1 (IMPα1) but not with Glyoxalase 1 (GLX1). (D) Among interacting partners of AP2C1 (IPs-AP2C1), only Acyl-coA oxidase 1 (ACX1) interacted with AP2C2. (E) Calcium dependent protein kinase 3 (CPK3) did not interact with AP2C1, AP2C2 or AP2C3. (F) IMPα1 also interacted with MPK3, MPK4, MPK6 and AP2C1, but not AP2C3. The positive control is AP2C1 & MPK6. The negative controls are either AP2C2 or IMPα1 with empty vector. β-galactosidase activity values are the average of the measurements from three reactions.

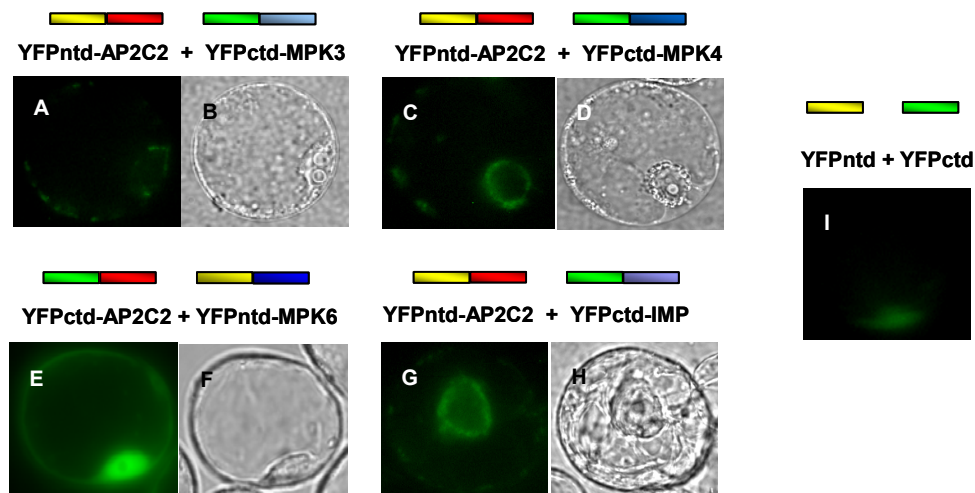


Figure 3.2. BiFC images demonstrate that AP2C2 interacts with MPK4, MPK6 and IMP α 1 but not with MPK3 in protoplasts. Either N-terminal domain (NTD) (yellow) or C-terminal domain (CTD) (green) of split YFP was fused to AP2C2 (red box), MPK3, MPK4, MPK6 (blue boxes) and IMP α 1 (purple box). Each pairs of split YFP fusion proteins were co-transformed into *Arabidopsis* protoplasts. The fluorescent microscope images show that except (A) MPK3, AP2C2 interacts with (C) MPK4 in the nucleus, (E) MPK6 in nucleus/cytoplasm and (G) IMP α 1 in the nucleus. (B,D,F,H) are corresponding bright field images. (I) is the negative control.

3.2. Subcellular localisation of AP2C2

3.2.1. cAP2C2 sequence

Shown the cDNA of AP2C2 (At1g07160) 1143 bp 380 amino acids, containing chloroplast transit peptide IMP α 1 (cTP, green letters, 67 amino acids) predicted by ChloroP (www.cbs.dtu.dk/services/) and kinase interaction motif (KIM, pink letters) at the N-terminus and 11 catalytic subdomains (orange and blue letters) (Bork et al., 1996).

3.2.2. Subcellular localization of AP2C2 predicted by bioinformatics

The localisation of AP2C2 proteins in the cell is the clue to reveal the functions of the protein. Protein sequences prediction analysis suggested AP2C2 targeting to chloroplast. The ChloroP server of the Centre for Biological Sequence Analysis (CBS), Technical University of Denmark DTU (<http://www.cbs.dtu.dk/index.shtml>) predicted the presence of chloroplast transit peptides (cTP) in the N-terminal domain of a AP2C2 protein and the location of potential cTP cleavage sites approximately at amino acid 68 from the N-terminal end of the protein (Figure 3.3.A.).

cTP

atg tcg tct tca gtt gcc gtt tgc aac tca ccg gtg ttc tct ccg tct tcg tct ctt
M S S S V A V C N S P V F S P S S S L
ttc tgc aac aaa ccg ttg aac act tct ccg gca cat gaa acc cta acc ctg tct ctt
F C N K P L N T S P A H E T L T L S L
tcc cat ctc aat cct ccc gtt tct tct act tct cct tcc gcc gcg tct ccc aca tct
S H L N P P V S S T S P S A A S P T S
ccg ttc tgc ctc cgt ctc ctg aaa ccg ccg gct aaa cta ggg ttt gga tcg gac tct
P F C L R L L K P P A K L G F G S D S

KIM

ggt ccg gga agc att ctg aag agg aaa cga ccg acg acg ctt gat ata ccg gtg gct
G P G S I L K R K R P T T L D I P V A
ccg gtt ggt att gca gct cct ata tcg aat gca gat acg ccg agg gag gag agt aga
P V G I A A P I S N A D T P R E E S R
gca gtg gag agg gaa ggt gat ggt tac tct gtt tat tgc aag aga ggt aaa aga gaa
A V E R E G D G Y S V Y C K R G K R E

Subdomain I

gct atg gag gat cgt ttc tct gcc atc act aat ctt caa gga gat ccc aaa cag
A M E D R F S A I T N L Q G D P K Q

Subdomain II

gca ata ttc gga gtc tat gat ggt cac gga gga cca aca gcg gct gag ttt gcg gct
A I F G V Y D G H G G P T A A E F A A

Subdomain III

aag aac ttg tgt agt aac att ctt ggc gag ata gtt ggt ggg agg aac gag tca aag
K N L C S N I L G E I V G G R N E S K
att gaa gaa gct gta aaa cgt ggt tat cta gcg act gat tct gag ttt ctc aag gaa
I E E A V K R G Y L A T D S E F L K E

Subdomain IV

aaa aac gtt aag ggc ggc tcg tgc tgt gtc acg gct ctg atc agc gac gga aat ctt
K N V K G G S C C V T A L I S D G N L

subdomain V

gtg gtg gcc aat gct ggt gac tgc cgt gct gtt ttg agc gtt gga gga ttc gcg gag
V V A N A G D C R A V L S V G G F A E

subdomain Va

gcc ttg act tct gac cac cgc cct tcc aga gat gat gaa cga aac aga att gag agc
A L T S D H R P S R D D E R N R I E S

subdomain Vb

tcg
S

ggc ggt tat gtg gat aca ttc aat agt gtt tgg aga att caa gga tca tta gcg gta
G G Y V D T F N S V W R I Q G S L A V

subdomain VI

subdomain

VII

tct aga gga ata gga gat gct cat ctc aaa caa tgg ata ata tct gaa cca gag ata
S R G I G D A H L K Q W I I S E P E I
aat att ctc cga atc aat ccc caa cac gag ttc ttg atc tta gca tca gat ggt cta
N I L R I N P Q H E F L I L A S D G L

subdomain VIII

subdomain IX

tgg gac aag gtt agt aat cag gag gca gta gac ata gct cga cca ttt tgc aaa ggg
W D K V S N Q E A V D I A R P F C K G
acc gat cag aaa cgg aag cca ttg ctg gct tgc aag aag ctc gtt gac ctc tct gta
T D Q K R K P L L A C K K L V D L S V

subdomain X

subdomain XI

tca cga ggc tcc ttg gac gat att agt gtg atg ttg att cag ttg tgc cac ctc ttc
S R G S L D D I S V M L I Q L C H L F

tga
stop

3.2.3. Subcellular localisation of AP2C2 in planta.

To investigate the intracellular localisation of AP2C2, the pGreenII-2x35S-TL-gAP2C2-GFP plasmid was transformed transiently into *Arabidopsis* protoplasts. In protoplasts, green fluorescence could be detected in plastids and in the nucleus (Figure 3.3.B.). In constitutive overexpressing AP2C2-GFP plants under the control of 35S promoter, green fluorescence could be detected in the chloroplasts of stomata cells (Figure 3.3.D.).

To verify that AP2C2 localised in plastids of cells, AP2C2-GFP was co-expressed together with the plastid targeting CFP (Pt-CFP) (first 79 amino acid of the small subunit of tobacco rubisco) or the peroxisomal targeting signal 1 (PTS1, Ser-Lys-Leu)-CFP (Px-CFP) in *Arabidopsis* protoplasts. The organelle marker plasmids were obtained from Andreas Nebenführ, University of Tennessee, USA (Nelson et al., 2007). The fluorescent images demonstrated that AP2C2-GFP was co-localised with the plastid targeting protein CFP (Figure 3.3.F-H.) but not with the peroxisome targeting protein-CFP (Figure 3.3.I-K.).

3.3. Subcellular localisation of IMP α 1 in protoplasts

To investigate the location of IMP α 1 in plant cells, the pGreenII0029-2x35S-TL-IMP α 1-YFP plasmid was transformed into *Arabidopsis* protoplasts. Yellow fluorescence could be detected strongly in the nucleolus and weakly in the nucleoplasm (Figure 3.4.A.). To verify IMP α 1 localisation, IMP α 1-YFP was co-expressed together with the peroxisomal targeting signal 1 (PTS1, Ser-Lys-Leu)-CFP (Px-CFP) in *Arabidopsis* protoplasts. The fluorescent images demonstrated that IMP α 1-YFP was not co-localised with peroxisome targeting protein-CFP (Figure 3.4.C-E.).

3.4. Expression analysis of AP2C2.

3.4.1. Differential expression *in silico* of AP2C1 and AP2C2.

AP2C2 and its close homolog AP2C1 expression was analysed *in silico* according to the data retrieved from the AtGenExpress Visualization Tool (AVT) (<http://jsp.weigelworld.org/expviz/expviz.jsp> developed by Christian K. Widmer). Similar expression patterns for both genes were found in mature pollen and upon biotic and abiotic stress conditions. However, unique expression patterns of AP2C2 were also detected. During development, AP2C1 expression is stronger than AP2C2. Whereas AP2C2

uniquely expresses in mature pollen, *AP2C1* expresses either in mature pollen, roots and cotyledons (Figure 3.5.).

Both *AP2C1* and *AP2C2* are inducible genes. Their expressions are induced by environmental stresses, both biotic and abiotic stresses, strikingly by cyclohexamide and high salt. Some stresses induce similar *AP2C1* and *AP2C2* expressions, such as methyl jasmonate, abscisic acid, UVB, methyl violgen and mannitol. However, some other stresses affect differently *AP2C1* and *AP2C2* expression. For instance, whereas cold, drought and wounding strongly induce *AP2C1* expression, heat pathogens and seed imbibitions strongly induce *AP2C2* expression (Figure 3.6.). The catalase-deficient plant (*CAT2HP1*), which had approximately 20% catalase activity, demonstrated that upon high-light exposure for 3 hours, *AP2C2* transcript was upregulated 52.4 fold higher than the untreated one (Vanderauwera et al., 2005).

3.4.2. *AP2C2* transcript was upregulated in catalase-deficient plants.

The catalase-deficient plants *CAT2HP1* and *CAT2HP2* reported lower catalase activity levels. Using a spectrophotometric assay, the catalase activity retained 20 and 7% of total residual catalase activity level in 2-week-old *CAT2HP1* and *CAT2HP2* leaves, respectively (Vandenabeele et al., 2004). These plants accumulated high endogenous H_2O_2 after ozone treatment. Since *AP2C2* transcript was upregulated in catalase-deficient plants upon high-light stress, these plants were interesting as tools for the characterisation of *AP2C2* function. The *CAT2HP1*, *CAT2HP2* and empty vector control *PTHW* seeds were kindly distributed by Dr. Frank Van Breusegem, Belgium, for use in this study. Prior to use, catalase activity was measured in *CAT2HP1*, *CAT2HP2* and *PTHW* plants after strong-light irradiation. *CAT2HP1.9* and *CAT2HP2.5* plants with catalase activity of 13% and 1% respectively were selected for further experiments (Figure 3.7.A.).

To study the effect of high endogenous H_2O_2 on *AP2C2* expression, 1 month-old *CAT2HP1.9*, *CAT2HP2.5* and wild type were treated with catechin. Detached leaves were left in 1/2MS liquid medium for 3 hours. 100µg/ml catechin was added and incubated for 3 hours. RNA was extracted from frozen samples and subjected to RT-PCR using primers #406 and #407 (positional described in Figure 3.14.A.). The result showed higher upregulation of *AP2C2* in treated *CAT2HP1* plants compared to untreated wild type plants. In *CAT2HP2* plants *AP2C2* transcript was already detected before the induction and remained after induction (Figure 3.7.B.).

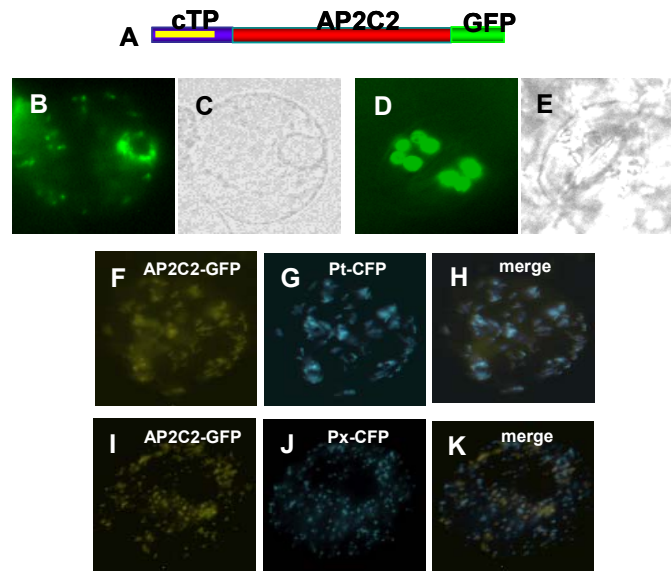


Figure 3.3. Subcellular localisation of AP2C2. (A) Schematic representation of AP2C2 protein. The protein contains N-terminal domain (purple box) and C-terminal domain (green box). The N-terminal domain is predicted to contain a 68 amino acids chloroplast transit peptide (cTP) (yellow line) (ChloroP, www.cbs.dtu.dk) (B) AP2C2-GFP was localises in plastids and in the nucleus of protoplasts (D) in chloroplasts in the stomata of overexpressing AP2C2-GFP plants. (F, I) AP2C2-GFP was co-transformed together with (G) the plastid targeting CFP (Pt-CFP) or (J) the peroxisomal targeting signal 1-CFP (Px-CFP) in *Arabidopsis* protoplasts. The fluorescent images demonstrated that AP2C2-GFP was co-localised with (H) plastid targeting protein-CFP but not (K) with peroxisome targeting protein-CFP. (C, E) are corresponding bright field images.

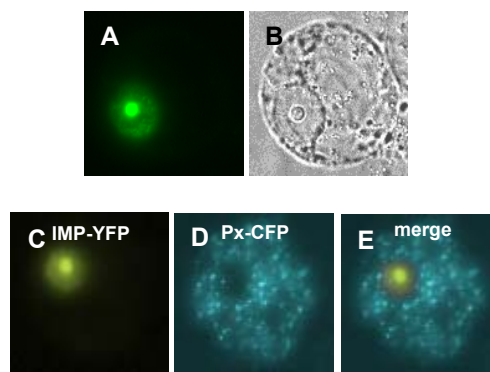


Figure 3.4. IMP-YFP nuclear and nucleolar localisation in *Arabidopsis* protoplasts. (A) *Arabidopsis* protoplasts were transformed by 35S::IMP-YFP. The fluorescence was detected strongly in the nucleolus and to some extent to the nucleoplasm. (B) corresponding bright field image. (C) IMP-YFP was co-transformed with (D) the peroxisome targeting signal 1-CFP (Px-CFP). The image shows that (E) IMP-YFP was not co-localised with peroxisome targeting protein-CFP.

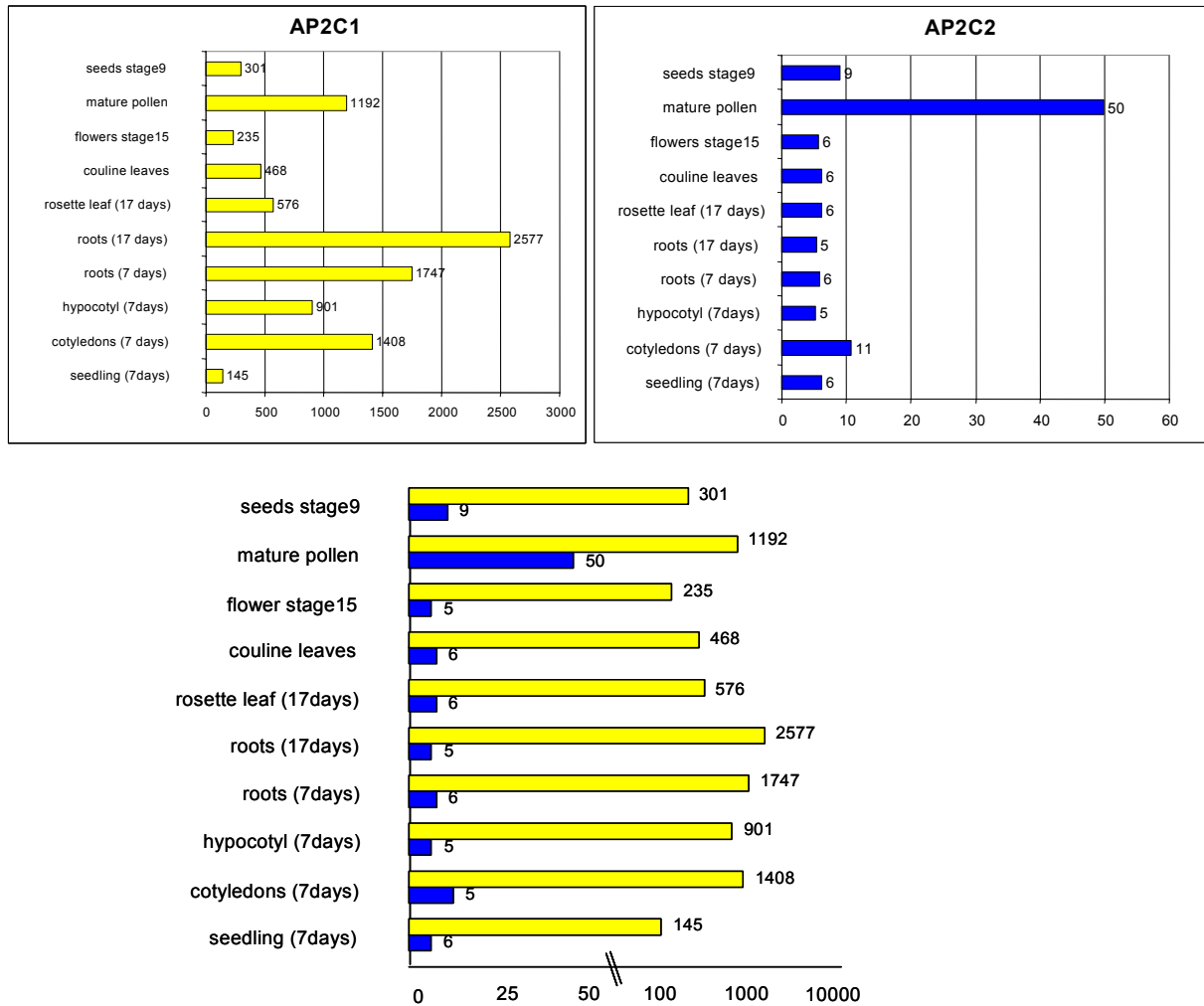


Figure 3.5. AP2C1 and AP2C2 expression *in silico* during development. *AP2C2* uniquely expresses in mature pollen, whereas *AP2C1* expresses more ubiquitously and especially in root and in mature pollen. Yellow bars represent *AP2C1* and blue bars represent *AP2C2*. Data from AtGenExpress Visualization Tool (AVT) <http://jsp.weigelworld.org/expviz/expviz.jsp> developed by Christian K. Widmer.

3.4.3. *AP2C2::GUS* reporter transgenic plants analysis

To investigate *AP2C2* expression in plants and to identify the inducers or conditions that induce *AP2C2* expression, promoter activation was studied using transgenic plants with promoter::*GUS* (*AP2C2::GUS*) reporter gene activity in the background of WT plants (*AP2C2::GUS*/WT) and CAT2HP1 plants (*AP2C2::GUS*/CAT2HP1). Reporter uidA gene (*GUS*), encoding a bacterial enzyme β -glucuronidase, was fused to 2 kb *AP2C2* promoter region sequence and introduced into plants by floral dip. Two independent transformants of *AP2C2::GUS*/WT and two independent transformants of *AP2C2::GUS*/CAT2HP1 were selected (one of *AP2C2::GUS*/WT plant was created by Vaiva Kazanaviciute). T3 homozygous lines were analysed for *AP2C2* promoter induction and β -glucuronidase production by histochemical staining using X-Glc as a substrate.

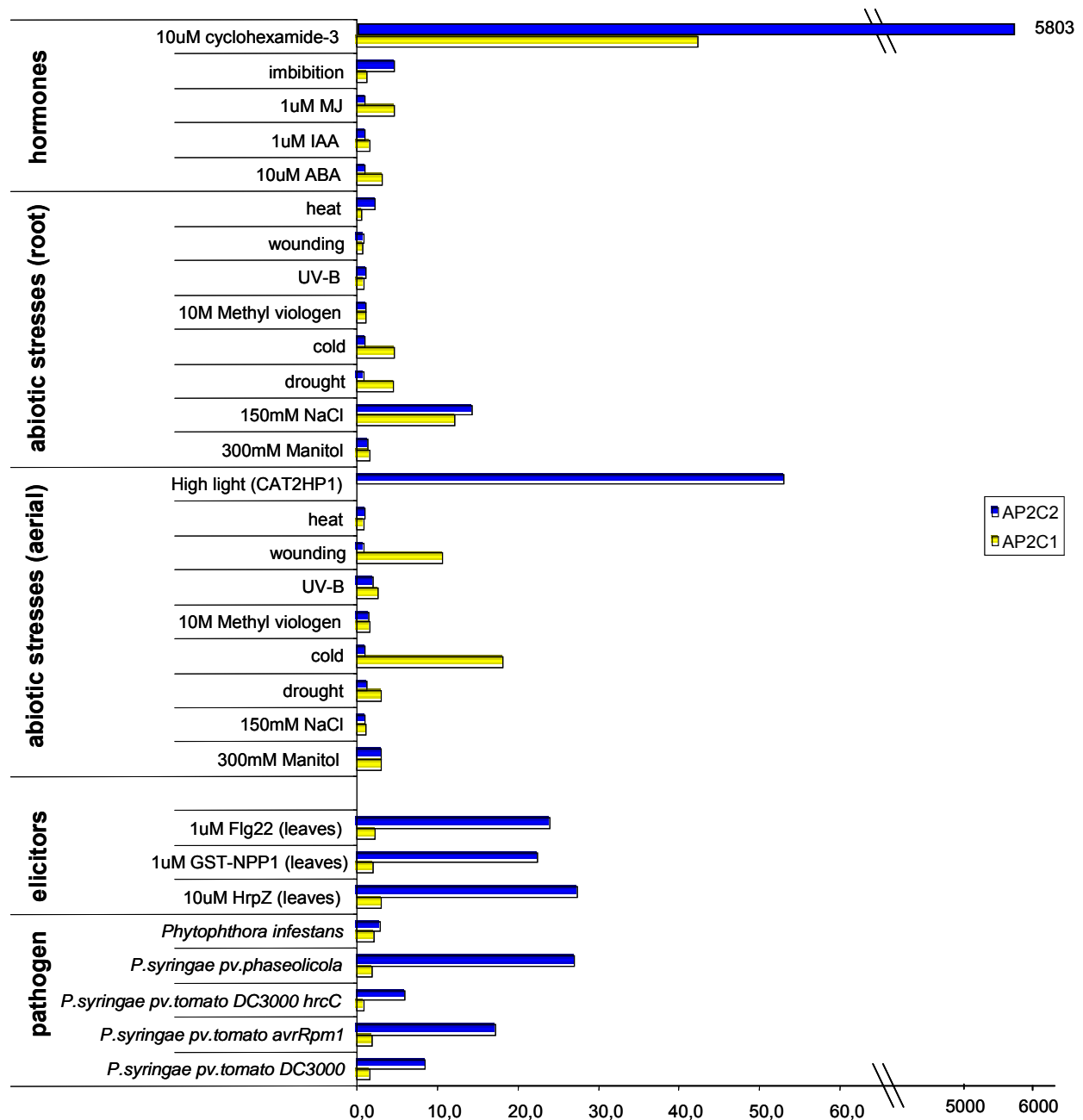


Figure 3.6. Comparison between *in silico* AP2C1 and AP2C2 expression under biotic and abiotic stresses. The expression of both genes (AP2C1 in yellow bars and AP2C2 in blue bars) was induced by cyclohexamide and high salt. MJ, ABA, UVB, methyl viologen and mannitol demonstrate approx. equal induction of both genes. Seed imbibitions, heat and pathogens induced stronger AP2C2 expression. Cold, drought and wounding induced stronger AP2C1 expression (data from AtGenExpress Visualization Tool (AVT) <http://jsp.weigelworld.org/expviz/expviz.jsp> developed by Christian K. Widmer). High light induces AP2C2 transcript 53 fold in catalase-deficient plant (CAT2HP1) compared to the untreated one (Vanderauwera et al., 2005).

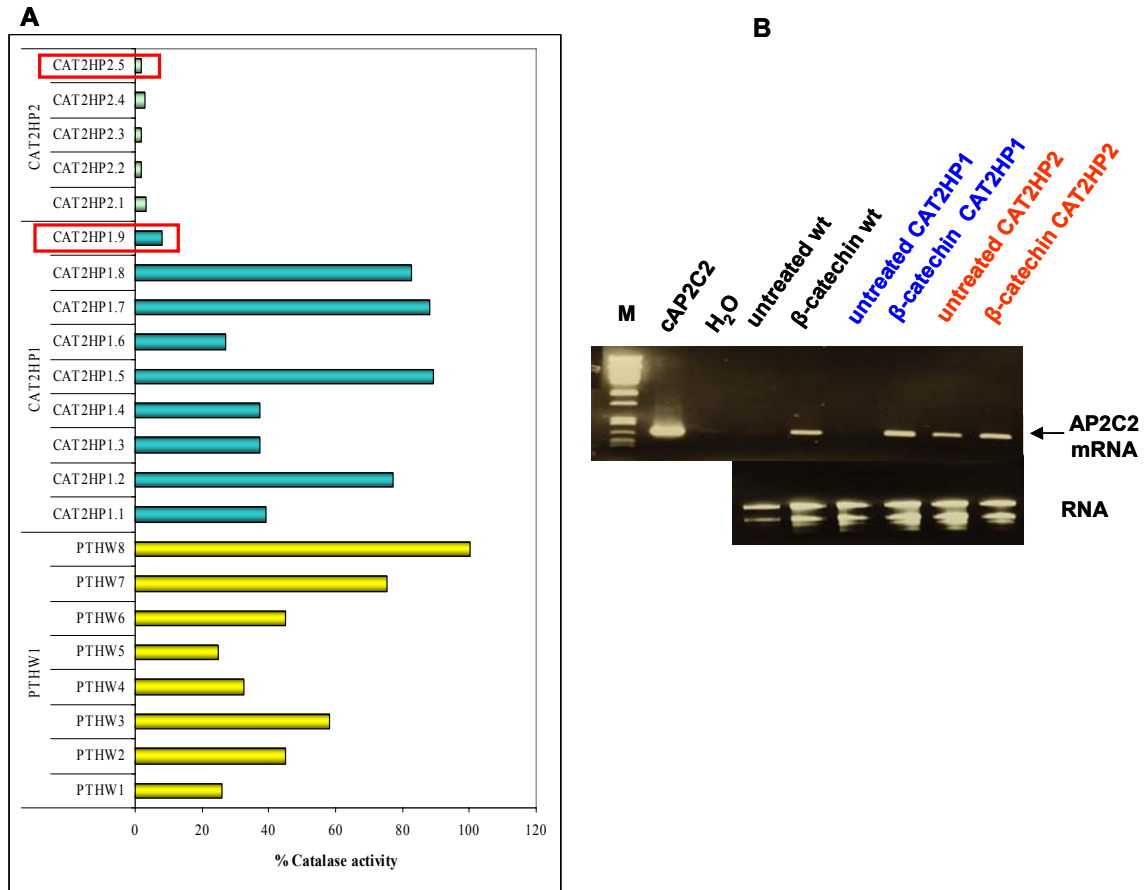


Figure 3.7. *AP2C2* transcript was upregulated in catalase-deficient plants. (A) Measurement of catalase activity by a spectrophotometric assay. The catalase-deficient plants CAT2HP1 and CAT2HP2 had lower catalase activity. Line CAT2HP1.9 and CAT2HP2.5 with remaining catalase activity of 13% and 1% respectively, were selected. The transgenic plants containing empty vector (PTHW) were used as references. **(B)** Using RT-PCR, *AP2C2* transcript was checked in wild type and catalase deficient plants after catechin treatment for 3 hr. The upregulation of *AP2C2* is higher in treated CAT2HP1 plants compared to treated WT plants. In CAT2HP2 plants *AP2C2* transcript was detected before induction and still remained after induction. M is a λ/*Pst*I DNA marker.

The developmental expression of *AP2C2* was studied using *AP2C2::GUS*/WT plants. GUS activity was detected strongly in mature pollen. The GUS staining could be observed in the anthers, in the generative tube and on the stigma (Figure 3.8.A.). In the case of shorter incubation for GUS activity, no GUS staining was observed in other parts of plants such as in root, in leaves or in flowers. *AP2C2::GUS* expression was induced under biotic and abiotic stresses such as wounding, cellulase treatment, strong light and UVC. The GUS staining could be found in roots, around wounded areas and at the hydratode point of leaves (Figure 3.8.B-F.).

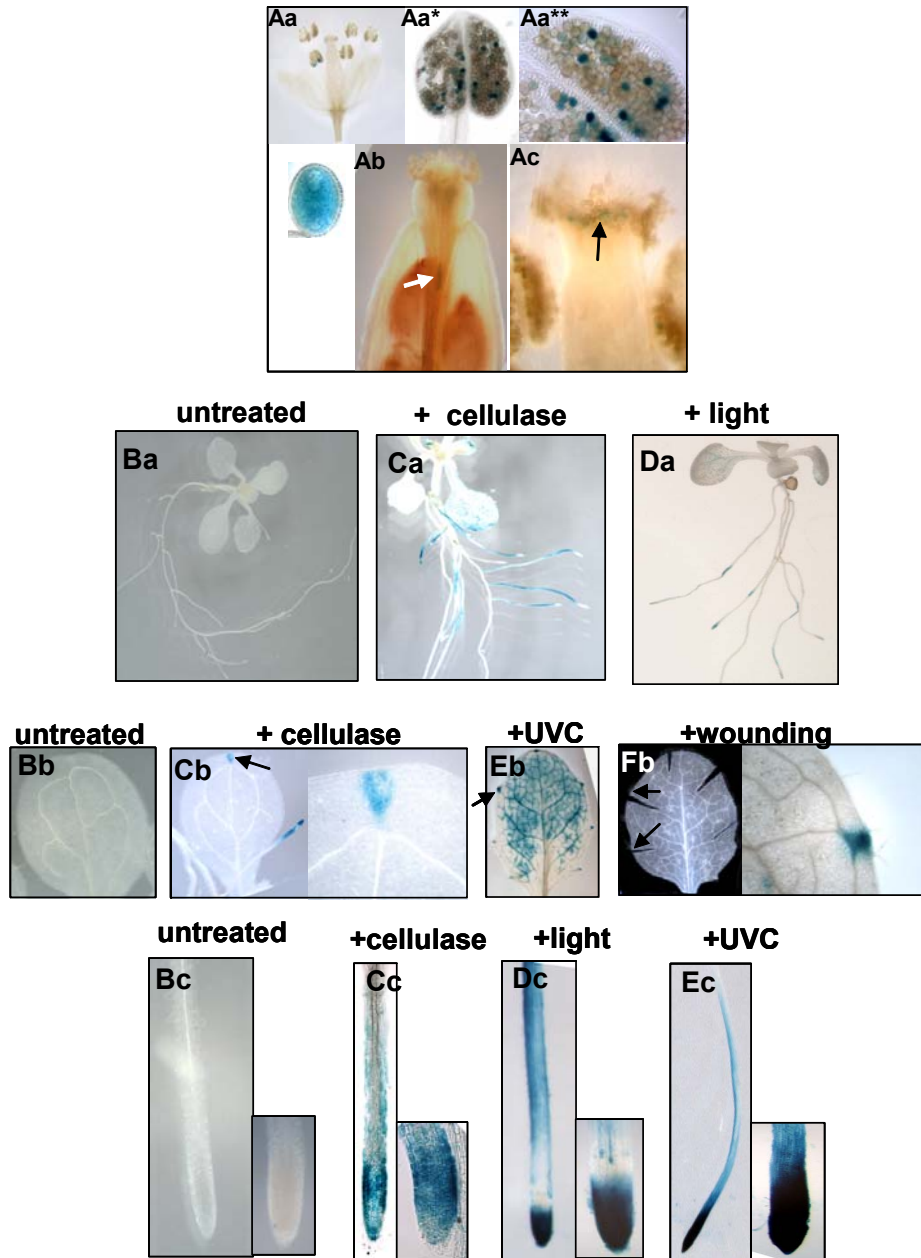


Figure 3.8. *AP2C2::GUS* activity in *Arabidopsis* WT plants during development and under stress conditions. GUS activity was detected (A) in mature pollen, which were (Aa) in the anthers, (Ab) in the generative tube and (Ac) on the stigma. (B-F) *AP2C2::GUS* is expressed upon stress in roots, weakly around the wounded area and at the hydratode point of leaves (arrow). (B) Untreated and treated plants by (C) Cellulase, (D) Strong light (E) UVC and (F) Wounding.

Using *AP2C2::GUS/CAT2HP1* plants, GUS staining was detected at the root tips of untreated plants. This GUS staining could be detected stronger in *AP2C2::GUS/CAT2HP1* plants than in *AP2C2::GUS/wt* plants after induction by strong light, cellulase or wounding. The induction was observed at the hydratode point of leaves, in stomata and in roots (Figure 3.9.).

Taken together, promoter *AP2C2* is induced upon stress. GUS activity could be detected upon stress at the place where there is ROS accumulation, for example at the hydratode point of leaves, in roots, wounded areas or stomata cells.

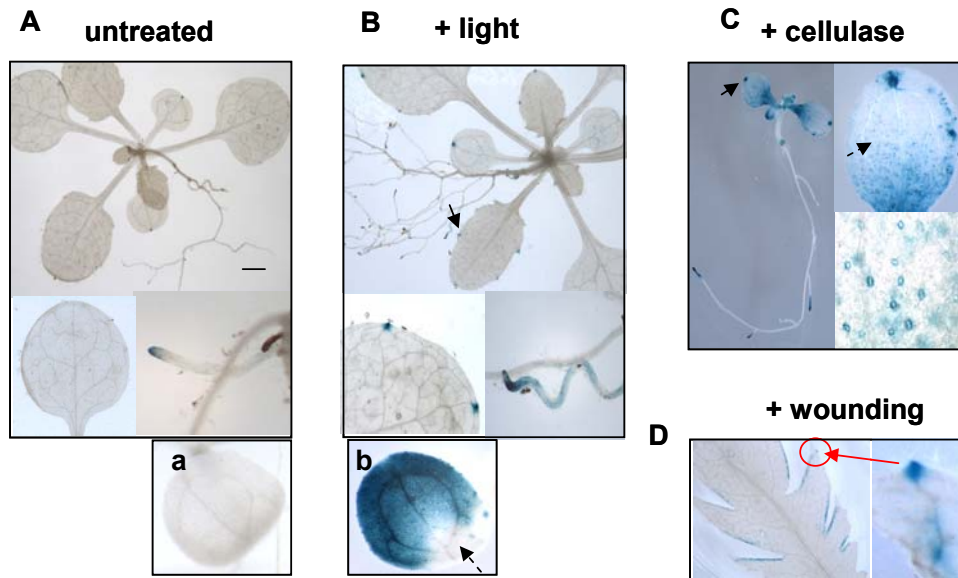


Figure 3.9. *AP2C2*::GUS expression in catalase-deficient plants (*AP2C2*:GUS/*CAT2HP1*). (A) Untreated 2 week-old plant (B) 2 week-old plant exposed to strong light (a) Untreated 5 day-old seedling (b) 5 day-old seedling exposed to strong light (C) Cellulase treatment (D) Wounding. The GUS staining is detected at the hydratode point of leaves (arrow), in stomata (dash arrow) and in root.

3.4.4. *AP2C2* transcript was induced upon stresses.

2 month-old plants were subjected to different stresses including spraying with 0.1 mg/ml cellulase for 30 min, UVC irradiation for 3 hours, 100µg/ml catechin for 3 hours or wounding for 3 hours. RNA was extracted from frozen leaves and RT-PCR was performed for *AP2C2* transcript amplification using primers #406 and #407. Whereas no *AP2C2* transcript was detected in untreated WT plants, the *AP2C2* transcript was strongly induced by cellulase, wounding, catechin and UVC respectively (Figure 3.10.).

Table 3.3. Analysis of *AP2C2::GUS* expression in *AP2C2:GUS/wt* and *AP2C2:GUS/CAT2HP1* plants.

Stress	stress conditions	ages (dpg)	GUS staining		
			wt	CAT2HP1	GUS localisation
untreated	no stress	1-7	-	-	
		14	-	+	at root tip
abiotic stresses					
cold	put seedlings grown in 1/2MS agar plates in +4°C for 3 hr	1-7	-	-	
heat	put seedlings grown in 1/2MS agar plates in 37°C for 3 hr	1-7	+	+	roots
		14	+	+	roots
strong light	put seedlings grown in 1/2MS agar plates under strong light for 3 hr	1-7	-	+	wt-roots CAT2HP1-cotyledons, stomata
		14	+	+	wt-root tip CAT2HP1-hydratode of leaf, roots
UVB	put seedlings grown in 1/2MS agar plates under UVB (302nm) for 30 min and recovery for 3 hr	1-7	-	-	
UVC	put seedlings grown in 1/2MS agar plates under UVC for 15 min and recovery for 3 hr	1-7	+	+	colyledons/roots
	put plants grown in soil under UVC for 30 min and recovery for 3 hr and recovery for 3 hr	14	+	nt	root,hydratode,leaves
freezing	put seedlings grown in 1/2MS agar plates in -10°C for 30 min and recovery for 3 hr	1-7	+	nt	root
high salt	add 250mM NaCl to seedlings grown in 1/2MS liquid media for 1 hr	1-7	-	nt	
wounding	wound attached leaves for 3 hr by blade or wire brush	14	+	+	around wounded area/at hydratode of leaf
H ₂ O ₂	add 20mM H ₂ O ₂ to seedlings grown in 1/2MS liquid media for 1 hr	1-7	-	nt	
Pathogen elicitors					
flg22	add 100nM flg22 to seedlings grown in 1/2MS liquid media for 1 hr	1-7	+	nt	root
cellulase	add 0.1mg/ml cellulase to seedlings grown in 1/2MS agar media for 3 hr	1-7	+	+	wt-root, hydratode point of leaves CAT2HP1-root, hydratode point and stomata of leaves
xylanase	add 1mg/ml xylanase to seedlings grown in 1/2MS liquid media for 1 hr	1-7	+	nt	cotyledon
Hormones					
ABA	add 50,10,200,1000 uM ABA to seedlings grown in 1/2MS liquid media for 1 hr	1-7	-	nt	
auxin	add 5,50,500,1000uM NAA to seedlings grown in 1/2MS liquid media for 1 hr	1-7	-	nt	
JA	add 10,20,50,100uM MeJA to seedlings grown in 1/2MS liquid media for 1 hr	1-7	-	-	
SA	add 10,20,50,1000 uM SA to seedlings grown in 1/2MS liquid media for 1 hr	1-7	-	nt	
cytokinin	add 1mM BAP to seedlings grown in 1/2MS liquid media for 1 hr	1-7	-	nt	
ET	add 10uM ACC to seedlings grown in 1/2MS liquid media for 1 hr	1-7	-	nt	

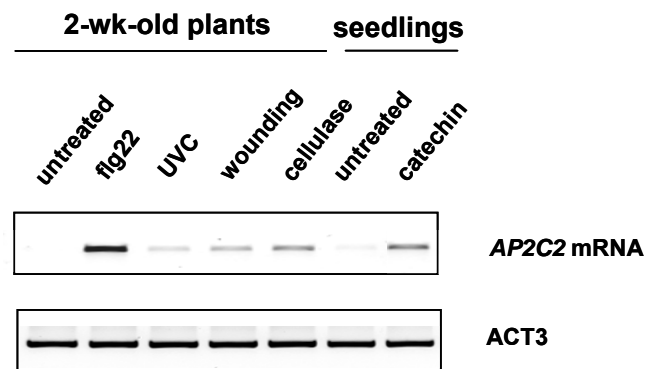


Figure 3.10. *AP2C2* transcript was induced upon stresses. 2 month-old plants were stressed by: adding 100nM flg22 for 3 hr, spraying with 0.1 mg/ml cellulase for 30 min, UVC irradiation for 3 hr, adding catechin for 3 hr and wounding for 3 hr before freezing leaves for RNA extraction. RT-PCR was performed from isolated total mRNA. *ACT3* –control.

3.5. Analysis of phosphatase activity of *AP2C2*

3.5.1. Creation of pGEX-*AP2C2* wild type and loss-of-function mutations plasmids

AP2C2 is a putative protein phosphatase of type 2C (PP2C) and is grouped in cluster B according in sequence similarity to *Medicago sativa* PP2C MP2C (Schweighofer et al., 2004). Its close homolog *AP2C1* (At3g30020) was well characterised as a negative regulator of MAPK signalling by inactivation of MPK4 and MPK6 (Schweighofer et al., 2007), suggesting the possible function of *AP2C2* as a negative regulator of MAPK signalling. Moreover, the Y2H results demonstrated that *AP2C2* directly interacted with MPK3, MPK4 and MPK6, leading to the question if this interaction affects the enzymatic activity of MAP kinases. To investigate whether *AP2C2* is a PP2C phosphatase and also if it acts as a MAPK phosphatase, enzymatic activity and substrates specificity of *AP2C2* was studied using GST fusion proteins: PP2C cluster A (GST-HAB1 and GST-ABI2), PP2C cluster B (GST-*AP2C1* and GST-*AP2C2*) and GST as a negative control.

To produce GST-*AP2C2* protein, pGEX-c*AP2C2* plasmid was created. cDNA of *AP2C2* was cloned into pGEX-4T-1 vector. The resulting pGEX-*AP2C2* was transformed into DH5α *E.coli* competent cells. The positive clones were selected by ampicillin resistant marker.

To produce GST-*AP2C2* loss-of-function (phosphatase inactive enzyme) proteins, three pGEX-*AP2C2*-lof mutation plasmids were constructed. The pGEM-c*AP2C2* was mutated by site directed mutagenesis method using 3 pairs of specific primers, introducing 3 single point mutations in c*AP2C2*. The *AP2C2*-lof1 (G155D) mutation was designed according to

the G180D mutation found in *ABII* gene in the conserved motif which is involved in metal binding and catalysis (Das et al., 1996; Sheen, 1998) (Figure 3.11.A.). The AP2C2-lof2 (G155R) mutation was applied mutation at the same point as AP2C2-lof1 but exchanged with a different amino acid. The last mutation, AP2C2-lof3 (R287A) was designed according to the MP2C-lof mutation in the highly conserved motif among eukaryotic PP2Cs C-terminal part of the protein (Figure 3.11.B.). The point mutations were verified by sequencing before cloning into pGEX-4T-1 vector and transformed into DH5 α *E.coli* competent cells and positive clones were selected by ampicillin resistance.

The GST-AP2C2 proteins (wild type and lof mutations) were extracted and purified. The quantity and quality of the proteins were checked by 10%SDS-PAGE. The expected size of GST-AP2C2 is 67.2 KDa (Figure 3.12.A.). The protein amount was calculated according to Bradford assay (§ 2.6.2) and SDS-PAGE (§ 2.6.3). 0.1-1 ug of the protein was used for *in vitro* phosphatase activity assay.

A		B	
SubdomainII		Subdomain VI	
MP2C (G159)	LAFFGVFDGHG	MP2C (R289)	GSLAVSRGIGDRHLK
AP2C1 (G172)	QAIFGVYDGHG	AP2C1 (R304)	GSLAVSRGIGDAQLK
AP2C2 (G155)	QAIFGVYDGHG	AP2C2 (R287)	GSLAVSRGIGDAHLK
AP2C3 (G163)	NAFFGVFDGHG	AP2C3 (R297)	GTLAVSRGIGDRYLK
AP2C4 (G153)	KSFFGVYDGHG	AP2C4 (R284)	GILAVSRGIGDAHLK
ABI1 (G174)	AHFFGVYDGHG	ABI1 (R313)	GVLAMSRSIGDRYLK
ABI2 (G162)	AHFFGVYDGHG	ABI2 (R303)	GVLAMSRSIGDRYLK
AtPP2CA (G139)	HHFYGVFDGHG	AtPP2CA (R293)	GVLAMSRSIGDNYLK
	G>D ↑		↑
	G168D <i>abi2-1</i>		R289A MP2C-lof

Figure 3.11. Creation of AP2C2 loss-of-function mutations. (A) AP2C2-lof1 (G155D) and (B) AP2C2-lof3 (R287A) were created by site directed mutagenesis. The mutations are corresponding to *abi1-1* mutation and MP2C-lof, respectively. The point mutations are in the conserved motif which is involved in metal binding and catalysis in conserved C-terminal part of the PP2C phosphatases.

3.5.2. Recombinant GST-AP2C2 protein has Mg²⁺-dependent PP2C phosphatase activity and MAPK phosphatase activity *in vitro*.

GST-phosphatase fusion proteins (AP2C1, AP2C2, HAB1 and ABI2) were incubated with a radio-labelled casein substrate in the presence of okadaic acid in the phosphatase buffer for 1 hour at 30°C. Protein phosphatases remove ³²P from the substrate and release free radio-phosphate into supernatant. The phosphatase activity was reported as the radioactivity count per minute per mg protein (CPM/mg). The result demonstrated that

PP2Cs, both cluster A (HAB1 and ABI2) and cluster B (AP2C1 and AP2C2), had phosphatase activity toward the phosphorylated casein substrate (Figure 3.12.A.).

To study the substrate specificity, GST-MPK6-lof was labelled with radio-phosphate by GST-MEK4 and used as a substrate for phosphatase activity assay. The reaction performed was similar as that for substrate casein. The result demonstrated that only the PP2Cs cluster B (AP2C1 and AP2C2) had MAPK phosphatase activity at 30 and 60 min after incubation, whereas PP2Cs cluster A (HAB1 and ABI2) did not reveal phosphatase activity toward MPK6 (Figure 3.12.B.). The phosphatase activity depended on Mg^{2+} cofactor, since MPK6 phosphatase activity of GST-AP2C2 was abolished by adding EDTA (Figure 3.12.C.)

3.5.3. Phosphatase activity of AP2C1 is strongly reduced by loss-of-function mutations in metal binding site and catalytic part.

Plasmid pGEX-AP2C1-lof2 (G178D) (constructed by Alois Schweighofer) was used in this study. The loss-of-function mutation was created according to the G180D mutation in *ABII* gene in the conserved motif involved in metal binding and catalysis (Das et al., 1996; Sheen, 1998) (Figure 3.12.D.). The result showed that the MPK6 phosphatase activity of GST-AP2C1-lof2 is reduced 70% of the GST-AP2C1-wt protein activity (Figure 3.12.E.).

3.6. MAP kinases are inactivated by AP2C2 in protoplasts

Since AP2C2 could inactivate MPK6 *in vitro* (phosphatase assay of GST recombinant proteins), it was important to test whether AP2C2 could inactivate MAPKs in protoplasts. To study the MAP kinase inactivation by AP2C2 in protoplasts, plasmids pSP72-2x35S-TL-gAP2C2-Myc were co-transformed with pGreenII0229-2x35S-TL-AtMPK3-HA or pGreenII0229-2x35S-TL-AtMPK4-HA or pGreenII0229-2x35S-TL-AtMPK6-HA (by Vaiva Kazanaviciute) in the presence of upstream activators pJS-delta ANP1-HA or pRT-AtMKK2-gof-Myc into *Arabidopsis* protoplasts. Whereas the amount of MAPKs, Δ ANP1-HA and MKK2-Myc plasmids, used in this assay was always the same (5 μ g), the amount of AP2C2 was increased from 0, 0.05, 0.1, 0.5, 1 to 5 μ g. Total protein extracts from protoplasts were used to pull down the MAP kinase complexes with anti-HA antibody, and the immunoprecipitate was used for *in vitro* kinase assay toward MBP substrate. The consistent results between MPK3, MPK4 and MPK6 demonstrated that kinase activities decreased parallel with the increasing amount of AP2C2 protein (Figure 3.13.)

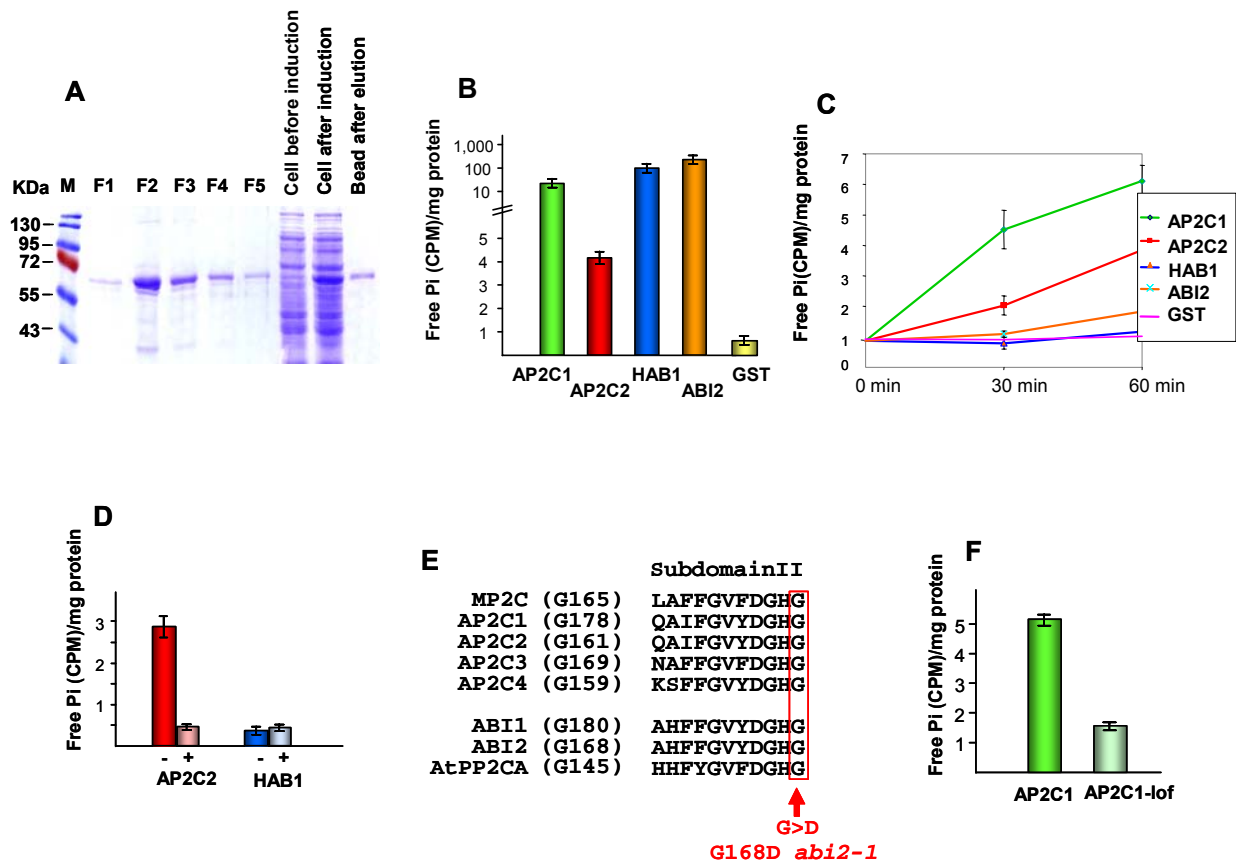


Figure 3.12. Recombinant PP2C proteins from cluster B have Mg^{2+} -dependent MAPK phosphatase activity, which is strongly reduced by loss-of-function mutation in catalytic part. Phosphatase activities of PP2C proteins both from cluster A (HAB1 and ABI2) and cluster B (AP2C1 and AP2C2) were measured as free radio-phosphate released after incubation of purified GST-PP2C proteins with the substrates. **(A)** 5 fractions (F1-F5) of purified GST-AP2C2 protein (M.W. 67.2 KDa) were checked on 10%SDS-PAGE. Cell before/after induction and bead after elution were included in the gel. M is PageRuler® prestained protein ladder marker. **(B)** Both cluster A and B PP2Cs have phosphatase activity toward artificial substrate casein. Whereas **(C)** only PP2C cluster B have MAPK phosphatase activity toward MPK6-lof. **(D)** MAPK phosphatase activity is abolished by adding 10mM EDTA and is reduced in AP2C1 loss-of-function **(E)** glycine change to aspartic acid in Mg^{2+} coordination site **(F)** MPK6 phosphatase activity of AP2C1-lof is reduced 70% of the wt protein activity. Standard errors represent the average of 3 measurements.

3.7. Characterization of *ap2c2* knockout plants

ap2c2 knockout mutant T2 seeds (GK-316F11) caused by T-DNA insertion was obtained from GABI-Kat collection. The 10 plants which could survive on selective medium containing sulfadiazine were further analysed. PCR, using the set of primers which were composed of *AP2C2* gene specific primers (#179 and #180) and T-DNA binding LB (#398) and RB (#393) primers, demonstrated that T-DNA inserted within *AP2C2* gene consisted of two inverted repeat LB-RB/RB-LB. Nucleotide sequencing revealed the site

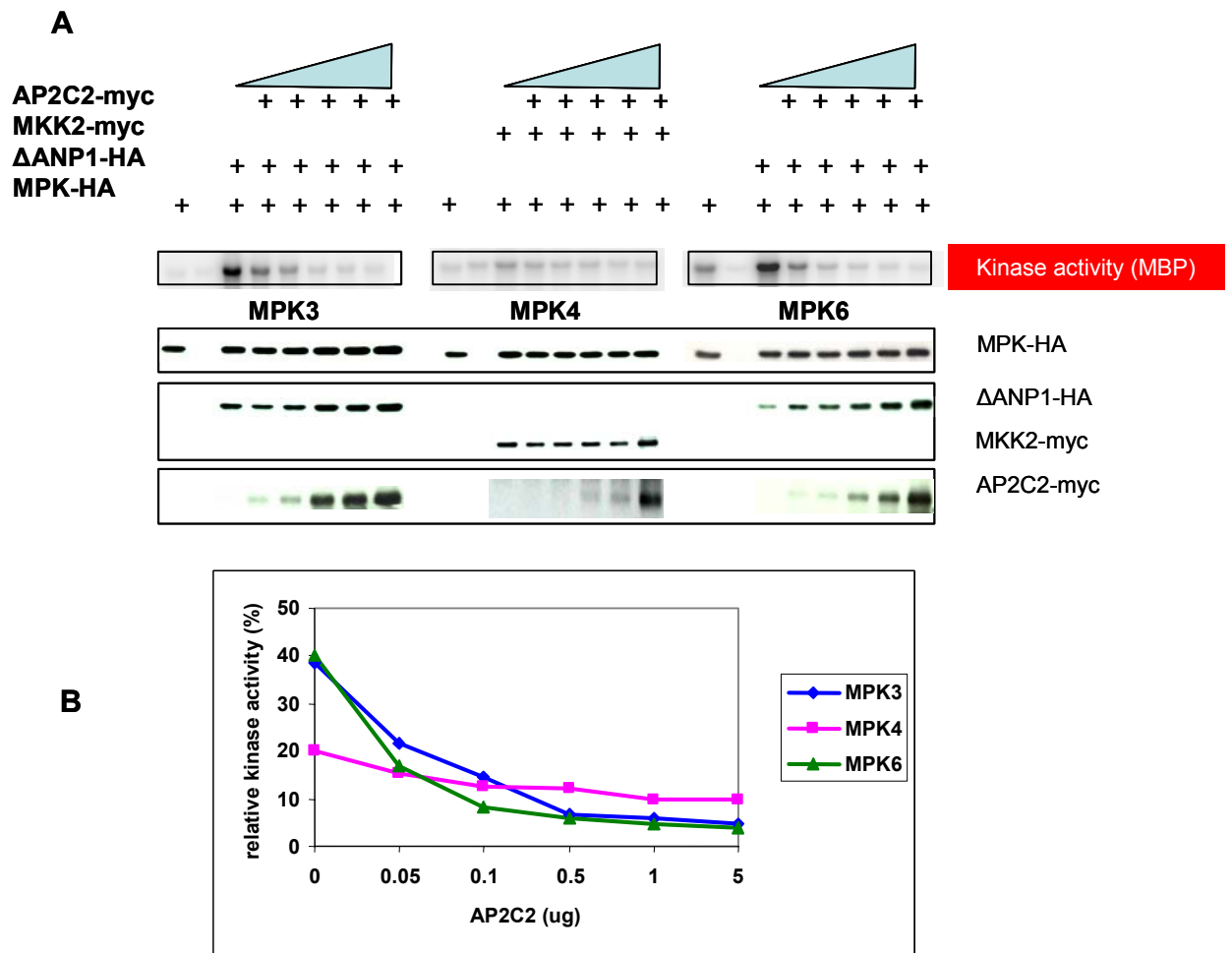


Figure 3.13. MAP kinases are inactivated by AP2C2 in protoplast. (A) AP2C2-myc together with MPKs-HA and upstream activator, ΔANP1-HA or MKK2-Myc, were co-transformed into *Arabidopsis* protoplasts. The proteins were immunoprecipitated with HA antibody and used in *in vitro* kinase assay toward MBP. Increasing the amount of AP2C2 from 0, 0.05, 0.1, 0.5, 1 to 5 μg in samples 3-8 resulted in decreasing MPK3, MPK4 and MPK6 activities respectively. Sample 1 contained only MPKs. Only H₂O was added in sample 2. (B) Quantification of kinase activities in protoplasts with respect to the different amount of AP2C2 according to the above experiment.

of T-DNA insertion in the 1st intron, approximately 534 bp downstream ATG (Figure 3.14.A.). However, Southern blotting analysis revealed multiple T-DNA insertion in the plants (data not shown). To get rid of the multiplicity of T-DNA insertions and select the line with a single T-DNA insertion in AP2C2 gene, *ap2c2* knockout line #7 was used for crossing back with wild type plant. After back crossing with wild type, F1 plants bearing T-DNA were detected by PCR and sulfadiazine resistant marker. F2 plants were analysed for homozygous T-DNA insertion by PCR. Line #7.2.1 was selected (Figure 3.14.B.). F3 plants were checked for single T-DNA insertion by Southern blotting. gDNA of wild type and knockout leaves were digested with *Bgl*II and electrophoresis on 0.8% agarose gel for 2.50 hr. After DNA was transferred to nitrocellulose filter it was probed with the

fluorescent labelled DNA fragment recognising left border of T-DNA. The two expected bands of size 8326 and 3676 bp were detected. Southern blotting confirmed line #7.2.1.6 as a single T-DNA insertion line (Figure 3.14.C.). Moreover, T3 plant line #7.2.1.6 was checked for *AP2C2* transcript using RT-PCR primers #406 and #407. The results showed null expression of *AP2C2* in *ap2c2* line #7.2.1.6 after treatment with flg22 (Figure 3.14.D.). Finally, the homozygous single T-DNA insertion *ap2c2* plant #7.2.1.6 was selected for further study. Western blotting analysis, using phospho (S/T)-MAPK antibody, demonstrated that *ap2c2* #7.2.1.6 had higher phospho-threonine MAPK protein amount than WT plants, especially 10 and 30 min after cellulase treatment (Figure 3.14.E.). These results confirmed that *AP2C2* is responsible for dephosphorylating MAPKs at the activation loop.

3.8. Characterization of *AP2C2* overexpressing transgenic plants

Transgenic plants, constitutively overexpressing *AP2C2* were produced by Vaiva Kazanaviciute using *Agrobacterium* mediated floral dip. Full length cDNA of *AP2C2* was fused to a sequence encoding green fluorescent protein (GFP), C-myc (Myc) and hemagglutinin (HA) in plant expression vectors and introduced into the wild type *Arabidopsis* plants. Cauliflower mosaic virus (CaMV) 35S promoter fusion with the tobacco etch virus translational leader (TL) was used to ensure high protein expression (Restrepo et al., 1990). T1-T2 plants were selected on medium containing kanamycin. T3-T4 plants were analysed for protein abundance by western blotting using epitope tags antibodies. The proteins were extracted from leaves and separated on 10% SDS-PAGE. By cDNA sequences, *AP2C2*-tag proteins size were expected as 66.8 KDa for *AP2C2*-GFP, 55.8 KDa for *AP2C2*-Myc and 42.5 KDa for *AP2C2*-HA. However, the protein bands detected by Western blotting were lower than the expected bands as 66.8 KDa for *AP2C2*-GFP, 55.8 KDa for *AP2C2*-Myc and 42.5 KDa for *AP2C2*-HA. The lines with high protein expression were selected for further study including *AP2C2*-GFP OE #11.2.6, *AP2C2*-Myc OE # 3.2.5.6 and *AP2C2*-HA OE # 1.2.3

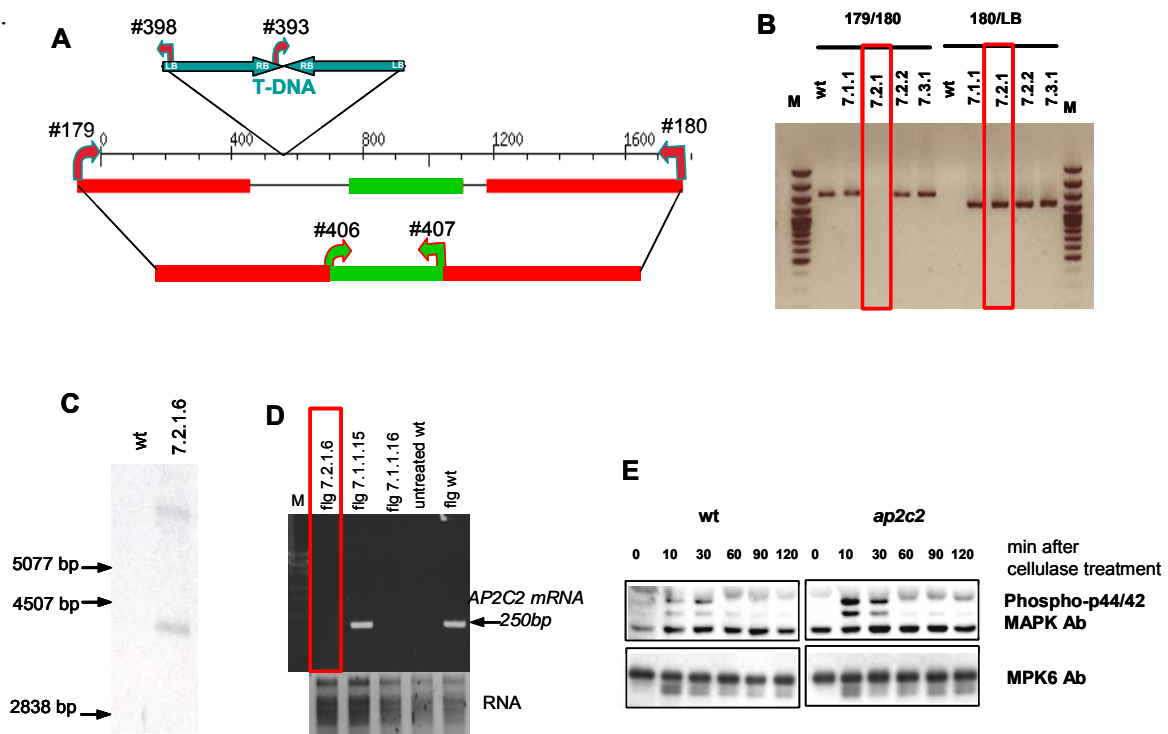


Figure 3.14. Characterisation of *ap2c2* plant line. *ap2c2* T2 seeds line GK-316F11 obtained from GABI-Kat was analysed. **A)** Schematic diagram shows inverted repeat T-DNA insertion (LB-RB RB-LB) at the first intron of *AP2C2* gene, approximately 534 bp downstream ATG. Red and green bars represent exons. Red arrows indicate primers used for PCR and green arrows indicate primers for RT-PCR. **B)** PCR analysis of wt and *ap2c2* F2 leaves after crossing back with wild type plant. T-DNA insertion was detected as 800 bp and 1.2 Kb amplified products by primers LB and #179/#180 respectively, whereas the wild type *AP2C2* gene specific primers #179 and #180 amplified product of 1.5 Kb size. The F2 plant #7.2.1.6 was identified as homozygous knockout and selected for further studies. M is a 100bp ladder DNA marker. **C)** The copy numbers of T-DNA insertion in *ap2c2* F2 plants was determined by Southern blotting. gDNA of wild type and knockout leaves were digested with *Bgl*II electrophoresed on 0.8% agarose gel for 2.50 hr. Filter-transferred DNA was probed with the fluorescent labelled DNA fragment recognising left border of T-DNA. The expected sizes were 8,326 and 3,676 bp as shown compared to wild type. **D)** Expression of *AP2C2* was checked by RT-PCR using primers #406 and #407 as indicated in the diagram A. Leaves were treated with 100nM flg22 for 30 min. The result shows null *AP2C2* expression of flg22-treated plants #7.2.1.6 and #7.1.1.16. M is a λ /*Pst*I marker. **(E)** Western blot analysis using phospho-MAPK antibody detected higher amount of phospho-threonine/phospho-tyrosine active loop MAPK protein in *ap2c2* plants than in wild type plants after cellulase treatment.

3.9. AP2C2 inactivated MAPKs in plant.

In order to verify the function of *AP2C2* as a negative regulator of MAPKs, (in addition to *in vitro* and in protoplasts experiments), the MAPKs inactivation effect of *AP2C2* was tested *in planta*. MPK3, MPK4 and MPK6 kinases were immunoprecipitated, and their

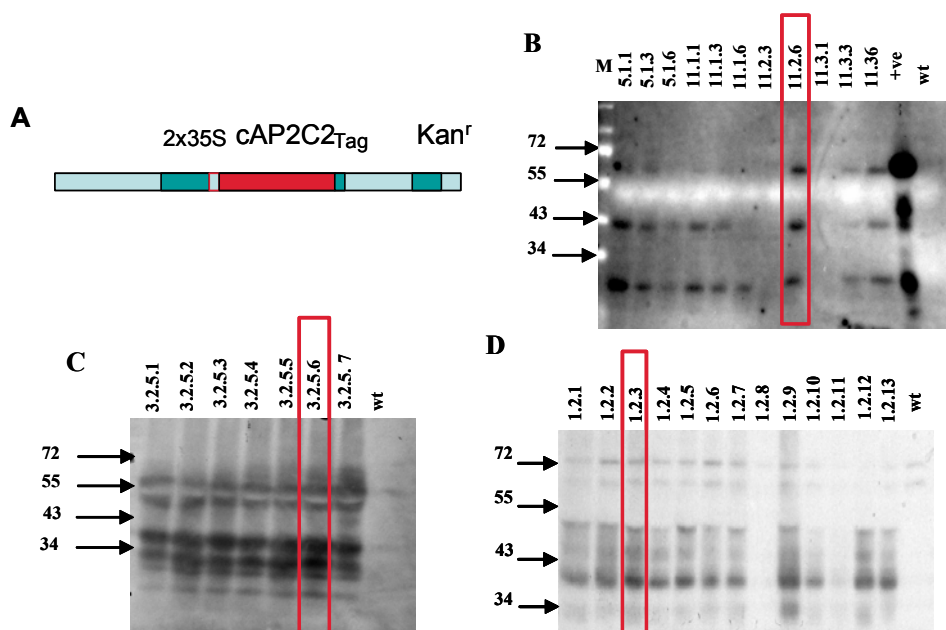


Figure 3.15. Identification of AP2C2 overexpressing transgenic plants. T3 and T4 transgenic lines were analysed for the expression of AP2C2-tag proteins as quantified by western blot analysis on 1%SDS-PAGE using GFP, Myc and HA antibodies. (A) Schematic diagram showed the part of plasmid containing AP2C2cDNA under control of 35S promoter, leader and termination signal tagged with GFP, Myc, or HA. **(B)** Line AP2C2-GFP #11.2.6 was selected for further analyses. MW 66.8 KDa, +ve is AP2C1-GFP –a positive control **(C)** line AP2C2-Myc # 3.2.5.6 was selected, MW 55.8 KDa **(D)** Line AP2C2-HA # 1.2.3 was selected, MW 42.5 KDa

activity assays were performed on MBP substrate in WT plants and in plants with altered AP2C2 levels. Two month-old *ap2c2*, AP2C2 OE and WT plants were sprayed with 0.1 mg/ml cellulase. Leaves were collected and frozen for 0, 10, 30, 60, 90 and 120 min after treatment. After protein extraction, MPK3, MPK4 and MPK6 were immunoprecipitated with specific antibody to each kinase (Cardinale et al., 2000). The results showed that the activity of MPK3, MPK4 and MPK6 were significantly lower in AP2C2 OE leaves than in WT leaves after cellulase treatment. At the same time, analysis of *ap2c2* plants revealed strongly elevated MPK3 and MPK6 kinases activity after cellulase treatment, whereas MPK4 activity was not significant changed compared to the WT (Figure 3.16.). The estimation of MAPKs protein levels by Western blotting from the same protein extracts showed that upon cellulase treatment, protein amounts of all three MAP kinases tested did not change, supporting the idea that kinase activities are regulated by posttranslational mechanisms.

Taken together, analysis of *ap2c2* plants and plants with constitutive overexpressing of AP2C2 protein confirmed AP2C2 role in negative regulation of stress activated MPK3, MPK4 and MPK6

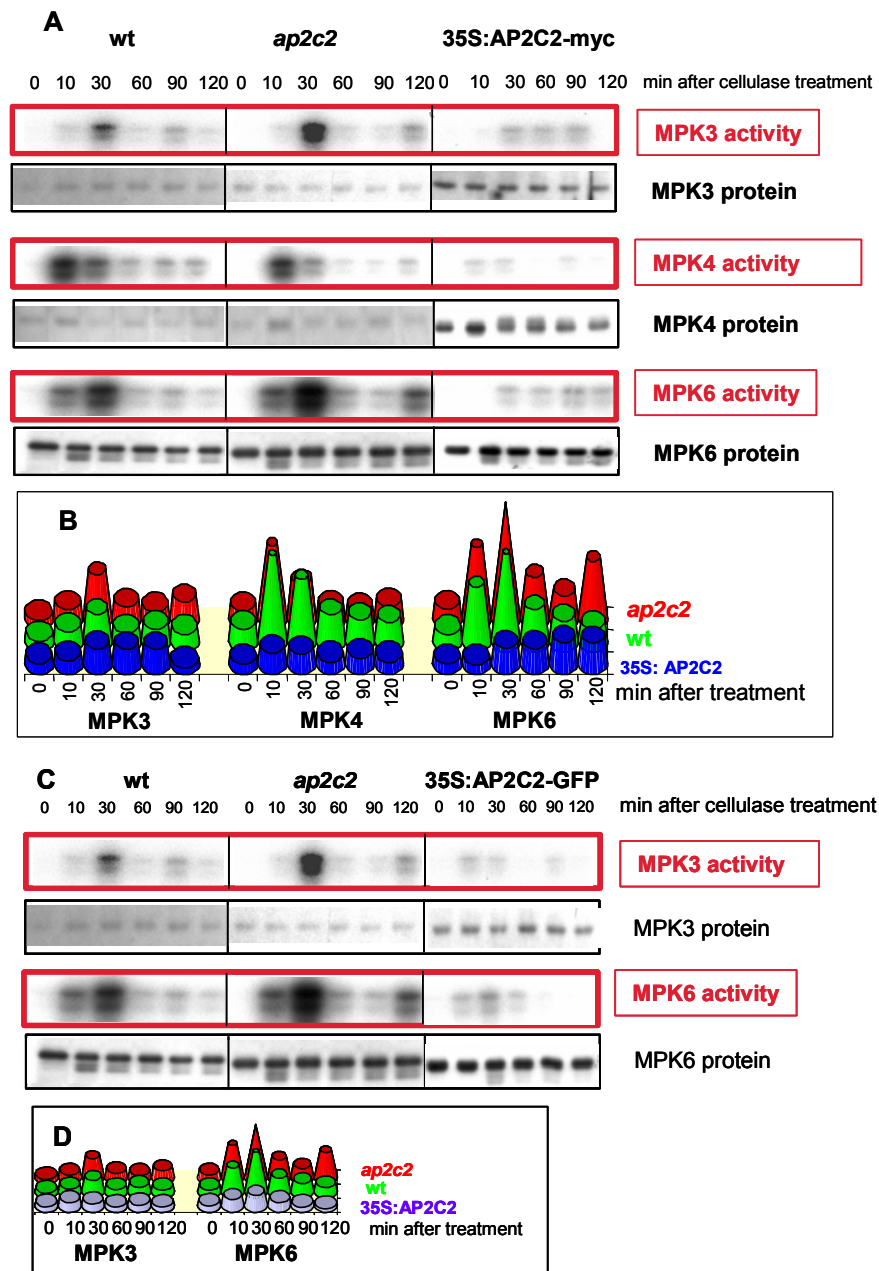


Figure 3.16. AP2C2 inactivates MAPKs in planta and *ap2c2* plants have enhanced stress-MAPK activities. 2 month-old plants were sprayed with 0.1mg/ml cellulase and leaves were collected after 0, 10, 30, 60, 90 and 120 min. MPK3, MPK4 and MPK6 antibodies were applied to immunoprecipitate kinases from proteins extracts. The IPs were used for *in vitro* kinase assays toward MBP substrate. **(A)** MPK3, MPK4 and MPK6 kinases were transiently activated between 10 and 30 min after stress. *ap2c2* plants had stronger kinase activities, whereas AP2C2-myc OE had lower kinase activities compared with WT plants. At 120 min, MPK6 activity of *ap2c2* came up again. **(C)** AP2C2-GFP OE had lower kinase activities compared with *ap2c2* and WT plants. **(B, D)** Quantification of kinase activities by ImageQuant in WT, *ap2c2* and AP2C2 OE plants according to the above experiments.

3.10. *Thionin2.1*, JA-responsive transcript, was transiently upregulated in *ap2c2* plant after stresses.

As found in this work, one of the interacting partners of AP2C2 is Acyl-coA oxidase 1, ACX1. ACX1 is the enzyme in jasmonate biosynthesis (octadecanoid biosynthesis) pathway. It catalyses the first step of the core β -oxidation cycle that also produces H_2O_2 byproduct. It has been reported that biotic and abiotic stresses, such as pathogen and wounding, generate signals that activate a phosphorylation cascade that regulates JA biosynthesis and signalling (Kazan and Manners, 2008; Schweighofer and Meskiene, 2008). To investigate if AP2C2 affects JA signalling pathway, expression of *Thionin2.1* (*Thi2.1*) transcript, which is the JA-responsive gene, was determined in 2 month-old WT plant and plants with altered AP2C2 levels. After wounding, leaves were collected at 3 and 6 hours. RNA was extracted and RT-PCR was performed. The results demonstrated that JA-responsive *Thi2.1* transcript was upregulated in *ap2c2* leaves but not in wild type or AP2C2 OE plants. The expression of *Thi2.1* was affected by interplay between AP2C1 and AP2C2 expression due to altered AP2C2 levels in AP2C2 modified plants. This demonstrates the effect of AP2C2 expression on *AP2C1* and *thi2.1* transcripts. In WT plants after wounding, both *AP2C1* and *AP2C2* transcripts were induced, leading to no *Thi2.1* expression. In *ap2c2* plants at 3 hours after wounding, *Thi2.1* was strongly induced. However, later on at 6 hours after wounding, the increased *AP2C1* was observed and less *Thi2.1* transcript detected. In AP2C2 OEs, higher amount of *AP2C2* could be detected even before the induction by stress. Interestingly, at 3 hours after wounding in AP2C2 OEs, internal *AP2C2* was not detected but was detected again at 6 hours after wounding. No *AP2C1* and *thi2.1* expression was detected in AP2C2 OE plants (Figure 3.17.).

3.11. Modification of AP2C2 expression in plants affects seed germination and seedling survival.

Since AP2C2 expression was induced in response to stress, it was tested whether plants with altered AP2C2 levels responded to stress differently than WT plants. Seed germination and seedling survival was observed in *ap2c2*, AP2C2 OE and WT seedlings using *mpk6* (characterized by Vaiva Kazanaviciute) as a control. 50 seeds of each line were sterilized and sown on the 1/2 MS medium plates without or with stress factors, including

0.25 μ M methyl viologen (PQ), 0.1M NaCl and 10 μ M methyl jasmonate (MJ). The plates were kept at 4°C for 3 days before transferring to growth chamber

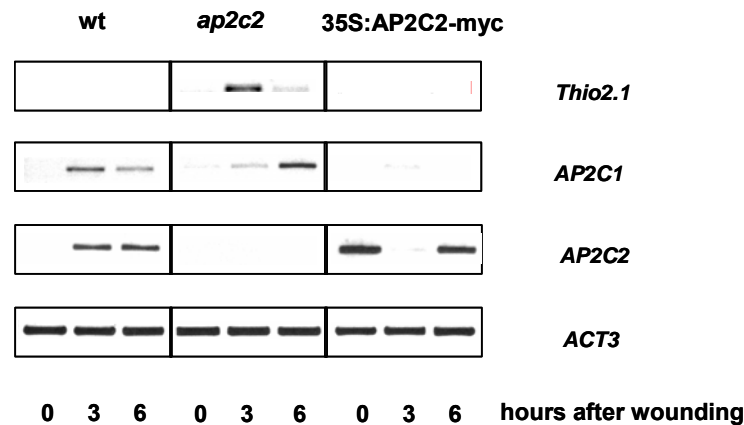


Figure 3.17. *Thionin2.1*, a JA-responsive transcript, was transiently upregulated in *ap2c2* plant after stresses. After wounding, leaves were collected at 3 and 6 hr. RNA was extracted and RT-PCR was performed. The result showed JA-responsive *Thi2.1* was upregulated only in *ap2c2* plant but not in wild type or AP2C2 OE plants. In *ap2c2* plant, at 3 hpw when no *AP2C2* and low *AP2C1*, *thi2.1* transcript was upregulated. At 6 hpw the transcript was reduced when *AP2C1* transcripts came up. Whereas in WT plant where *AP2C1* and *AP2C2* transcripts co-upregulated or in AP2C2 OE plant where high level of *AP2C2* transcript lead to no *thi2.1* transcript both at 3 and 6 hpw.

One day after placing the plates in growth chamber (1 DPG), the number of germinated seeds with emerging of radical were counted under binocular microscope. Whereas there was no significant difference in the number of seed germination between plant lines in 1/2 MS media, there was difference of the number of seed germination between lines grown under stress conditions. Under 0.25 μ M PQ and 0.1M NaCl, *ap2c2* seeds germinated better than AP2C2 OE seeds, approximately 50% and 30% respectively. However, there was no significant difference in the number of *ap2c2* and AP2C2 OE seeds, including WT seed germination, under 10 μ M MJ. The number of *ap2c2* seed germination was higher than WT when grown under 0.25 μ M PQ (55%) and 0.1M NaCl (80%). The number of AP2C2 OE seed germination was significantly higher than WT only when grown under 0.1M NaCl (60%) but not 0.25 μ M PQ or 10 μ M MJ (Figure 3.18.A.).

In addition to seed germination, the survival of seedlings was observed at 7 day-post germination (7 DPG). The number of seedling survival was counted as green cotyledons of seedlings. Interestingly, only under 0.25 μ M PQ but not on 1/2 MS medium, 0.1M NaCl or 10 μ M MJ, seedlings showed significant difference in survival between lines. Under

0.25 μ M PQ, AP2C2 OE seedlings could not survive at all, while *ap2c2* seedlings could survive 50 fold more than WT (Figure 3.18.B.).

Taken together, plants with no phosphatase (*ap2c2* knockout plants) were more tolerant to oxidative stress conditions, including paraquat and high salinity. *ap2c2* seeds could germinate better and survive more than WT and AP2C2 OE plants under oxidative stress conditions.

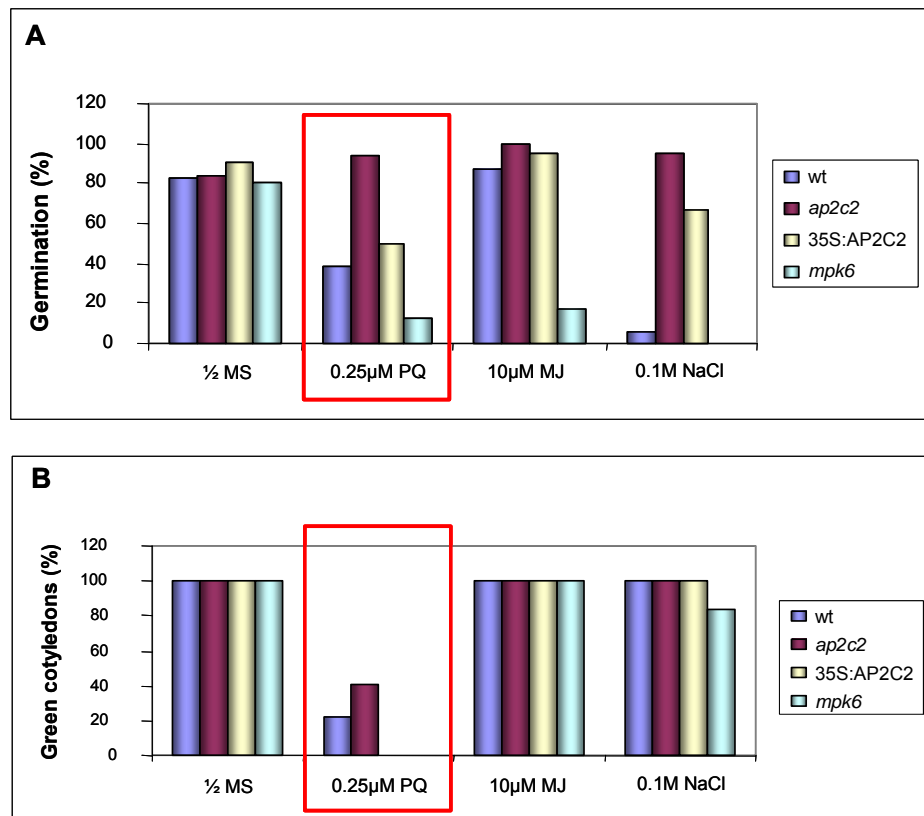


Figure 3.18. Modification of AP2C2 expression in plants affects seeds germination and seedlings survival. (A) The number of seed germination under stress conditions of WT, *ap2c2* and AP2C2 OE plants with *mpk6* as a control. Under 0.25 μ M PQ and 0.1M NaCl, the number of *ap2c2* seed germination was more than WT and OE AP2C2. No difference of germination between lines grown in JA containing medium. (B) The number of seedling survival under stress conditions at seven day post germination. Seedlings grown under 0,25uM PQ survive more than WT. AP2C2 OE seedlings could not survive at all. No difference of seedling survival between lines grown in JA or high salt. Each bar represented the average of 50 seedlings.

3.12. Modification of AP2C2 expression in plants affects root phenotype under stress conditions.

The reduction of root growth by NaCl is closely correlated with an increase of cellular H₂O₂ level (Lin and Kao, 2001). AP2C2 expression was induced by oxidative stress. Since AP2C2 negatively affected stress-responsive MAPK cascade (activated by cellulase, see Figure 3.16.), the modification of AP2C2 expression in plants might affect other stress signalling pathways and stress responses which may lead to modulation of root phenotype under stress. We observed root phenotype including primary roots and lateral roots of 10 *ap2c2*, AP2C2 OE and WT seedlings grown under 1/2 MS medium and medium containing 0.1M NaCl. On 1/2 MS medium, *ap2c2* seedlings showed longer primary root than WT seedlings. Obvious phenotype was observed under high salt environment. The length of *ap2c2* roots was longer than WT. Whereas the primary root length of AP2C2 OE showed not much difference compared with WT, the AP2C2 OE seedlings had longer lateral root (Figure 3.19.).

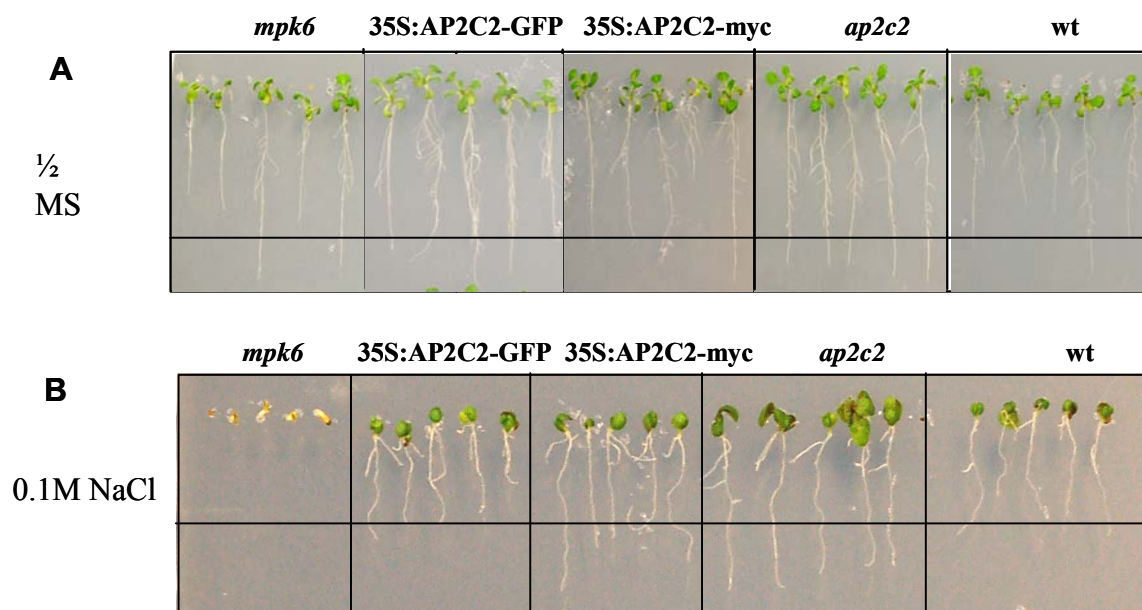


Figure 3.19. Modification of AP2C2 expression in plants affects root phenotype under stress conditions. (A) Under normal growth condition, the primary root length of *ap2c2* and AP2C2 OE are approximately the same with a bit longer roots of *ap2c2*. (B) Under high salt condition, the primary root of *ap2c2* seedlings are significantly longer than those of WT.

3.13. Production and characterisation of AP2C2 RNAi plants

To gain more insight on AP2C2 functions, AP2C2 loss-of-function RNAi-induced AP2C2 knockdown plants were produced. The CATMA 1a06210 DNA fragment of *cAP2C2* according to the AGRICOLA project was amplified and cloned into pGEM-Teasy vector as inverted repeats interrupted by an intron. The Catma-intron-amtaC DNA cassette was subcloned into pENTRY 4 entry vector. Finally, the DNA cassette was exchanged to pB7GWIWG2-I Gateway vector, resulting in pB7GWIWG2-I-AP2C2-RNAi plasmid. The plasmid was transformed into *Arabidopsis* WT plants. The T1 plants bearing the Catma AP2C2-RNAi cassette were selected by Basta resistance. The T2 plants were analysed by RT-PCR for AP2C2 transcript after flg22 treatment. The lines which had lower AP2C2 transcript were selected. Plant line #1050.2.2, which had AP2C2 transcript of approximately 20% compared with treated WT, was selected (Figure 3.20.).

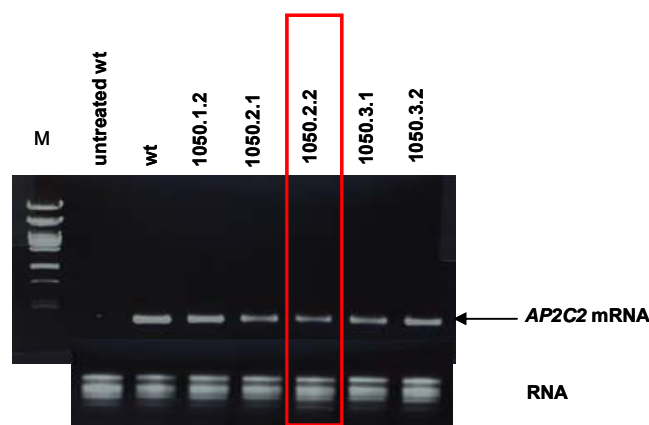


Figure 3.20. Characterisation of AP2C2 RNAi plants. Plasmid pB7GWIWG2-I containing AP2C2 Catma 1a06210-RNAi was transformed into *Arabidopsis* WT plants. The positive Basta selection T2 plants were checked for AP2C2 transcript. The flg22 treated plant lines #1050.2.2, which had AP2C2 transcript approximately 20% compared with flg22 treated WT, was selected. M is a λ /PstI DNA marker.

3.14. No difference in sensitivity to *Pseudomonas syringae* DC3000 of AP2C2 modified plants.

To investigate the effect of AP2C2 on plant susceptibility to bacterial pathogen, leaves of WT, AP2C2-GFP OE, AP2C2-myc OE and AP2C2 RNAi plants were inoculated with virulent *Pseudomonas syringae* DC3000 by syringe infiltration of a 5×10^5 cfu/ml of bacterial suspension to leaves. The number of bacteria grown on the NYG(A) plates

containing rifampicin and cyclohexamide were counted in leaf tissue at 0, 1, 2 days after infection. Results showed no significant difference of the number of bacterial colonies in the tested plants (Figure 3.21.).

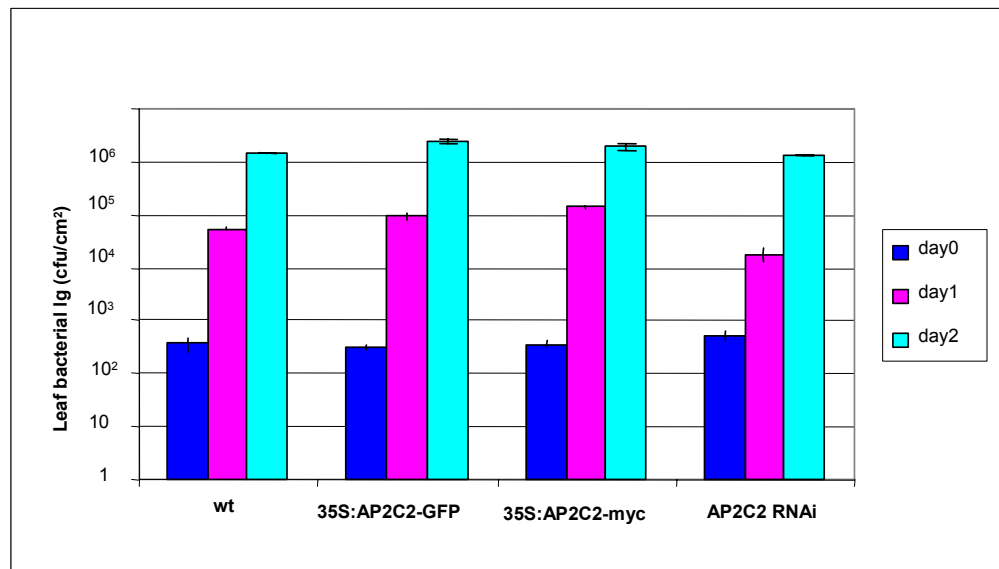


Figure 3.21. No difference in sensitivity to *Pseudomonas syringae* DC3000 of AP2C2 modification plants. Leaves of WT, AP2C2-GFP OE, AP2C2-Myc OE and AP2C2 RNAi plants were inoculated with virulent *P.syringae* DC3000 by syringe infiltration of a 5×10^5 cfu/ml of bacterial suspension into 6 week-old leaves. Bacterial growth in leaf tissue was monitored 0,1,2 days after infection. Data represents log₁₀ (cfu/cm²) \pm standard deviation of triple samples.

3.15. *ap2c2 mkp1* plants demonstrate developmental phenotypes.

An *Arabidopsis* dual specificity (DSP) phosphatase AtMKP1 mutant *mkp1* was found to be hypersensitive to genotoxic stress treatment (UVC). Growth of the *mkp1* mutant under standard conditions is similar as WT, indicating a stress-specific function of AtMKP1 as a crucial regulator of the MAP kinase activity response to genotoxic stress (Ulm et al., 2001). Since AP2C2 and MKP1 function at the same target/pathway, it was interesting to check if there is a relation between the regulations of these phosphatases. Therefore double KO plants were produced by genetic crossing. We observed that single KO parent plants, *ap2c2* or *mkp1*, grown in normal growth long day conditions, showed no obvious phenotype difference from WT plants, whereas the double knockout *ap2c2 mkp1* plants demonstrated abnormalities in development both during growth and fertility. The plants carrying homozygous *mkp1* with either heterozygous or homozygous *ap2c2* were small and showed retarded growth (Figure 3.22.A.).

In addition to growth, the *ap2c2 mkp1* plants showed reduced fertility. The plants carrying homozygous *mkp1* and heterozygous *ap2c2* produced less seeds. The stronger fertility phenotype was detected in the plant with homozygous knockout of both genes. It produced only two seeds (Figure 3.22.B.).

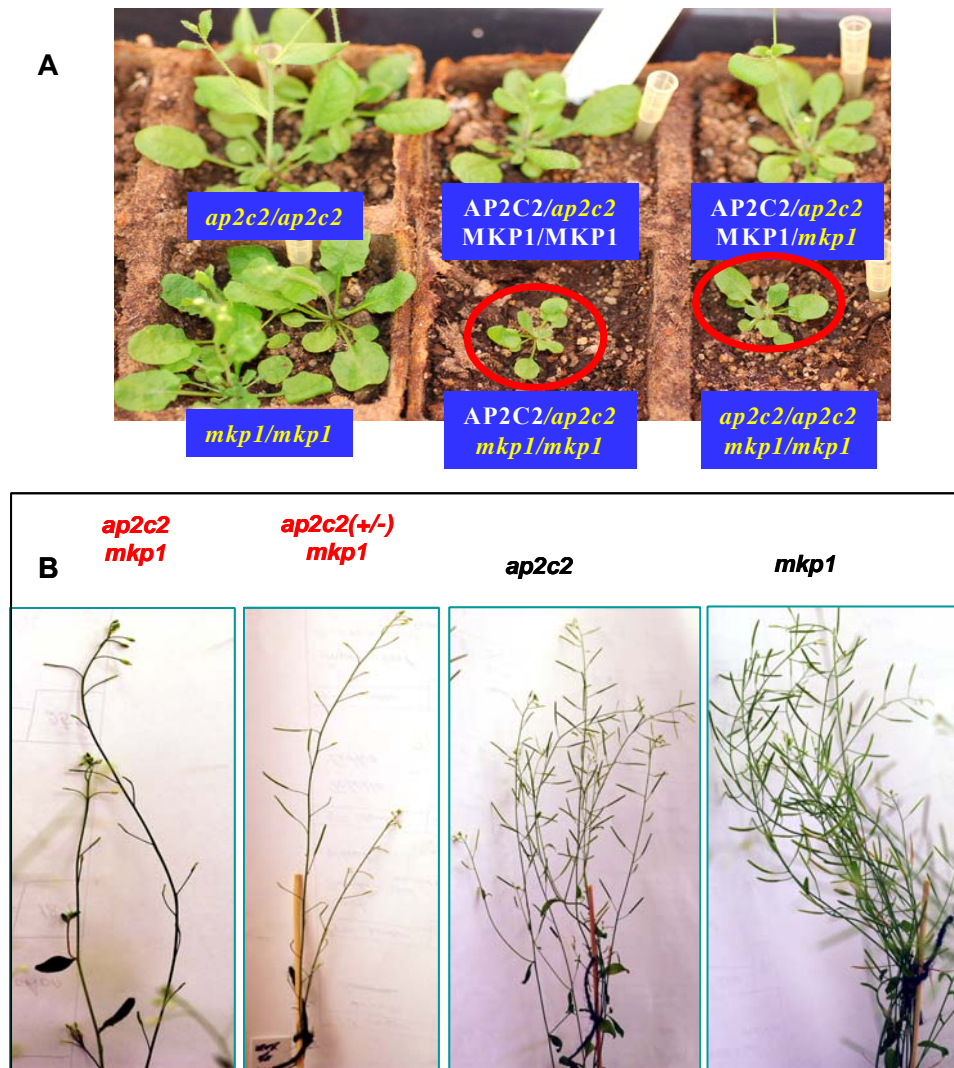


Figure 3.22. *ap2c2 mkp1* plants have obvious developmental phenotypes. F2 plants grown in normal long day conditions showed phenotype similar to single parent knockout plant, *ap2c2* or *mkp1*. **(A)** Plants carrying homozygous *mkp1* and either heterozygous or homozygous *ap2c2* showed retarded growth and were smaller than WT. **(B)** Plants carrying homozygous *mkp1* with either homozygous or heterozygous *ap2c2* have reduced fertility. They produce less seeds. In the homozygous knockout of both genes plant, severe seed abortion occurred. They produce only one or two mature seeds per plant.

3.16. *ap2c1/2* plants had longer primary root

As AP2C1 and AP2C2 are close homolog, they might share some substrates and work redundantly. Therefore, we produced double knockout plants of both genes, which might present stronger phenotypes compared with the single knockout parent, *ap2c1* or *ap2c2*. Since *ap2c2* already had primary root longer than WT grown under normal growth conditions, the root length of *ap2c1/2* plants was monitored under normal growth conditions. The primary root length of WT, *ap2c1*, *ap2c2* and *ap2c1/2* seedlings grown in 1/2MS media was observed under normal growth conditions. After 5 days of germination, the primary root length was measured. The results showed significant differences of primary root length of studied plants. Strikingly *ap2c1/2* seedlings had much longer primary root length than WT ($P = 0$), *ap2c1* ($P = 0.002$) and *ap2c2* ($P = 0.021$) single knockout parental seedlings. Compared to the WT, *ap2c2* seedling root length was significantly longer ($P = 0.029$), whereas *ap2c1* seedlings root length was less different ($P = 0.186$). The root length of *ap2c1* and *ap2c2* were not significantly different ($P = 0.281$) (Figure 3.23.A,B.).

3.17. AP2C2 complements fertility phenotype in *ap2c2* (+/-) *acx1/5* plants.

It has been seen that wound-induced JA accumulation was abolished in a mutant that is impaired in Acyl-coA oxidases (the core enzyme in β -oxidation cascade of JA biosynthesis) both *ACX1* and its close related paralog, *ACX5*. The severe JA deficiency in *acx1/5* double mutants was accompanied by reduced pollen viability and fertility. Treatment of *acx1/5* plants with JA restored the normal seed set (Schilmiller et al., 2007). *ACX1* is identified as the substrate of AP2C2 by Y2H, suggesting the possible role of AP2C2 involved with JA biosynthesis. In addition to that, AP2C1, an interacting protein with *ACX1* (Kazanaviciute, 2006), was shown to negatively control wound JA amounts (Schweighofer et al., 2007). We hypothesized that AP2C2 may act as a negative regulator of JA biosynthesis, thus knockout of AP2C2 expression could complement the fertility phenotype of *acx1/5* plants. To examine the hypothesis, *ap2c2* was crossed with *acx1/5* double knockout plants (provided by Gregg A. Howe, Michigan State University, USA) to produce triple knockout *ap2c2/acx1/acx5* plants. In *ap2c2/AP2C2/acx1/5* T2 plants demonstrated better fertility compared to the *acx1/5* plants (Figure 3.24.).

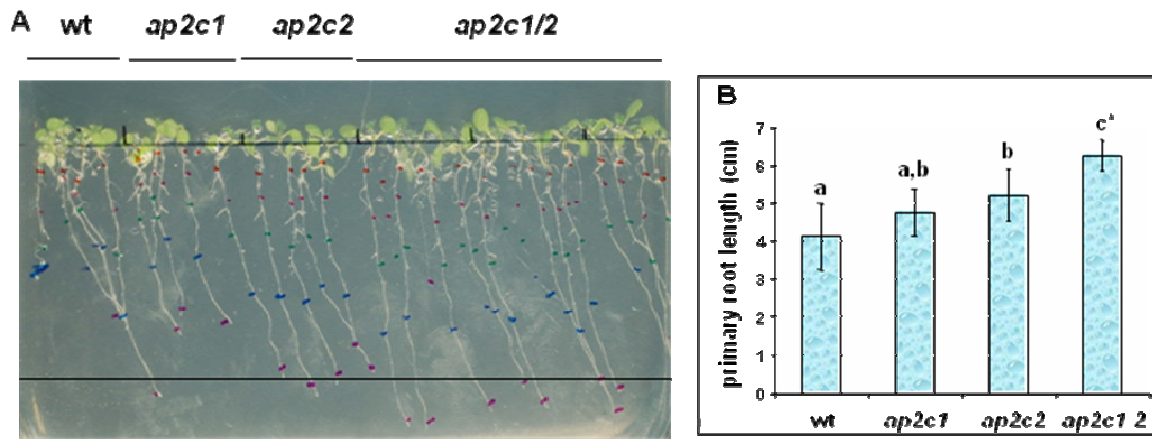


Figure 3.23. *ap2c1/2* plants have longer primary root. (A) *ap2c1/2* seedlings grown in $\frac{1}{2}$ MS media have longer primary roots than WT, *ap2c1* and *ap2c2* seedlings. *ap2c2* seedlings root length was significantly longer than *ap2c1* seedlings root length compared to WT. The root length of *ap2c1* and *ap2c2* were not much different (B) 10-30 seedlings represent for each bar chart according to the picture A. Mean root length was measured representing an average of 25 measurements is reported. Data are presented as average (n=10-30).



Figure 3.24. Less AP2C2 complements fertility phenotype in *ap2c2/AP2C2* *acx1/5* plants. The 3 month-old plants of heterozygous *ap2c2/AP2C2* in *acx1/5* plants produce siliques containing normal seed sets compared with the *acx1/5* plants.

3.18. Production of ethylene in wounded WT, *ap2c2* and AP2C2 OE plants

It has been reported that *Arabidopsis* MPK6 is required for ethylene induction. Phosphorylation of ACS2 and ACS6 (1-aminocyclopropane-1-carboxylic acid synthase, the rate-limiting enzyme of ethylene biosynthesis) by MPK6 leads to the stabilisation and accumulation of ACS proteins and, thus, elevated levels of cellular ACS activity and ethylene production (Liu and Zhang, 2004). Moreover, constitutive overexpression of AP2C1, leading to suppression of MPK6 activation by wounding, results in strongly reduced wound ethylene levels in leaves. As MPK6 is inactivated by AP2C2, it suggests the possible role of AP2C2 in ethylene biosynthesis via MPK6. We assumed that plants with higher AP2C2 protein amounts, which have lower MPK6 activity, may produce less ethylene compared with WT after stress. Therefore, the expanding leaves of 2 month-old WT, *ap2c2* and AP2C2 OE plants, were wounded and kept in air-tight sealed vials for 24 hours prior to ethylene measurement using gas chromatography, FID detection. Results showed that the AP2C2-GFP OE plants had statistically significant lower ET production compared to WT ($P = 0.027$), while another overexpressing AP2C2-Myc plants had not significant lower ET production ($P = 0.353$). Both *ap2c1/2* and *ap2c2* had tendency, but not significant, of higher ET production ($P = 0.685$ and $P = 0.443$ respectively) (Figure 3.25.).

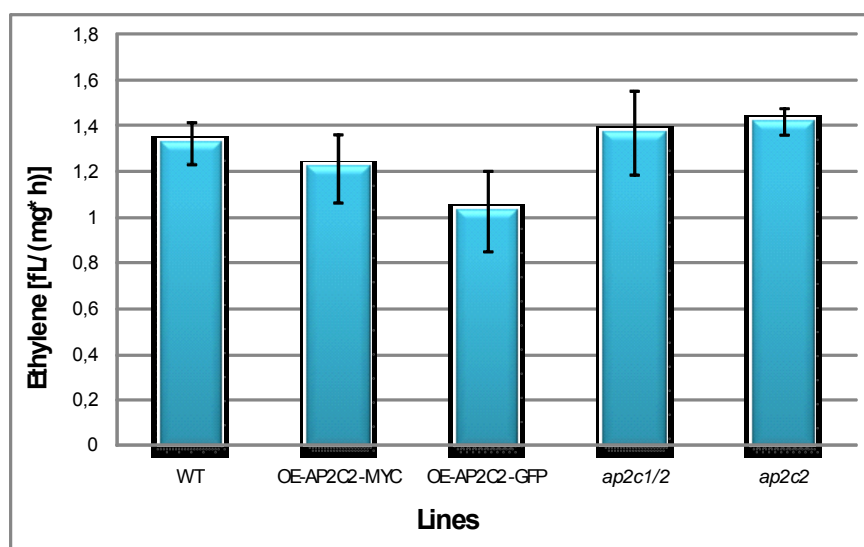


Figure 3.25. Production of ethylene in wounded AP2C2 modification plants. Approximately 0.5 g of 2 month-old leaves of wild type, 35S::AP2C2-Myc and 35S::AP2C2-GFP, *ap2c1/2*, and *ap2c2* were wounded and put into sealed 21.5 ml vial. The headspace-released wound-induced ethylene was measured after 24 hours. The OE AP2C2-GFP plants produced significantly higher ET than WT. Standard errors from the measurements of three samples are indicated. $P < 0.05$.

4. DISCUSSION

AP2C2 was classified as a putative *Arabidopsis* protein Ser/Thr phosphatase type 2C (PP2C) of cluster B by the amino acids homology to alfalfa MP2C (Schweighofer et al., 2004). According to MP2C and its close homolog, *Arabidopsis* AP2C1, the function of AP2C2 was assumed to be involved with stress response. The results obtained from this work together with the previous reports support the hypothesis that AP2C2 function as a regulator of stress response, especially response to ROS signalling, under biotic and abiotic stresses and may be involved in regulation of JA in development.

AP2C2 expression is induced by ROS

AP2C2 is an inducible gene. Its expression is highly specific and very low under normal growth condition, detected only in mature pollen according to microarray analysis (AtGenExpress) and promoter AP2C2::GUS reporter analysis. However, the expression of AP2C2 is stronger induced by biotic and abiotic stress factors. Heat and cyclohexamide induce AP2C2 transcript much higher than AP2C1. Our results demonstrated that GUS activity could be detected in AP2C2::GUS plants subjected to flg22, cellulase, UVC, wounding and paraquat. Whereas cellulase induced AP2C2 expression stronger than that of AP2C1, methyl jasmonate (MJ) induced AP2C1 expression but not the AP2C2. Moreover, the AP2C2 transcript could be detected by RT-PCR after the WT plants were subjected to cellulose, UVC, wounding or catechin.

Furthermore, the location of AP2C2 expression could be detected at the site of ROS accumulation, for example at the hydrotode point of stressed leaves (e.g. by cellulase, UVC or wounding) or around wounded area.

The expression of AP2C2 is stronger observed in the condition of higher ROS production, for example in catalase deficient plants, CAT2HP1. These plants accumulate higher H₂O₂ upon ozone or high light treatment (Vandenabeele et al., 2004). Interestingly, only AP2C2 but not AP2C1 transcript was upregulated 52.4 fold in CAT2HP1 plants exposed to high light stress (Vanderauwera et al., 2005). In this study, stronger GUS activity could be detected in AP2C2::GUS in the background of CAT2HP1 plants (AP2C2::GUS/CAT2HP1), than in the background of WT plants (AP2C2::GUS/WT), both treated or untreated (e.g. cellulase, high light or wounding) conditions. In the background

of catalase deficient plants (*AP2C2::GUS/CAT2HP1*), *AP2C2::GUS* was already induced even without any treatment. The GUS activity could be detected at the distal part of the roots. After induction by stresses, the GUS activity was stronger induced in roots, the hydratode points of leaves, stomata cells and around wounded area than in *AP2C2::GUS/WT* plants exposed to the same stresses.

Taken together, the results suggested that *AP2C2* expression is responding to biotic and abiotic stress factors, which induce ROS production. The expression pattern of *AP2C2* has some similarity and some specificity compared to *AP2C1*, suggesting both the unique and redundant functions between *AP2C1* and *AP2C2*.

AP2C2 acts as a negative regulator of ROS-induced MAPK signalling.

AP2C2 interacts with MPK3/4/6 in yeast.

Several evidences support the idea that *AP2C2* functions as a negative regulator of ROS-induced MAPK signalling. First, *AP2C2* protein contains MAP kinase interaction motif (KIM) in the N-terminus, suggesting its potential substrates to be MAPKs. Furthermore, MPK6 was isolated from *Arabidopsis* cDNA library using *AP2C2* as bait. The specific interaction of *AP2C2* with only MPK3/4/6 out of the tested 18 MAPKs demonstrated high specificity of *AP2C2* interactions. The identified interacting partners of *AP2C1* and *AP2C2* suggested the similarity and the difference in their functions. For instance, while they shared the same substrates MPK4/6, only *AP2C2* but not *AP2C1* interacts with MPK3 (Schweighofer et al., 2007). The interaction between *AP2C2* and MPK3/4/6 was validated using split YFP in protoplasts. Subcellular localization of *AP2C2* and its interacting complexes was similar as detected for *AP2C1* (Schweighofer et al., 2007). Both *AP2C2*/MPK4 and *AP2C2*/MPK6 complexes are associated with the nucleus. *AP2C2*/MPK6 complex was detected also in cytoplasm. These result suggested that *AP2C2* interacts with MAPKs in the nucleus or cytoplasm. However, it is not clear when the complexes were formed, before or after translocation into the nucleus. The interaction between *AP2C2* and MPK3 is ambiguous. The fluorescence signal detected in the cell was weak and not clear enough to be able to identify the site of interaction. The reason might be because the interaction between these proteins is not stable (Drori et al., 2004), alternatively new experiments have to be performed in protoplasts to verify this interaction.

The interaction between AP2C2 and MAPKs leads to MAPKs dephosphorylation.

In vitro phosphatase assay using GST-protein fusion demonstrated that AP2C2 has Mg^{2+} -dependent MAPK phosphatase activity, which can be abolished by EDTA. It has been reported that mutation in the metal coordinating residues in catalytic part at glycine 180 (G180) in *abi1-1* and *abi2-1* reduce phosphatase activity of the proteins (Das et al., 1996; Leung et al., 1997) and the mutation at G174D abolished phosphatase activity of ABI1 (Sheen, 1998). Similarly, AP2C1-lof1 (G172D) and AP2C1-lof2 (G178D) corresponding to ABI1 (G174D) and ABI1 (G180D) respectively, were generating inactive phosphatase proteins. The missense mutation of AP2C1-lof2 from glycine to aspartic acid (G178D) reduced 70% of the wild type phosphatase activity, suggesting the importance of the metal coordinating residues of catalytic part on phosphatase activity. Therefore, similar loss-of-function mutations of AP2C2 were produced in this work for future testing of phosphatase activity on MAPKs and to generate mutant plants.

ap2c2 plants demonstrated higher phosphorylation of serine/threonine MAPKs after cellulase treatment detected by Phospho-MAPK antibody. These result together with published data (Meskiene et al., 2003) confirmed the idea that AP2C2 (Ser/Thr phosphatase) dephosphorylates activated-MAPKs at threonine residues of pTEpY motif on MAPKs.

AP2C2 inactivates MAPKs through threonine dephosphorylation.

MPK3/4/6 inactivation by AP2C2 was demonstrated in protoplasts and *in planta*. In protoplasts, the increase amount of AP2C2 leads to the decrease MPK3/4/6 kinase activities activated by Δ ANP1 or MKK2 (Kovtun et al., 2000). In plants, modification of AP2C2 levels affected MPK3/4/6 kinase activity upon cellulase treatment. Whereas *ap2c2* plants had higher kinase activity, AP2C2 overexpressors, oppositely, demonstrated inactivation. Interestingly, in *ap2c2* MPK3/6 could be re-activated earlier than in wild type plants, demonstrating the narrower re-setting time in *ap2c2* plant during stress. These result confirmed the idea that MAPKs activity is regulated by AP2C2. However, the results of MPK4 activity in *ap2c2* plants are ambiguous. Whereas AP2C2 overexpressing plants had obviously lower kinase activity, *ap2c2* plants did not show enhanced MPK4 kinase activity, which would be expected for the knock out plants if AP2C2 is regulating MPK4. The possible explanation might be that under cellulase treatment, AP2C2 might not be a direct regulator of MPK4 in WT plants or it might be regulating MPK4 in specific cells (e.

g. pollen). However, due to constitutive and abundant production of AP2C2 in leaves of overexpressing plants, leading to high MAPK phosphatase activity, MPK4 kinase activity is affected.

Plants lacking both AP2C2 and MKP1 have obvious phenotypes.

The *Arabidopsis* MKP1 was reported as MAPK phosphatase (Ulm et al., 2001). Its interaction with MPK6 regulates MAPK activity and plant stress response. The *mkp1* mutant demonstrated hypersensitivity to genotoxic stress but had a normal development (Ulm et al., 2002). Since both AP2C2 and MKP1 regulate the same target group, MAPKs, they might act as functionally redundant or regulate MAPKs in different pathways. Interestingly, whereas *ap2c2* or *mkp1* develop normally under normal growth conditions, the homozygous of *ap2c2 mkp1* plants demonstrated obvious developmental phenotypes. They were small, had retarded growth and infertility, suggesting converging functions of AP2C2 and MKP1 in development.

AP2C2 localizes in plastids and is associated with the nucleus of the cell.

The localization of AP2C2 was predicted to be in plastids according to the putative chloroplast transit peptide (cTP) sequences identified at the N-terminus of the protein. Our results demonstrated that AP2C2-GFP is localized in plastids and associated with the nucleus of *Arabidopsis* protoplasts. The plastid localization of AP2C2 was confirmed by co-localization with fluorescent plastid marker (Nelson et al., 2007). The fluorescence images demonstrated that AP2C2 localized within the plastids, but not in peroxisomes. However, it could not be excluded the peroxisome localization of AP2C2. AP2C2 might translocate into peroxisome in some specific situation. For examples under high light stress or photorespiration, which produces high amount of H₂O₂ in peroxisomes, lead to AP2C2 induction. AP2C2-GFP localized in chloroplast of stomata cells and in unidentified, small, round organelles (“stromule”) in the roots of AP2C2 overexpressing plants.

Taken together, AP2C2 functions as a negative regulator of stress-activated MAPKs. AP2C2 might directly interact and inactivate MAPK3/4/6. The interaction of AP2C2 and MAPKs might be via KIM motif located in the N-terminal part of AP2C2. MAPK phosphatase activity of AP2C2 very probably dephosphorylates threonine residue of pTEpY motif of MAPKs. The site of action of AP2C2 on MAPKs might be in the nucleus or in the cytoplasm of the cell. AP2C2 function is redundant with another MAPK

phosphatase MKP1 as *ap2c2/mkp1* plants had developmental phenotype compared with *ap2c2* or *mkp1* plants.

Plants lacking AP2C2 grow better and are more tolerant to oxidative stresses.

Salinity and paraquat cause oxidative stress in plant. The toxicity of higher ROS level in the cell leads to cell death. To cope with the stress, plants have the sophisticated signalling system to respond to stress. AP2C2 is believed to be one of the components of ROS signalling regulator. Modification of AP2C2 in plants affects physiological and developmental response of plant to stress. Several evidences demonstrated that AP2C2 acts as a negative regulator of ROS signalling. For instance, *ap2c2* plants were more tolerant to stress than wild type. They germinated better and survived better than wild type in media containing paraquat or high salt. The negative role of AP2C2 in stress might be related to MAPKs, because the *mpk6* plants were much more sensitive to stress. However, the conflicting data was obtained in AP2C2 overexpressors, especially the germination of AP2C2 overexpressors under high salt. Oppositely with *mkp6*, AP2C2 overexpressors are more tolerant to high salt. They germinated better than wild type but less than *ap2c2*. This might be explained that the high amount of AP2C2 in AP2C2 OE plants interfere with the proteins required for this response. Moreover, the experiment on germination and seedling survival was done only once (one set of 50 seedlings of each). To produce convincing results, two more sets of experiment need to be performed with more seeds and including the complemented lines of *ap2c2* with AP2C2 under its own promoter.

In addition to seedling germination and survival, root growth is another developmental response of plants to ROS. There is evidence that ROS production is essential for root growth. The increasing of cellular H₂O₂ level by salt correlated with the reduction of root growth (Lin and Kao, 2001). This idea support the result that roots of *ap2c2* are longer than WT and AP2C2 OE plants grown in ½ MS medium. The difference is even more obvious in *ap2c1/2* double knockout plants, suggesting the additive action of both phosphatases on similar substrates or towards the same downstream target.

Taken together, AP2C2 functions as a negative regulator of stress responses in plants. The lacking of AP2C2 plants makes plant more resistant to stress. Moreover, AP2C1 and AP2C2 might work redundantly in stress response.

AP2C2 might acts as a regulator of JA biosynthesis and pollen development.

Jasmonates (JAs) comprise a class of signalling molecules that regulate both stress responses and development in plants (Browse and Howe, 2008). Based on AP2C2 interaction with Acyl-coA oxidase 1 (ACX1) in yeast, we hypothesised that AP2C2 might regulate JA biosynthesis. Upregulation of *Thionin2.1*, which is an inducible JA-responsive transcript (Epple et al., 1997) upon wounding in *ap2c2* plants but not in WT plants suggests the possible role of AP2C2 in regulation of *Thi2.1* expression. However, this experiment was done only once and needs to be repeated. Together with the report that *ap2c1* plants produced higher JA levels and upregulated JA-responsive *PDF1.2* transcript (Schweighofer et al., 2007), our data support the hypothesis that AP2C2 might negative regulate JA biosynthesis. ACX catalyses the first step of β -oxidation reaction with H_2O_2 as a by-product in peroxisomes. It might be that the accumulated H_2O_2 during stress induce AP2C2 expression at the site of stress application (e.g around wounding area) and then act as signalling molecules in balancing between the productions and signalling of JA. However, the upregulation of AP2C2 may be partially negatively regulate ACX and thereby control JA biosynthesis.

In addition to stress response, JA is also required for male fertility in *Arabidopsis* (Browse, 2005). Among 5 ACX family members, ACX1 and ACX5 are prominently express in mature pollen (Table 4.1.). The disruption of both genes in *acx1/5* plants depletes JA in flower buds to a level that leads to pollen infertility (Schilmiller et al., 2007). The *acx1/5* plants are producing fewer seed-containing siliques and fewer viable seeds than the WT. Reduction of AP2C2 in the heterozygous triple knockout *ap2c2/AP2C2/acx1/5* plants already could restore the fertility phenotype of *acx1/5* plants. These plants produced more seed-containing siliques. The explanation might be that without AP2C2, plants produced more JA in flowers and therefore improve fertility of *acx1/5* plants. In the absence or reduction of AP2C2, the other ACXs, which are expressed nearby or in pollen may act in JA biosynthesis required for normal pollen maturation and thereby help to overcome the lack of function of ACX1/5 in pollen (Table 4.1.).

Table 4.1. ACXs expression in different parts of plants. Data presented by AtGenExpress (AVT) as Absolute values, Mean-normalized values in blanket. ACX1-At4g16760, ACX2-At5g65110, ACX3-At1g06290, ACX4-At3g51840, ACX5-At2g35690

Parts of plant	ACX1	ACX2	ACX3	ACX4	ACX5
senescing leaves	2078 (1.78)	3133 (1.87)	2322 (3.49)	1628 (1.57)	95 (1.14)
sepals	5174 (4.45)	4610 (2.76)	2351 (3.54)	2319 (2.24)	141 (1.70)
petals	2036 (1.75)	6695 (4.01)	2243 (3.37)	2768 (2.67)	243 (2.93)
stamens	2528 (2.17)	2333 (1.40)	2054 (3.09)	2342 (2.26)	532 (6.40)
mature pollen	2024 (1.74)	1904 (1.14)	911 (1.37)	1341 (1.29)	342 (4.12)

There is another explanation for the complementation of the fertility phenotype in *ap2c2/AP2C2 acx1/5* plants that it might be via OPDA production. It was reported that OPDA, the C18 precursor in the biosynthesis of JAs, is itself a potent gene regulator in the wound response and the protection of plants against fungal pathogen in the absence of JA (Stintzi et al., 2001). Microarray analysis showed that OPDA not only upregulates COI1-dependent genes, but also COI1-independent genes that do not respond to JA, suggesting that OPDA may function cooperatively with JA (Taki et al., 2005). However, *opr3* plants demonstrated that JA, but not OPDA is the active signalling molecule that regulates pollen development, since the application of JA, but not OPDA, restored the fertility (Stintzi and Browse, 2000). Even though it can not be excluded that the reduction of AP2C2 might change the signalling and OPDA might be involved with the restoration of seeds fertilization in *ap2c2/AP2C2 acx1/5* plants.

Because ACX protein members have MAPK phosphorylation residues (Serine or Threonine) on the molecules, the alternative mechanism that AP2C2 regulates JA biosynthesis via MAPKs can be proposed (Table 4.2.). Two MAPKs, SIPK and WIPK, which are activated in tobacco after herbivore larva attack, mediate the transcript levels of gene encoding phytochrome biosynthesis enzymes or directly regulate the stability or activity of the enzymes by phosphorylation (Wu et al., 2008). This report supports our idea that AP2C2 might regulate the enzymes in JA biosynthesis pathway via MAPKs.

Table 4.2. Predicted MAPK phosphorylation sites on ACXs proteins. S/T (in red) followed by P is subjected to be the MAPK phosphorylation sites (Caspersen et al., 2007). NetPhos 2.0 Server - Technical University of Denmark ([http://www.cbs.dtu.dk/services/Net Phos/](http://www.cbs.dtu.dk/services/NetPhos/)).

	Amino acid position	Phosphorylation sites	score	
ACX1	215	LEDH S PLPN	0.939	*S*
ACX5	215	LDDH S PLPG	0.947	*S*
ACX2	36	SPSL T PSPS	0.861	*T*
	214	FVID T PNDG	0.835	*T*
ACX3	217	FVIN T PCES	0.979	*T*
ACX4	92	PFHI T PKLG	0.939	*T*
	357	TGQM T PGQA	0.809	*T*

Taken together, these results suggest the possible function of AP2C2 as a negative regulator of pollen development, possibly through JA biosynthesis. AP2C2 might act at the ACX1/5-dependent pathway of JA biosynthesis or independently of it.

However, many questions related to this function of AP2C2 are still open and waiting to be answered. Does AP2C2 really interact with ACX1 (or other ACXs) in plants and if so, is this interaction direct? Which manner does AP2C2 regulate JA biosynthesis and if dephosphorylation/inactivation of the enzyme(s) in the pathway is taking place? What is the role of AP2C2 in pollen development?

AP2C2 is a putative negative regulator of ethylene biosynthesis

According to the findings that MAPK MPK6 regulates ET production by phosphorylating and stabilizing ACS2/ACS6 (Liu and Zhang, 2004), the recent report that AP2C1, a MAPK phosphatase, regulates the levels of stress-ET in plants (Liu and Zhang, 2004; Schweighofer et al., 2007), and due to our result that AP2C2 interacts with and inactivates MPK6, the levels of stress-ET in plants with modified AP2C2 expressions were investigated. The result obtained in this study exhibit a reduction of ET levels compared with the WT and *ap2c1/2* or *ap2c2* after wounding. How AP2C2 controls the ethylene biosynthesis is not clear, but most probably it happens by regulating MPK6, which regulates and stabilises ACS - a rate limiting enzyme of ET biosynthesis

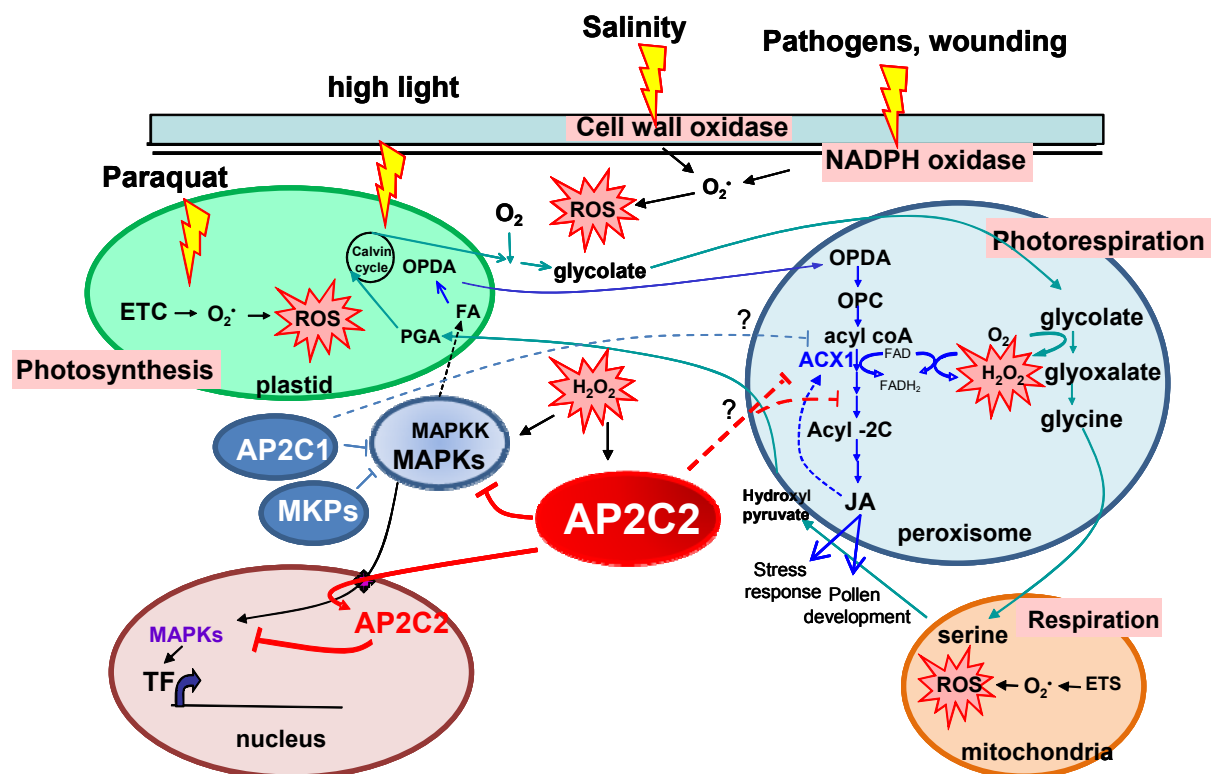


Figure 4.1. Diagram proposed functions of AP2C2. AP2C2 is proposed to act as a regulator of stress response and development in plants. Its expression is induced by stress factors. AP2C2 functions as a negative regulator of MAPKs by interacting and dephosphorylating activated MAPKs, leading to MAPKs inactivation. AP2C2 might act as a regulator of JA biosynthesis which is involved with stress response and pollen development. The mechanism of AP2C2 regulation on JA biosynthesis is not known until now, but might through ACXs enzyme in the JA biosynthesis pathway or might be via MAPK cascades (as described in text). The function of AP2C2 is suggested to be redundant to AP2C1 or MKP1.

5. REFERENCES

- Adie, B.A.T., Perez-Perez, J., Perez-Perez, M.M., Godoy, M., Sanchez-Serrano, J.-J., Schmelz, E.A., and Solano, R.** (2007). ABA Is an Essential Signal for Plant Resistance to Pathogens Affecting JA Biosynthesis and the Activation of Defenses in *Arabidopsis*. *Plant Cell* **19**, 1665-1681.
- Apel, K., and Hirt, H.** (2004). REACTIVE OXYGEN SPECIES: Metabolism, Oxidative Stress, and Signal Transduction. *Annual Review of Plant Biology* **55**, 373-399.
- Asai, T., Tena, G., Plotnikova, J., Willmann, M.R., Chiu, W.-L., Gomez-Gomez, L., Boller, T., Ausubel, F.M., and Sheen, J.** (2002). MAP kinase signalling cascade in *Arabidopsis* innate immunity **415**, 977-983.
- Babbs, C.F., Pham, J.A., and Coolbaugh, R.C.** (1989). Lethal hydroxyl radical production in paraquat-treated plants. *Plant Physiol.* **90**, 1267-1270.
- Baker, A., Graham, I.A., Holdsworth, M., Smith, S.M., and Theodoulou, F.L.** (2006). Chewing the fat: [beta]-oxidation in signalling and development. *Trends in Plant Science* **11**, 124-132.
- Barford, D., and Neel, B.G.** (1998). Revealing mechanisms for SH2 domain mediated regulation of the protein tyrosine phosphatase SHP-2. *Structure* **6**, 249-254.
- Bechtold, U., Richard, O., Zamboni, A., Gapper, C., Geisler, M., Pogson, B., Karpinski, S., and Mullineaux, P.M.** (2008). Impact of chloroplastic- and extracellular-sourced ROS on high light-responsive gene expression in *Arabidopsis*. *J. Exp. Bot.* **59**, 121-133.
- Beers, R.F., Jr., and Sizer, I.W.** (1952). A Spectrophotometric method for measuring the breakdown of hydrogen peroxide by catalase. *J. Biol. Chem.* **195**, 133-140.
- Bogre, L., Ligterink, W., Meskiene, I., Barker, P.J., Heberle-Bors, E., Huskisson, N.S., and Hirt, H.** (1997). Wounding Induces the Rapid and Transient Activation of a Specific MAP Kinase Pathway. *Plant Cell* **9**, 75-83.
- Bork, P., Brown, N.P., Hegyi, H., and Schultz, J.** (1996). The protein phosphatase 2C (PP2C) superfamily: Detection of bacterial homologues. *Protein Sci* **5**, 1421-1425.
- Bowler, C., and Fluhr, R.** (2000). The role of calcium and activated oxygens as signals for controlling cross-tolerance. *Trends in Plant Science* **5**, 241-246.
- Brodersen, P., Petersen, M., Nielsen, H.B., Zhu, S., Newman, M.-A., Shokat, K.M., Rietz, S., Parker, J., and Mundy, J.** (2006). *Arabidopsis* MAP kinase 4 regulates salicylic acid- and jasmonic acid/ethylene-dependent responses via EDS1 and PAD4. *The Plant Journal* **47**, 532-546.
- Browse, J.** (2005). Jasmonate: An Oxylin Signal with Many Roles in Plants Vitamins & Hormones. In *Plant Harmones*, G. Litwack, ed (Academic Press), pp. 431-456.
- Browse, J., and Howe, G.A.** (2008). New Weapons and a Rapid Response against Insect Attack. *Plant Physiol.* **146**, 832-838.
- Cardinale, F., Jonak, C., Ligterink, W., Niehaus, K., Boller, T., and Hirt, H.** (2000). Differential Activation of Four Specific MAPK Pathways by Distinct Elicitors. *J. Biol. Chem.* **275**, 36734-36740.
- Carol, R.J., Takeda, S., Linstead, P., Durrant, M.C., Kakesova, H., Derbyshire, P., Drea, S., Zarsky, V., and Dolan, L.** (2005). A RhoGDP dissociation inhibitor spatially regulates growth in root hair cells **438**, 1013-1016.

- Caspersen, M.B., Qiu, J.-L., Zhang, X., Andreasson, E., Næsted, H., Mundy, J., and Svensson, B. (2007). Phosphorylation sites of Arabidopsis MAP kinase substrate 1 (MKS1). *Biochimica et Biophysica Acta (BBA) - Proteins & Proteomics* **1774**, 1156-1163.
- Chassot, C., Buchala, A., Schoonbeek, H.J., Métraux, J.P., and Lamotte, O. (2008). Wounding of Arabidopsis leaves causes a powerful but transient protection against Botrytis infection. *The Plant Journal* **55**, 555-567.
- Chen, W., Provart, N.J., Glazebrook, J., Katagiri, F., Chang, H.-S., Eulgem, T., Mauch, F., Luan, S., Zou, G., Whitham, S.A., Budworth, P.R., Tao, Y., Xie, Z., Chen, X., Lam, S., Kreps, J.A., Harper, J.F., Si-Ammour, A., Mauch-Mani, B., Heinlein, M., Kobayashi, K., Hohn, T., Dangl, J.L., Wang, X., and Zhu, T. (2002). Expression Profile Matrix of Arabidopsis Transcription Factor Genes Suggests Their Putative Functions in Response to Environmental Stresses. *Plant Cell* **14**, 559-574.
- Chen, Y.-F., Etheridge, n., and Schaller, G.E. (2005). Ethylene Signal Transduction. *Ann Bot* **95**, 901-915.
- Cheong, Y.H., Chang, H.-S., Gupta, R., Wang, X., Zhu, T., and Luan, S. (2002). Transcriptional Profiling Reveals Novel Interactions between Wounding, Pathogen, Abiotic Stress, and Hormonal Responses in Arabidopsis. *Plant Physiol.* **129**, 661-677.
- Chung, J.-S., Zhu, J.-K., Bressan, R.A., Hasegawa, P.M., and Shi, H. (2008). Reactive oxygen species mediate Na⁺-induced SOS1 mRNA stability in Arabidopsis. *The Plant Journal* **53**, 554-565.
- Clark, K.L., Larsen, P.B., Wang, X., and Chang, C. (1998). Association of the Arabidopsis CTR1 Raf-like kinase with the ETR1 and ERS ethylene receptors. *Proceedings of the National Academy of Sciences of the United States of America* **95**, 5401-5406.
- Clough, S.J., and Bent, A.F. (1998). Floral dip: a simplified method for Agrobacterium-mediated transformation of Arabidopsis thaliana. *The Plant Journal* **16**.
- Das, A.K., Helps, N.R., Cohen, P.T.W., and Barford, D. (1996). Crystal structure of the protein serine/threonine phosphatase 2C at 2.0 Å resolution. *The EMBO Journal* **15**, 6798-6809.
- Dat, S., Vandenabeele, S., Vranova, E., Montagu, V.M., Inze, D., and Breusegem, F.V. (2000). Dual action of the active oxygen species during plant stress responses. *CMLS Cellular and Molecular Life Sciences* **57**, 779-795.
- Davletova, S., Schlauch, K., Coutu, J., and Mittler, R. (2005). The Zinc-Finger Protein Zat12 Plays a Central Role in Reactive Oxygen and Abiotic Stress Signaling in Arabidopsis. *Plant Physiol.* **139**, 847-856.
- Doczi, R., Brader, G., Pettko-Szandtner, A., Rajh, I., Djamei, A., Pitzschke, A., Teige, M., and Hirt, H. (2007). The Arabidopsis Mitogen-Activated Protein Kinase Kinase MKK3 Is Upstream of Group C Mitogen-Activated Protein Kinases and Participates in Pathogen Signaling. *Plant Cell* **19**, 3266-3279.
- Dombrecht, B., Xue, G.P., Sprague, S.J., Kirkegaard, J.A., Ross, J.J., Reid, J.B., Fitt, G.P., Sewelam, N., Schenk, P.M., Manners, J.M., and Kazan, K. (2007). MYC2 Differentially Modulates Diverse Jasmonate-Dependent Functions in Arabidopsis. *Plant Cell* **19**, 2225-2245.
- Drori, K.B., Shichrur, K., Katz, A., Oliva, M., Angelovici, R., Yalovsky, S., and Ohad, N. (2004). Detection of protein-protein interactions in plants using bimolecular fluorescence complementation. *The Plant Journal* **40**, 419-427.

- Ellis, C., and Turner, J.G.** (2001). The Arabidopsis Mutant *cev1* Has Constitutively Active Jasmonate and Ethylene Signal Pathways and Enhanced Resistance to Pathogens. *Plant Cell* **13**, 1025-1033.
- Ellis, C., Karafyllidis, I., Wasternack, C., and Turner, J.G.** (2002). The Arabidopsis Mutant *cev1* Links Cell Wall Signaling to Jasmonate and Ethylene Responses. *Plant Cell* **14**, 1557-1566.
- Epple, P., Apel, K., and Bohlmann, H.** (1997). Overexpression of an Endogenous Thionin Enhances Resistance of Arabidopsis against *Fusarium oxysporum*. *Plant Cell* **9**, 509-520.
- Foreman, J., Demidchik, V., Bothwell, J.H.F., Mylona, P., Miedema, H., Torres, M.A., Linstead, P., Costa, S., Brownlee, C., Jones, J.D.G., Davies, J.M., and Dolan, L.** (2003). Reactive oxygen species produced by NADPH oxidase regulate plant cell growth **422**, 442-446.
- Foyer, C.H., and Noctor, G.** (2005). Redox Homeostasis and Antioxidant Signaling: A Metabolic Interface between Stress Perception and Physiological Responses. *Plant Cell* **17**, 1866-1875.
- Gray, W.M., Muskett, P.R., Chuang, H.-w., and Parker, J.E.** (2003). Arabidopsis SGT1b Is Required for SCFTIR1-Mediated Auxin Response. *Plant Cell* **15**, 1310-1319.
- Gupta, R., Huang, Y., Kieber, J., and Luan, S.** (1998). Identification of a dual-specificity protein phosphatase that inactivates a MAP kinase from Arabidopsis. *The Plant Journal* **16**, 581-589.
- Hellens, R.P., Edwards, E.A., Leyland, N.R., Bean, S., and Mullineaux, P.M.** (2000). pGreen: a versatile and flexible binary Ti vector for *Agrobacterium*-mediated plant transformation. *Plant Molecular Biology* **42**, 819-832.
- Huang, Y., Li, H., Hutchison, C.E., Laskey, J., and Kieber, J.J.** (2003). Biochemical and functional analysis of CTR1, a protein kinase that negatively regulates ethylene signaling in Arabidopsis. *The Plant Journal* **33**, 221-233.
- Ichimura, K., Mizoguchi, T., Yoshida, R., Yuasa, T., and Shinozaki, K.** (2000). Various abiotic stresses rapidly activate Arabidopsis MAP kinases ATMPK4 and ATMPK6. *The Plant Journal* **24**, 655-665.
- Jefferson, R.A., Burgess, S.M., and Hirsh, D.** (1986). beta-Glucuronidase from *Escherichia coli* as a gene-fusion marker. *Proceedings of the National Academy of Sciences of the United States of America* **83**, 8447-8451.
- Karimi, M., Inzé, D., and Depicker, A.** (2002). GATEWAY(TM) vectors for *Agrobacterium*-mediated plant transformation. *Trends in Plant Science* **7**, 193-195.
- Kazan, K., and Manners, J.M.** (2008). Jasmonate Signaling: Toward an Integrated View. *Plant Physiol.* **146**, 1459-1468.
- Kazanaviciute, V.** (2006). Functional analysis of an Arabidopsis PP2C phosphatase. Ph.D Thesis.
- Kerk, D., Bulgrien, J., Smith, D.W., Barsam, B., Veretnik, S., and Gribskov, M.** (2002). The Complement of Protein Phosphatase Catalytic Subunits Encoded in the Genome of Arabidopsis. *Plant Physiol.* **129**, 908-925.
- Kotchoni, s.O., and Gachomo, e.W.** (2006). The reactive oxygen species network pathways: an essential prerequisite for perception of pathogen attack and the acquired disease resistance in plants. *J. Biosci.* **31**, 389-404.
- Kovtun, Y., Chiu, W.-L., Tena, G., and Sheen, J.** (2000). Functional analysis of oxidative stress-activated mitogen-activated protein kinase cascade in plants. *PNAS* **97**, 2940-2945.

- Langebartels, C., Wohlgemuth, H., Kschieschan, S., Grün, S., and Sandermann, H.** (2002). Oxidative burst and cell death in ozone-exposed plants. *Plant Physiology and Biochemistry* **40**, 567-575.
- Laurie-Berry, N., Joardar, V., Street, I.H., and Kunkel, B.N.** (2006). The *Arabidopsis thaliana* JASMONATE INSENSITIVE 1 Gene Is Required for Suppression of Salicylic Acid-Dependent Defenses During Infection by *Pseudomonas syringae*. *Molecular Plant-Microbe Interactions* **19**, 789-800.
- Lee, J.S., and Ellis, B.E.** (2007). *Arabidopsis* MAPK Phosphatase 2 (MKP2) Positively Regulates Oxidative Stress Tolerance and Inactivates the MPK3 and MPK6 MAPKs. *J. Biol. Chem.* **282**, 25020-25029.
- Leung, J., Merlot, S., and Giraudat, J.** (1997). The *Arabidopsis* ABSCISIC ACID-INSENSITIVE2 (ABI2) and ABI1 Genes Encode Homologous Protein Phosphatases 2C Involved in Absciscic Acid Signal Transduction. *Plant Cell* **9**, 759-771.
- Li, J., Brader, G., and Palva, E.T.** (2004). The WRKY70 Transcription Factor: A Node of Convergence for Jasmonate-Mediated and Salicylate-Mediated Signals in Plant Defense. *Plant Cell* **16**, 319-331.
- Lin, C.C., and Kao, C.H.** (2001). Cell wall peroxidase activity, hydrogen peroxide level and NaCl-inhibited root growth of rice seedlings. *Plant and Soil* **230**, 135-143.
- Liu, J., and Zhu, J.-K.** (1998). A Calcium Sensor Homolog Required for Plant Salt Tolerance. *Science* **280**, 1943-1945.
- Liu, J., Ishitani, M., Halfter, U., Kim, C.-S., and Zhu, J.-K.** (2000). The *Arabidopsis thaliana* SOS2 gene encodes a protein kinase that is required for salt tolerance. *Proceedings of the National Academy of Sciences of the United States of America* **97**, 3730-3734.
- Liu, J.-X., Srivastava, R., Che, P., and Howell, S.H.** (2007). Salt stress responses in *Arabidopsis* utilize a signal transduction pathway related to endoplasmic reticulum stress signaling. *The Plant Journal* **51**, 897-909.
- Liu, Y., and Zhang, S.** (2004). Phosphorylation of 1-Aminocyclopropane-1-Carboxylic Acid Synthase by MPK6, a Stress-Responsive Mitogen-Activated Protein Kinase, Induces Ethylene Biosynthesis in *Arabidopsis*. *Plant Cell* **16**, 3386-3399.
- Lorenzo, O., Piqueras, R., Sanchez-Serrano, J.J., and Solano, R.** (2003). ETHYLENE RESPONSE FACTOR1 Integrates Signals from Ethylene and Jasmonate Pathways in Plant Defense. *Plant Cell* **15**, 165-178.
- Mellersh, D., G, Foulds, I.V., Higgins, V.J., and Heath, M.C.** (2002). H₂O₂ plays different roles in determining penetration failure in three diverse plant-fungal interactions. *The Plant Journal* **29**, 257-268.
- Meskiene, I., Bögre, L., Glaser, W., Balog, J., Brandstötter, M., Zwerger, K., Ammerer, G., and Hirt, H.** (1998). MP2C, a plant protein phosphatase 2C, functions as a negative regulator of mitogen-activated protein kinase pathways in yeast and plants. *Proceedings of the National Academy of Sciences of the United States of America* **95**, 1938-1943.
- Meskiene, I., Baudouin, E., Schweighofer, A., Liwosz, A., Jonak, C., Rodriguez, P.L., Jelinek, H., and Hirt, H.** (2003). Stress-induced Protein Phosphatase 2C Is a Negative Regulator of a Mitogen-activated Protein Kinase. *J. Biol. Chem.* **278**, 18945-18952.
- Mittler, R.** (2006). Abiotic stress, the field environment and stress combination. *Trends in Plant Science* **11**, 15-19.
- Mittler, R., Vanderauwera, S., Gollery, M., and Van Breusegem, F.** (2004). Reactive oxygen gene network of plants. *Trends in Plant Science* **9**, 490-498.

- Mur, L.A.J., Kenton, P., Atzorn, R., Miersch, O., and Wasternack, C.** (2006). The Outcomes of Concentration-Specific Interactions between Salicylate and Jasmonate Signaling Include Synergy, Antagonism, and Oxidative Stress Leading to Cell Death. *Plant Physiol.* **140**, 249-262.
- Ndamukong, I., Abdallat, A.A., Thurow, C., Fode, B., Zander, M., Weigel, R., and Gatz, C.** (2007). SA-inducible Arabidopsis glutaredoxin interacts with TGA factors and suppresses JA-responsive PDF1.2 transcription. *The Plant Journal* **50**, 128-139.
- Nelson, B.K., Cai, X., and Nebenführ, A.** (2007). A multicolored set of in vivo organelle markers for co-localization studies in Arabidopsis and other plants. *The Plant Journal* **51**, 1126-1136.
- Nuhse, T.S., Peck, S.C., Hirt, H., and Boller, T.** (2000). Microbial Elicitors Induce Activation and Dual Phosphorylation of the Arabidopsis thaliana MAPK 6. *J. Biol. Chem.* **275**, 7521-7526.
- Ort, D.R., and Good, N.E.** (1988). Textbooks ignore photosystem II-dependent ATP formation: is the Z scheme to blame? *Trends in Biochemical Sciences* **13**, 467-469.
- Ort, D.R., and Baker, N.R.** (2002). A photoprotective role for O₂ as an alternative electron sink in photosynthesis? *Current Opinion in Plant Biology* **5**, 193-198.
- Ouaked, F., Rozhon, W., Lecourieux, D., and Hirt, H.** (2003). A MAPK pathway mediates ethylene signaling in plants. *EMBO Journal* **22**, 1282-1288.
- Pavet, V., Olmos, E., Kiddle, G., Mowla, S., Kumar, S., Antoniow, J., Alvarez, M.E., and Foyer, C.H.** (2005). Ascorbic Acid Deficiency Activates Cell Death and Disease Resistance Responses in Arabidopsis. *Plant Physiol.* **139**, 1291-1303.
- Penninckx, I.A.M.A., Thomma, B.P.H.J., Buchala, A., Metraux, J.-P., and Broekaert, W.F.** (1998). Concomitant Activation of Jasmonate and Ethylene Response Pathways Is Required for Induction of a Plant Defensin Gene in Arabidopsis. *Plant Cell* **10**, 2103-2114.
- Petersen, M., Brodersen, P., Naested, H., Andreasson, E., Lindhart, U., Johansen, B., Nielsen, H.B., Lacy, M., Austin, M.J., Parker, J.E., Sharma, S.B., Klessig, D.F., Martienssen, R., Mattsson, O., Jensen, A.B., and Mundy, J.** (2000). Arabidopsis MAP kinase 4 negatively regulates systemic acquired resistance. *Cell* **103**, 1111-1120.
- Pitzschke, A., Forzani, C., and Hirt, H.** (2006). Reactive Oxygen Species Signaling in Plants. *Antioxidants & Redox Signaling* **8**, 1757-1764.
- Rentel, M.C., Lecourieux, D., Ouaked, F., Usher, S.L., Petersen, L., Okamoto, H., Knight, H., Peck, S.C., Grierson, C.S., Hirt, H., and Knight, M.R.** (2004). OXI1 kinase is necessary for oxidative burst-mediated signalling in Arabidopsis **427**, 858-861.
- Restrepo, M.A., Freed, D.D., and Carrington, J.C.** (1990). Nuclear Transport of Plant Potyviral Proteins. *Plant Cell* **2**, 987-998.
- Rizhsky, L., Davletova, S., Liang, H., and Mittler, R.** (2004). The Zinc Finger Protein Zat12 Is Required for Cytosolic Ascorbate Peroxidase 1 Expression during Oxidative Stress in Arabidopsis. *J. Biol. Chem.* **279**, 11736-11743.
- Rodriguez, F.I., Esch, J.J., Hall, A.E., Binder, B.M., Schaller, G.E., and Bleeker, A.B.** (1999). A Copper Cofactor for the Ethylene Receptor ETR1 from Arabidopsis. *Science* **283**, 996-998.
- Rodriguez, S.-M.C., Adams-Phillips, L., Liu, Y., Wang, H., Su, S.-H., Jester, P.J., Zhang, S., Bent, A.F., and Krysan, P.J.** (2007). MEKK1 Is Required for flg22-Induced MPK4 Activation in Arabidopsis Plants. *Plant Physiol.* **143**, 661-669.

- Rossel, J.B., Wilson, P.B., Hussain, D., Woo, N.S., Gordon, M.J., Mewett, O.P., Howell, K.A., Whelan, J., Kazan, K., and Pogson, B.J. (2007). Systemic and Intracellular Responses to Photooxidative Stress in Arabidopsis. *Plant Cell* **19**, 4091-4110.
- Sagi, M., and Fluhr, R. (2006). Production of Reactive Oxygen Species by Plant NADPH Oxidases. *Plant Physiol.* **141**, 336-340.
- Schilmiller, A.L., Koo, A.J.K., and Howe, G.A. (2007). Functional Diversification of Acyl-Coenzyme A Oxidases in Jasmonic Acid Biosynthesis and Action. *Plant Physiol.* **143**, 812-824.
- Schopfer, P. (2001). Hydroxyl radical-induced cell-wall loosening *in vitro* and *in vivo*: implications for the control of elongation growth. *The Plant Journal* **28**, 679-688.
- Schweighofer, A., and Meskiene, I. (2008). Regulation of stress hormones jasmonates and ethylene by MAPK pathways in plants. *Molecular BioSystems* **4**, 799-803.
- Schweighofer, A., Hirt, H., and Meskiene, I. (2004). Plant PP2C phosphatases: emerging functions in stress signaling. *Trends in Plant Science* **9**, 236-243.
- Schweighofer, A., Kazanaviciute, V., Scheikl, E., Teige, M., Doczi, R., Hirt, H., Schwanninger, M., Kant, M., Schuurink, R., Mauch, F., Buchala, A., Cardinale, F., and Meskiene, I. (2007). The PP2C-Type Phosphatase AP2C1, Which Negatively Regulates MPK4 and MPK6, Modulates Innate Immunity, Jasmonic Acid, and Ethylene Levels in Arabidopsis. *Plant Cell* **19**, 2213-2224.
- Schweikert, C., Liskay, A., and Schopfer, P. (2000). Scission of polysaccharides by peroxidase-generated hydroxyl radicals. *Phytochemistry* **53**, 565-570.
- Seo, S., Katou, S., Seto, H., Kenji Gomi, and Ohashi, Y. (2007). The mitogen-activated protein kinases WIPK and SIPK regulate the levels of jasmonic and salicylic acids in wounded tobacco plants. *The Plant Journal* **49**, 899-909.
- Shah, J. (2003). The salicylic acid loop in plant defense. *Current Opinion in Plant Biology* **6**, 365-371.
- Sheen, J. (1998). Mutational analysis of protein phosphatase 2C involved in abscisic acid signal transduction in higher plants. *Proceedings of the National Academy of Sciences of the United States of America* **95**, 975-980.
- Shi, H., Ishitani, M., Kim, C., and Zhu, J.-K. (2000). The Arabidopsis thaliana salt tolerance gene SOS1 encodes a putative Na⁺/H⁺ antiporter. *Proceedings of the National Academy of Sciences of the United States of America* **97**, 6896-6901.
- Shibuya, E.K., Polverino, A.J., Chang, E., Wigler, M., and Ruderman, J.V. (1992). Oncogenic ras triggers the activation of 42-kDa mitogen-activated protein kinase in extracts of quiescent *Xenopus* oocytes. *Proceedings of the National Academy of Sciences of the United States of America* **89**, 9831-9835.
- Smith, H., Hicks, G.R., and Raikhel, N.V. (1997). Importin [alpha] from Arabidopsis thaliana Is a Nuclear Import Receptor That Recognizes Three Classes of Import Signals. *Plant Physiol.* **114**, 411-417.
- Spoel, S.H., Johnson, J.S., and Dong, X. (2007). Regulation of tradeoffs between plant defenses against pathogens with different lifestyles. *Proceedings of the National Academy of Sciences* **104**, 18842-18847.
- Stintzi, A., and Browse, J. (2000). The Arabidopsis male-sterile mutant, *opr3*, lacks the 12-oxophytodienoic acid reductase required for jasmonate synthesis. *Proceedings of the National Academy of Sciences of the United States of America* **97**, 10625-10630.

- Stintzi, A., Weber, H., Reymond, P., Browse, J., and Farmer, E.E.** (2001). Plant defense in the absence of jasmonic acid: The role of cyclopentenones. *Proceedings of the National Academy of Sciences of the United States of America* **98**, 12837-12842.
- Suzuki, N., and Mittler, R.** (2006). Reactive oxygen species and temperature stresses: A delicate balance between signaling and destruction. *Physiologia Plantarum* **126**, 45-51.
- Takahashi, F., Yoshida, R., Ichimura, K., Mizoguchi, T., Seo, S., Yonezawa, M., Maruyama, K., Yamaguchi-Shinozaki, K., and Shinozaki, K.** (2007). The Mitogen-Activated Protein Kinase Cascade MKK3-MPK6 Is an Important Part of the Jasmonate Signal Transduction Pathway in Arabidopsis. *Plant Cell* **19**, 805-818.
- Takatsume, Y., Izawa, S., and Inoue, Y.** (2006). Methylglyoxal as a Signal Initiator for Activation of the Stress-activated Protein Kinase Cascade in the Fission Yeast *Schizosaccharomyces pombe*. *J. Biol. Chem.* **281**, 9086-9092.
- Taki, N., Sasaki-Sekimoto, Y., Obayashi, T., Kikuta, A., Kobayashi, K., Ainai, T., Yagi, K., Sakurai, N., Suzuki, H., Masuda, T., Takamiya, K.-i., Shibata, D., Kobayashi, Y., and Ohta, H.** (2005). 12-Oxo-Phytodienoic Acid Triggers Expression of a Distinct Set of Genes and Plays a Role in Wound-Induced Gene Expression in Arabidopsis. *Plant Physiol.* **139**, 1268-1283.
- Teige, M., Scheikl, E., Eulgem, T., Dóczi, R., Ichimura, K., Shinozaki, K., Dangl, J.L., and Hirt, H.** (2004). The MKK2 Pathway Mediates Cold and Salt Stress Signaling in Arabidopsis. *Molecular Cell* **15**, 141-152.
- Tena, G., Asai, T., Chiu, W.-L., and Sheen, J.** (2001). Plant mitogen-activated protein kinase signaling cascades. *Current Opinion in Plant Biology* **4**, 392-400.
- Topfer, R., Matzeit, V., Gronenborn, B., Schell, J., and Steinbiss, H.-H.** (1987). A set of plant expression vectors for transcriptional and translational fusions. *Nucl. Acids Res.* **15**, 5890-.
- Torres, M.A., and Dangl, J.L.** (2005). Functions of the respiratory burst oxidase in biotic interactions, abiotic stress and development. *Current Opinion in Plant Biology* **8**, 397-403.
- Torres, M.A., Jones, J.D.G., and Dangl, J.L.** (2006). Reactive Oxygen Species Signaling in Response to Pathogens. *Plant Physiol.* **141**, 373-378.
- Turner, J.G., Ellis, C., and Devoto, A.** (2002). The Jasmonate Signal Pathway. *Plant Cell* **14**, S153-164.
- Ulm, R., Revenkova, E., di Sansebastiano, G.-P., Bechtold, N., and Paszkowski, J.** (2001). Mitogen-activated protein kinase phosphatase is required for genotoxic stress relief in Arabidopsis. *Genes Dev.* **15**, 699-709.
- Ulm, R., Ichimura, K., Mizoguchi, T., Peck, S.C., Zhu, T., Wang, X., Shinozaki, K., and Paszkowski, J.** (2002). Distinct regulation of salinity and genotoxic stress responses by Arabidopsis MAP kinase phosphatase 1. *EMBO* **21**, 6483-6493.
- Vandenabeele, S., Vanderauwera, S., Vuylsteke, M., Rombauts, S., Langebartels, C., Seidlitz, H.K., Zabeau, M., Montagu, M.V., Inzé, D., and Breusegem, F.V.** (2004). Catalase deficiency drastically affects gene expression induced by high light in Arabidopsis thaliana. *The Plant Journal* **39**, 45-58.
- Vanderauwera, S., Zimmermann, P., Rombauts, S., Vandenabeele, S., Langebartels, C., Groussin, W., Inzé, D., and Van Breusegem, F.** (2005). Genome-Wide Analysis of Hydrogen Peroxide-Regulated Gene Expression in Arabidopsis Reveals a High Light-Induced Transcriptional Cluster Involved in Anthocyanin Biosynthesis. *Plant Physiol.* **139**, 806-821.

- Wahid, A., Gelani, S., Ashraf, M., and Foolad, M.R.** (2007). Heat tolerance in plants: An overview. *Environmental and Experimental Botany* **61**, 199-223.
- Walter, M.H.** (1989). The induction of phenylpropanoid biosynthetic enzymes by ultraviolet light or fungal elicitor in cultured parsley cells is overridden by a heat-shock treatment. *Planta* **177**, 1-8.
- Wang, H., Chevalier, D., Larue, C., Cho, S.K., and C, W.J.** (2007). The protein phosphatases and protein kinases of *Arabidopsis thaliana*. *The Arabidopsis book*, 1-30.
- Wang, K.L.-C., Li, H., and Ecker, J.R.** (2002). Ethylene Biosynthesis and Signaling Networks. *Plant Cell* **14**, S131-151.
- Wildermuth, M.C., Dewdney, J., Wu, G., and Ausubel, F.M.** (2001). Isochorismate synthase is required to synthesize salicylic acid for plant defence **414**, 562-565.
- Wu, J., Hettenhausen, C., Schuman, M.C., and Baldwin, I.T.** (2008). A Comparison of Two *Nicotiana attenuata* Accessions Reveals Large Differences in Signaling Induced by Oral Secretions of the Specialist Herbivore *Manduca sexta*. *Plant Physiol.* **146**, 927-939.
- Xu, Q., Fu, H.-H., Gupta, R., and Luan, S.** (1998). Molecular Characterization of a Tyrosine-Specific Protein Phosphatase Encoded by a Stress-Responsive Gene in *Arabidopsis*. *Plant Cell* **10**, 849-858.
- Yoo, S.-D., Cho, Y.-H., Tena, G., Xiong, Y., and Sheen, J.** (2008). Dual control of nuclear EIN3 by bifurcate MAPK cascades in C₂H₄ signalling **451**, 789-795.
- Yuasa, T., Ichimura, K., Mizoguchi, T., and Shinozaki, K.** (2001). Oxidative Stress Activates ATMPK6, an *Arabidopsis* Homologue of MAP Kinase. *Plant Cell Physiol.* **42**, 1012-1016.
- Zhu, J.-K.** (2000). Genetic Analysis of Plant Salt Tolerance Using *Arabidopsis*. *Plant Physiol.* **124**, 941-948.

6. APPENDIX

6.1. Abbreviations

ABA	abscisic acid
ABI	abscisic acid insensitive
ACX	acyl CoA oxidase
ATP	adenosine triphosphate
AUX	auxin
AP2C	<i>Arabidopsis</i> protein phosphatase type 2C
BAC	bacterial artificial chromosome
BSA	bovine serum albumin
CaMV	cauliflower mosaic virus
CAT2HP	hair pin construct-containing catalase-deficient plant
CFP	cyan fluorescent protein
2,4-D	2,4-dichlorophenoxy acetic acid
DEPC	Diethyl Pyrocarbonate
Dex.SO ₄	dextrane sulphate
DMSO	dimethylsulfoxide
DMF	dimethylformamide
DSP	dual specificity protein tyrosine phosphatase
DTT	dithiothreitol
EDTA	ethylenediaminetetraacetic acid
EGTA	ethyleneglycol-bis(β -aminoethylether)-tetraacetic acid
ET	ethylene
FA	fatty acid
GFP	green fluorescent protein
gof	gain-of-function
GST	glutathione S-transferase
GTP	guanidine triphosphate
hr	hour
HA	hemagglutinin
HAB1	homology to <i>ABI1/ABI2</i>
HL	high-light

IMP	importin
IPTG	isopropyl- β -D-thiogalactoside
JA	Jasmonic acid
Kb	kilobase pair
kDa	kiloDalton
KIM	kinase interaction motif
KO	knockout
LB	brothLuria Bertani broth
Lof	loss-of-function
MAPK/MPK	mitogen-activated protein kinase
MAPKK/MKK	mitogen-activated protein kinase kinase
MBP	myelin basic protein
β -ME	β -mercaptoethanol
min	minute
MKP1MAP	kinase phosphatase1
MP2C	<i>Medicago</i> PP2C
MS	murashige Skoog medium
MW	molecular weight
Myc	myelocytomatosis
NLS	nuclear localization signal
OD	optical density
OE	overexpression
ONPG	o-nitrophenyl- β -D-galactopyranoside
PCR	polymerase chain reaction
PEG	polyethylene glycol
PMSF	phenylmethysulfonylfluoride
PP2A	protein phosphatase type 2A
PP2B	protein phosphatase type 2B
PP2C	protein phosphatase type 2C
PPM	protein phosphatase M
PPP	protein phosphatase P
PQ	paraquat or methyl viologen
RL	Kreceptor - like kinase

RT	room temperature
RT-PCR	reverse transcription PCR
SA	salicylic acid
SAMdC	S-adenosyl-L-methionine decarboxylase
SAMK	stress-activated MAP kinase
SAR	systemic acquired resistance
SD	synthetic dropout medium
SDS-PAGE	sodium dodecyl sulphate polyacrylamide gel electrophoresis
SIMK	stress-induced MAP kinase
ssDNA	single stranded DNA
TB	Terrific Broth
TCA	trichloroacetic acid
T-DNA	transferred DNA
WT	wild type
YFP	yellow fluorescent protein
YPD	yeast extract/peptone/dextone

Curriculum Vitae

Personal details

Name: Chonnanit Choopayak

Date of birth: April 21st, 1970

Place of birth: Bangkok, Thailand

Nationality: Thai

Education and Professional experiences

2004 – present PhD Thesis (Genetics), Group of Dr. Irute Meskiene, Department of Plant Molecular Biology, University of Vienna.

1998 – present Lecturer, Department of Biochemistry, Faculty of Medical Science, Naresuan University, Phitsanulok, Thailand.

1997 – 1998 Research Assistant, Group of Dr. Patcharee Lertrit Wichyanuwat, Department of Biochemistry, Mahidol University, Bangkok, Thailand.

1993 – 1996 M.Sc. Thesis (Biochemistry), Mahidol University, Bangkok, Thailand M.Sc. project: The mitochondrial cytochrome oxidase subunit III gene and protein sequence analysis in chloroquine resistant *Plasmodium falciparum*.

1987 – 1990 Bachelor degree (Nursing Science), Faculty of Nursing Science, Burapha University, Chonburi, Thailand.

Grants and Scholarships

2005 – present	Royal Thai government scholarship for PhD study
2004 – 2005	Naresuan University scholarship for PhD study
2002, 2003	Research grants for the exchange of scientists under Japan Society for The Promotion of Science and the National Research Council of Thailand (NRCT-JSPS)
1995	The King Prajadhipok and Queen Barni Memorial Foundation for Master degree study
1993 - 1994	The National Science and Technology Development Agency (NSTDA) for Master degree study

Conference Participations and Poster presentations

- Life Sciences, Graz, Austria, 22-24 September 2008. Poster: Characterization and Functional analysis of a novel PP2C phosphatase AP2C2 from Arabidopsis.
- 5th Tri-National Arabidopsis Meeting (TNAM 2008), Zürich, Switzerland, 10-13 September 2008. Poster: Jasmonate is controlled by PP2C phosphatases.
- PhD-Symposium 2008 : Young Scientist Association of the Medical University of Vienna (YSA2008), Vienna, Austria, 28-29 May 2008. Poster: The novel protein phosphatases with PP2C and MAPK-phosphatase activities from Arabidopsis
- 5th Austrian Proteome Research Symposium, Vienna, Austria, 24-25 September 2007.
- 4th Tri-National Arabidopsis Meeting (TNAM 2007), Vienna, Austria, 12-15 September 2007. Poster: Identification of the substrates and expression patterns of the novel Arabidopsis PP2C-type phosphatase.
- 32nd FEBS Congress: Molecular machines (FEBS 2007), Vienna, Austria, 7-12 July 2007. Poster: Identification of the substrates and expression patterns of the novel Arabidopsis PP2C-type phosphatase.
- 24th Annual Missouri Plant Biology Symposium: Plant Protein Phosphorylation Dephosphorylation and Plant Proteomics Mini-Symposium, Missouri, USA, 22-24 May 2007. Poster: Proteomics of Protein Phosphatase Target: Application of TAP-tagged PP2Cs in Arabidopsis.
- XVII International Botanical Congress, Vienna, Austria, 17-23 July 2005.